A CODE FOR MULTIPHASE REACTIVE TRANSPORT MODELING OF CONCENTRATED SOLUTIONS UNDER EXTREME DRY CONDITIONS

PhD Thesis

Hydrogeology Group (GHS)

Dept Geotechnical Engineering and Geosciences, Universitat Politecnica de Catalunya, UPC-BarcelonaTech

Institute of Environmental Assessment and Water Research (IDAEA), Spanish Research Council (CSIC)

Author:

Ing. Pablo Andrés Gamazo Rusnac

Advisors:

Dr. Jesús Carrera

Dr. Maarten Saaltink

December, 2010

This thesis was co-funded by the Technical University of Catalonia (UPC) with a grant "*BECA UPC PER A LA RECERCA*", and by the Hydrogeology Group (GHS) through the projects: "*Tecnologías avanzadas de generación, captura y almacenamiento de CO_2. Almacenamiento Geológico de CO_2 (PSS-120000-2008-31). Entidad financiadora: Ministerio de Ciencia e Innovación*" and "*Atenuación natural y tratamiento pasivo de drenajes ácidos de minas en la cuenca del río Odiel. (CTM2007-66724-C02-01). Entidad financiadora: Ministerio de Ciencia e Innovación*."

Pal' Ale

I. Abstract

Multiphase Reactive Transport (MPRT) modelling involves simulating flow of fluid phases, transport of species and energy, and reactions between species within the same or different phases. Reactive transport codes decouple phase flow calculations from reactive transport. This approach has been successfully applied to a wide range of MPRT problems, but it may be unsuitable for problems like the chemical evolution of unsaturated tailings or the salinization of soils, where concentrated solutions or extremely dry conditions are be reached. The amount of liquid water in these cases can be so small that both vapor and water in hydrated minerals can be significant for the water balance. Wissmeier and Barry (2008) developed a code which couples chemical sink-sources and water flow, but only for cases where transport is limited to unsaturated liquid phase. However, under these extreme conditions gas transport becomes important and water activity, which controls vapor pressure, is affected by capillary and salinity effects. Moreover, certain mineral paragenesis (the ones that produce invariant points) fix water activity, causing the geochemistry to control vapor pressure, which is a key gas flow variable. Thus, a fully coupled solution of phase fluxes and reactive transport is required for these conditions.

The main objective of this thesis is to develop a general MPRT code capable of representing the effect of geochemistry on flow and transport for concentrated solutions under extreme dry conditions. As a secondary objective, the behavior of some cases under such conditions is studied. Different aspects of this code and different cases are discussed through the chapters of this thesis.

First, coupling of salinity and vapor pressure (and thus evaporation rate) is discussed, and a method for computing the evolution of high salinity systems is presented. Special emphasis is placed on the treatment of invariant points, that are sets of minerals that fix water activity. The method is applied to a natural $MgSO_4$-rich brine evaporation experiment and to a simplified model of a perennial saline playa lake. The results indicate that mineral paragenesis can have a considerable influence on the evolution of shallow brine systems by fixing chemical composition for a significant portion of time.

Second, the evolution of concentrated solution in porous media is discussed. In this scenario evaporation is affected not only by salinity but also by capillary effects. Also transport is considered. A generalized compositional formulation for MPRT, which considers coupling effects between geochemical and hydrodynamic process problems, is presented. Some aspects related to its numerical solution are discussed as well. The advantages of the formulation are illustrated by simulating the effect of mineral dehydration on the hydrodynamic processes in a gypsum column that reaches extremely dry conditions. The results indicate this significantly affects the evolution of the system.

Finally, implementation of the code is presented. The importance of flexibility for reactive transport codes and the way how objects oriented programming can facilitate this feature is discussed. The code's main classes and their interactions are presented. The code is used to model a laboratory experiment where a sand column saturated with an MgSO4 solution is subject to evaporation. Extreme dry conditions and high salinity content are reached in this experiment. The interaction between hydrodynamic and geochemical processes on the model is analyzed. Model results shows that the occurrence of invariant points on the top of the domain can have an appreciable effect on the outlet of vapor from the column and on the distribution of salt precipitates along the column. In fact, invariant points explain spatial fluctuation of salt precipitates.

II. Resumen

La modelación de transporte reactivo multifase (TRMF) involucra la simulación del flujo de fases fluidas, el transporte de especies y energía, y las reacciones químicas. La mayoría de los códigos de transporte reactivo desacoplan los cálculos de flujos de fases del transporte reactivo. Este enfoque ha sido aplicado a diversos problemas de TRMF, pero puede resultar inadecuado para problemas como la evolución de pilas de desechos mineros o la salinización de suelos, donde pueden encontrarse soluciones concentradas o condiciones de extrema sequedad. En estos casos la cantidad de agua líquida puede ser tan pequeña que tanto el vapor cómo la precipitación mineral pueden afectar su balance. Wissmeier y Barry (2008) desarrollaron un código que acopla los términos fuente sumidero químico y los cálculos de flujo, pero solo para casos donde el transporte está limitado a la fase liquida. Sin embargo, bajo estas condiciones el transporte de gas puede ser importante y la actividad del agua, que controla la presión de vapor, se ve afectada por efectos capilares y de salinidad. Además, ciertas paragénesis (las que producen puntos invariantes) pueden fijar la actividad del agua, conduciendo a que la geoquímica controle la presión de vapor, que es una variable clave para el flujo de gas. Por lo tanto, una solución que acople el flujo de fases y el transporte reactivo es necesaria.

El principal objetivo de esta tesis es desarrollar un código de TRMF capaz de representar la influencia de la geoquímica sobre los flujos y el transporte para soluciones concentradas bajo condiciones de extrema sequedad. Como objetivo secundario se estudian algunos casos bajo estas condiciones.

En primer lugar, se discute el acoplamiento de la salinidad y la presión de vapor (y por tanto la evaporación), y se presenta un método para calcular la evolución de sistemas altamente salinos. Se hace especial énfasis en la valoración de puntos invariantes, donde la actividad del agua es controlada por el conjunto de minerales precipitados. El método es testeado modelando un experimento de evaporación de una salmuera natural rica en $MgSO_4$ y con un modelo simplificado de una laguna salada perene. Los resultados obtenidos indican que la paragénesis mineral puede tener una influencia considerable sobre la evolución de sistemas salobres al fijar la composición química durante un intervalo considerable de tiempo.

En segundo lugar, se discute la evolución de una solución concentrada en un medio poroso. En estas condiciones la evaporación se ve afectada no solo por efectos salinos sino también por capilares, y por procesos de transporte. Se presenta una formulación composicional

generalizada para TRMF que considera los efectos del acoplamiento entre procesos geoquímicos e hidrodinámicos, y se discuten algunos aspectos en relación a su solución numérica. Las ventajas de esta formulación se ilustran mediante la simulación del efecto de la deshidratación mineral en los procesos hidrodinámicos en una columna de yeso que alcanza condiciones de extrema sequedad. Los resultados indican que los efectos acoplados pueden tener una influencia significativa en la evolución de sistema.

Finalmente, se presenta la implementación del código. Se discute la importancia de la flexibilidad en los códigos de transporte reactivo y cómo la programación orientada a objetos puede facilitarla. Se presentan las principales clases del código y como las mismas interaccionan. El código se utiliza para modelar un experimento de evaporación de una columna de arena saturada en una solución de MgSO4. Se analiza la interacción entre procesos hidrodinámicos y geoquímicos. Los resultados obtenidos muestran que la ocurrencia de puntos invariantes en el extremo superior de la columna puede tener un efecto apreciable en la salida de vapor y en la aparición de sales en la columna. De hecho, los puntos invariantes explican la fluctuación espacial en la precipitación de sales.

III. Resum

La modelació del transport reactiu multifàsic (TRMF) involucra la simulació del flux de fases fluïdes, el transport de compostos químics i energia, i les reaccions químiques. La majoria dels codis de transport reactiu desacoblen els càlculs de flux de fases del transport reactiu. Aquesta metodologia que s'utilitza per resoldre diversos problemes de TRMF resulta inadequada per adreçá problemes com ara l'evolució de piles de deixalles mineres o la salinització de sòls a on poden trobar-se solucions concentrades o condicions d'extrema sequedat. En aquests casos la quantitat d'aigua líquida pot ser tan petita que tant el vapor com la precipitació mineral poden afectar el seu balanç. Wissmeier i Barry (2008) han desenvolupat un codi que acobla el terme font químic i els càlculs de flux, però solament serveix per a casos on el transport està limitat a la fase líquida. Tot i això, sota aquestes condicions, el transport de gas pot ser important i l'activitat de l'aigua que controla la pressió de vapor es pot veure afectada tan per efectes capil·lars com ara de la salinitat. A més, certes paragènesis (les que produeixen punts invariants) poden fixar l'activitat de l'aigua, produint que la geoquímica controli la pressió de vapor, la qual és una variable clau per simular correctament el flux de gas. Per tant, una solució que acobli el flux de fases i el transport reactiu és necessària.

El principal objectiu d'aquesta tesi és desenvolupar un codi de TRMF capaç de representar la influència de la geoquímica sobre els fluxes i el transport en solucions concentrades i condicions d'extrema sequedat. Com objectiu secundari s'estudien alguns casos sota aquestes condicions.

En primer lloc, es discuteix l'acoblament de la salinitat i la pressió de vapor (i per tant l'evaporació), i es presenta un mètode per calcular l'evolució de sistemes altament salins. Es fa especial èmfasi en la valoració de punts invariants, on l'activitat de l'aigua és controlada pel conjunt de minerals precipitats. El mètode és contrastat contra un experiment d'evaporació d'una salmorra natural rica en MgSO4 i amb un model simplificat d'una llacuna salobre perenne. Els resultats obtinguts indiquen que la paragènesis mineral pot tenir una influència considerable sobre l'evolució de sistemes salobres en fixar la composició química durant un interval considerable de temps.

En segon lloc, es discuteix l'evolució d'una solució concentrada en un mitjà porós. En aquestes condicions l'evaporació es veu afectada no solament per efectes de la salinitat sinó també per capil·lars, i per processos de transport. Es presenta una formulació composicional per TRMF que considera els efectes de l'acoblament entre processos geoquímics i hidrodinàmics, i es

discuteixen alguns aspectes en relació a la seva solució numèrica. Els avantatges d'aquesta formulació són il·lustrades mitjançant la simulació de l'efecte de la deshidratació mineral en els processos hidrodinàmics en una columna de guix en condicions d'extrema sequedat. Els resultats indiquen que els efectes acoblats poden tenir una influència significativa en l'evolució de sistema.

Finalment, presentem la implementació del codi. Es discuteix la importància de la flexibilitat en el desenvolupament de codis de transport reactiu mitjançant la programació orientada a objectes. Es presenten les principals classes que utilitza el codi i com interaccionen entre elles. El codi s'utilitza per modelar un experiment d'evaporació d'una columna de sorra saturada en una solució de MgSO4. La interacció entre processos hidrodinàmics i geoquímics és analitzada. Els resultats obtinguts mostren que l'aparició de punts invariants en l'extrem superior de la columna té un efecte apreciable en la valoració de la sortida de vapor i en la precipitació de sals en la columna. De fet, els punts invariants expliquen les fluctuacions espacials observades en la precipitació de sals.

IV. Agradecimientos

Quiero agradecer en primer lugar a mis directores Dr. Jesús Carrera y Dr. Maarten Saaltink por haber sabido orientar mi entusiasmo y dirigir mi esfuerzo durante el desarrollo del doctorado. También al Dr. Carlos Ayora por contribuir en mi formación geoquímica y por el tiempo que me ha dedicado.

Estoy especialmente agradecido a mis compañeros Sergio y Luit (ahora Dr. Sergio Bea y Dr. Luit Slooten) de los cuales aprendí mucho y recibí siempre un desinteresado apoyo. También con el Dr. Orlando Silva con el cual he trabajado con mucho gusto.

Estoy muy agradecido a todos mis compañeros de doctorado de la UPC y del instituto Jaume Almera, especialmente a Jordi Font, Gonzalo Sapriza ,Eduardo Castro, Alejandro Blanco y Manuela Barbieri con quienes he compartido tantos buenos momentos. Gracias al *Herr Doktor* Marcos Dentz por contribuir con el mantenimiento de mi estado físico. Quiero también agradecer a mis compañeros de despacho Meritxell Gran, Carmen Chaparro, Daniel Fernández y Estanislao Pujades por la buena atmosfera de trabajo que entre todos generamos durante los últimos años y especialmente a Marco Barahona por permitirme usar y abusar de su ordenador para correr modelos.

Quiero agradecer también a Jorge de los Santos por iniciarme en el mundo de la hidrogeología y por el apoyo brindado para comenzar el doctorado.

Estoy especialmente agradecido a mis padres y mi hermana, quienes siempre me apoyaron y alentaron a lo largo de mis estudios en Uruguay y España. También a los amigos fuera de España Alejandro Mouta, Fernando Alfonzo, Fabián Cedres, Gabriel Rügnitz, Fernando Rostagnol y Martín Alcalá quienes a pesar de la distancia no dejaron nunca de estar cerca.

Sin lugar a dudas me hubiese sido imposible realizar el doctorado sin el apoyo incondicional de mi esposa Johana, con quien compartí los momentos buenos y los no tanto. *Gracias querida por respaldarme y acompañarme en cada paso durante estos cinco años.* Y finalmente a mi hija Lucía, por la inagotable fuente de felicidad que es.

V. List of Contents

VI. List of figures

VII. List of Tables

1. Introduction

1.1. Motivation and objectives

Modeling multiphase reactive transport (MPRT) problems draws on numerous fields in the Earth sciences, including hydrology, geochemistry, biogeochemistry, soil physics, and fluid dynamics. It involves simulating several phenomena: flow of fluid phases, transport of species and energy and chemical reactions (Steefel et al. 2005). MPRT modeling has to deal not only with the individual difficulties of each of these phenomena but also with new ones associated to coupling effects (Lichtner 1996).

One of the major difficulties is the interaction between geochemical processes and the other phenomena. Geochemistry controls flow properties, such as viscosity and density. Moreover, chemical reaction can act as a source-sink term in the conservation equations of chemical species including water. This will also affect the conservation of fluid phases (either gas or liquid), since they are equal to the sum of all species that compose them.

The effect of transport processes on geochemistry has been studied from a reactive transport perspective (Xu and Pruess 1998, Saaltink et al. 2004, Mills et al. 2007). These authors deal with the complexity of geochemical and transport processes but they calculate phase flow separately. Effects of heterogeneous reactions on phase flow have been studied from a multiphase perspective (Abriola and Pinder, 1985, Forsyth and Shao, 1991, Olivella et al. 1996, Pruess et al. 1999, Pruess and Battistelli 2002), but these approaches do not include key geochemical processes, such as reactions between species of the same phase (e.g., complexation and hydrolysis), complex adsorption models or equilibrium with several mineral phases.

MPRT of concentrated solutions under extreme dry conditions (like vadose tailings, or soils with high a salt content) requires the features of both of the approaches mentioned above. Under these conditions the amount of liquid water can be so small that vapor and hydrated minerals becomes important for the water balance. Wissmeier and Barry (2008) developed a code that can model the effect of chemical sink-sources of water onr liquid flow, but only for cases where transport is limited to unsaturated liquid phase. However, under these conditions gas transport

can also be important and water activity, which controls vapor pressure, is affected by capillarity and salinity. Moreover, certain mineral paragenesis (the ones that produce invariant points) fix water activity, causing the geochemistry to control vapor pressure, which is a key flow variable (Risacher and Clement, 2001). Thus, a fully coupled solution of phase fluxes and reactive transport is required.

The main objective of this thesis is to develop a general multiphase reactive transport code capable of representing the influence of geochemistry over flux and transport processes for concentrated solutions under extreme dry conditions. As a secondary objective the behavior of some cases under these conditions is studied.

1.2. Thesis outline

Different aspects of the code which and different cases are studied through the chapters of this thesis.

In chapter 2 the effects of salinity on water activity and its influence on evaporation are discussed, and a method for computing the evolution of high salinity systems, like shallow salt lakes, is presented. Special emphasis is placed on the assessment of invariant points, where activity is controlled by the set of precipitated minerals. The method is applied to a natural $MgSO_4$-rich brine evaporation experiment and to a simplified model of a perennial saline playa lake.

In chapter 3 the evolution of concentrated solution in porous media is discussed. In this scenario evaporation is affected besides salinity by capillarity, and also transport processes have to be considered. A generalized compositional formulation for MPRT which considers coupling effects between geochemical and hydrodynamic process problems is introduced. Some aspects related to its numerical solution are discussed. The advantages of the formulation are illustrated by simulating the effect of mineral dehydration on the hydrodynamic processes in an unsaturated gypsum column that reaches extremely dry conditions.

In chapter 4 PROOST the code in which the formulation presented in chapter 3 was implemented is presented. This chapter discusses the importance of flexibility for reactive transport codes and the way how object oriented programming can facilitate this feature. It

presents the structure of Proost through classes and their interaction. The code is used to model a laboratory experiment of a sand column saturated in a MgSO4 solution subjected to evaporation. In this experiment extreme dry conditions and high salinity content are reached, and the interaction between hydrodynamic and geochemical process on the model are analyzed.

In chapter 5 main contributions of this thesis are summarized.

Chapter 2 is based on a submitted paper, and chapter 3 and 4 are based on papers in preparation.

In appendix I details about component matrix calculations are given. In appendix II code verification results are presented. Appendix III contains examples of PROOST input files.

2. Modeling the interaction between evaporation and chemical composition in a natural saline system[1]

2.1. Introduction

Natural saline systems occur broadly worldwide. They may be of significant hydrological, economic and ecological importance. Playas, sabkhas and saline lakes affect water resource assessments (Yechieli and Wood, 2002). They often represent the discharge point of regional water flow systems. These can significantly affect ground-water quality and flow due to high concentrations and density differences (Simmons and Narayan, 1998, Holzbecher, 2005). Evaporation is the critical process to understand the evolution of these natural systems. Evaporation also plays a leading role in the production of industrial salt (halite, magnesium, sodium sulphate, potassium chloride). Nearly all forms of salt production require evaporation of water to concentrate brine and ultimately produce salt crystals (Akridge, 2008). Evaporation is also a key process to understand the formation of evaporitic deposits (Jankowski and Jacobson, 1989,Donovan and Rose, 1994), and plays a main role in the formation of water-soluble efflorescent salts on tailings in arid climates (Acero et al., 2009). Such salts may increase the risk of human exposure to heavy metals such as Cu, Ni, and Zn through wind transport (Dold, 2006; Bea et al., 2010b). Understanding evaporation mechanisms in the formation of these salts is crucial for the design of remediation measures.

Ever since Dalton (1802), evaporation has been seen as a balance between vaporization and condensation. The latter depends on the quantity and energy of water molecules in the gas phase, which can be evaluated as proportional to vapor pressure, pv_{air}. Vaporization depends on the energy of liquid molecules to overcome the surface barrier. In hydrology, vaporization has been traditionally taken as proportional to the saturation vapor pressure, pv_{sat}, which is the one in equilibrium with a flat surface of pure water. Notice that pv_{sat} needs to be evaluated at water temperature, to measure indeed the energy of liquid water. This energy can be

[1] This chapter is based on the article with the same name submitted to the Journal of Hydrology. Bea, S.A., Saaltink, M.W., Carrera, J. and Ayora, C. are coauthors of this article.

significantly reduced as the free vibration of water molecules is impaired either because they tend to form solvatation spheres around solute ions or because water is under suction. That is both salinity and suction can reduce the energy of water (Jury and Horton, 2004). This reduction is quantified by water activity, a_w. Water activity is defined as the ratio between vapor pressure in equilibrium with the solution and the saturation vapor pressure. It can also be seen as an indicator about the "chemical availability of water" to react with other species or to evaporate. Because of this reduction, Dalton's law should read:

$$Ev = f_w \left(pv_{sat} \cdot a_w - pv_{air} \right) \tag{2-1}$$

Where Ev is the evaporation rate and f_w is a mass transfer coefficient that depends on weather conditions.

The activity of fresh water bodies can be considered constant and equal to one. Therefore chemical composition hardly influences the evaporation. However, in concentrated solutions, water activity decreases as salinity increases, thus affecting the evaporation rate and the chemical evolution of the system (Krumgalz et al., 2000).

The chemical evolution of brines under evaporation has been extensively studied (Hardie and Eugster, 1980, Eugster et al., 1980, Sanford and Wood, 1991, Wood and Sanford, 1990, and Yan et al., 2002). However, most of these works seek geochemical understanding. They typically take evaporation as given and do not pursue understanding evaporation dynamics. Ironically, geochemistry may exert a key control on evaporation rate. Hydrated minerals, as many efflorescent salts, can act as a water source or sink as they dissolve or precipitate, and can literally control water activity. To illustrate this effect, let us consider the coexistence in equilibrium of gypsum and anhydrite, which implies,

$$\begin{aligned} \left(Ca^{2+}\right)\left(SO_4^{2-}\right) a_w^2 &= K_{gypsum} \\ \left(Ca^{2+}\right)\left(SO_4^{2-}\right) &= K_{anhydrite} \end{aligned} \Rightarrow a_w = \sqrt{\frac{K_{gypsum}}{K_{anhydrite}}} \tag{2-2}$$

That is, the simultaneous presence of these minerals fixes water activity, thus controlling evaporation. This situation is termed invariant point and may exert a significant influence on the evolution of the system. In fact, if evaporation is the only mass exchange mechanism not only water activity will be fixed, but also all species activity. Dealing with invariant points involves mathematical modeling difficulties, to the point that they are normally ignored. Risacher and Clement (2001) discuss these difficulties and developed an algorithm to deal with them. Unfortunately, the method is rather involved.

The effect of invariant points on evaporation is strongly related to the liquid water source-sink that results from hydrated mineral dissolution-precipitation. This process is not always considered in saline lakes water balance and only a few works discuss it (e.g. Krumgalz et al., 2000, Sánchez-Moral et al., 2002).

In this work we study the influence of chemical reactions on the dynamics of brine evaporation through numerical simulation, with special focus on the treatment of invariant points. First we present a mathematical formulation that overcomes the difficulties of modeling invariant points of previous works. Then we apply the proposed formulation to simulate an experiment where a brine rich in SO_4^{2-} and Mg^{2+} is evaporated in a climatic chamber. Finally, we study by means of a simple model the interaction between mineral paragenesis and evaporation in a perennial saline playa lake with a seasonably varying air vapor pressure.

2.2. Proposed numerical formulation for brine evolution under evaporation.

Modeling the chemical evolution of brines during evaporation involves species mass balance, mass action law and energy balance. Energy balance controls temperature changes that can affect equilibrium constant and activity coefficient calculations. For simplicity, we will adopt isothermal conditions. However, energy balance could be added without significant changes on invariant points.

2.2.1. Governing equations

Two groups of equations need to be solved: mass balance and mass action equations. The latter can be written in a matrix notation (Saaltink et al., 1998) as:

$$\mathbf{S_e} \cdot \log \mathbf{a} - \log \mathbf{K} = 0 \tag{2-3}$$

where $\mathbf{S_e}$ is the stoichiometric matrix of size Ne (number of equilibrium reactions) x Ns (number of species), $\mathbf{a}$ is a vector with the activity of all (Ns) species and $\mathbf{K}$ is a vector with the equilibrium constants of all (Ne) reactions.

Mass balance equations can also be written in matrix form:

$$\frac{\Delta(\eta \mathbf{m})}{\Delta t} = \mathbf{f} + \eta \mathbf{S}_e^t \cdot \mathbf{r}_e \tag{2-4}$$

where η $\left[kg_{water}\right]$ is the mass of liquid water in the system, $\mathbf{m}$ $\left[mol/kg_{water}\right]$ is a vector with the molality of all chemical species, $\mathbf{f}$ $\left[mol/time\right]$ is a vector with external source-sink terms for each species (only affects water in case of evaporation), $\mathbf{S}_e^t$ is the transpose of the stoichiometric matrix, and $\mathbf{r}_e$ $\left[mol/time\right]$ is a vector containing the reaction rates of equilibrium reactions. Assuming **f** given, the system (2-3) and (2-4) contains Ne+Ns equations and unknowns (the molality of water is fixed, 55.6 mol water/kg water, but η is unknown).

For a better understanding of these vectors and matrices, we illustrate them by means of the following geochemical system:

$$H_2O \rightleftarrows H^+ + OH^- \qquad \text{(2-5)a}$$

$$Ca^{2+} + SO_4^{2-} + 2H_2O \rightleftarrows gypsum \qquad \text{(2-5)b}$$

$$Ca^{2+} + SO_4^{2-} \rightleftarrows anhydrite \qquad \text{(2-5)c}$$

The vector of concentration, sink source terms, reaction rates and stoichiometric matrix will be:

$$\mathbf{m} = \begin{pmatrix} m_{H_2O} \\ m_{H^+} \\ m_{SO_4^{2-}} \\ m_{Ca^{2+}} \\ m_{OH^-} \\ m_{gypsum} \\ m_{anhydrite} \end{pmatrix}; \mathbf{f} = \begin{pmatrix} f_{H_2O} \\ 0 \\ 0 \\ 0 \\ 0 \\ 0 \\ 0 \end{pmatrix}; \mathbf{r_e} = \begin{pmatrix} r_{H_2O} \\ r_{gypsum} \\ r_{anhydrite} \end{pmatrix}; S_e^t = \begin{bmatrix} -1 & -2 & 0 \\ 1 & 0 & 0 \\ 0 & -1 & -1 \\ 0 & -1 & -1 \\ 1 & 0 & 0 \\ 0 & 1 & 0 \\ 0 & 0 & 1 \end{bmatrix} \qquad \text{(2-6)}$$

Where we have assumed that f_{H_2O} is the only sink source term ($-f_{H_2O}$ is evaporation rate).

Notice that the columns of S_e^t represent the stoichiometry of (2-5).

2.2.2. Step 1 - Component definition

The equilibrium reaction rate terms in (2-4) can be eliminated by linearly combining the mass balance equations (Saaltink et al., 1998). To do so, we define the matrix $\mathbf{U}$ (also known as component matrix, (Ns-Ne)xNs) as:

$$\mathbf{U} \cdot \mathbf{S}_e^t = 0 \qquad \text{(2-7)}$$

Multiplying equation (2-4) times $\mathbf{U}$ ensures elimination of all equilibrium reaction rates. It also leads to the definition of components as $\mathbf{u} = \mathbf{U} \cdot \mathbf{m}$, which by virtue of (2-7) become linear combinations of species that are not affected by equilibrium reactions.

2.2.3. Step 2 – Component mass balance

Multiplying system (2-4) by $\mathbf{U}$ yields:

$$\frac{\Delta(\eta \mathbf{u})}{\Delta t} = \mathbf{U} \cdot \mathbf{f} \tag{2-8}$$

When mineral phases are present in equilibrium, Gibbs phase rule indicates that the system looses one degree of freedom for every additional mineral phase. Therefore the definition of components needs to be updated. There are several ways to achieve this goal, depending on the additional properties one may wish for components (see Molins et al., 2004). Here we will use the approach of Saaltink et al. (1998), where the initial components matrix **U** is multiplied by an elimination matrix to obtain the reduced component matrix. Matrix **U** and matrices **E** are given in Table 1 for cases where the system is in equilibrium with gypsum ($\mathbf{E}_{gyp}$) or with gypsum and anhydrite.

Multiplying equation (2-8)by $\mathbf{E}$ does indeed reduce the number of component mass balances:

$$\frac{\Delta(\eta \mathbf{u}')}{\Delta t} = \mathbf{f}' \tag{2-9}$$

Where $\mathbf{u}' = \mathbf{E} \cdot \mathbf{U} \cdot \mathbf{m}$ is the reduced component vector and $\mathbf{f}' = \mathbf{E} \cdot \mathbf{U} \cdot \mathbf{f}$ is the reduced component sink source

Table 2-1 – Different Matrices for the geochemical system of the example

Matrix $\mathbf{U}$

	H_2O	H^+	SO_4^{2-}	Ca^{2+}	OH^-	gyp	anh
u_{H_2O}	1	0	0	0	1	2	0
u_H	0	1	0	0	–1	0	0
u_{SO_4}	0	0	1	0	0	1	1
u_{Ca}	0	0	0	1	0	1	1

Matrix $\mathbf{E}_{gyp}$ (gypsum saturated)

	u_W	u_H	u_{SO_4}	u_{Ca}
u_{H_2O}	1	0	0	0
u_H	0	1	0	0
u_{SO_4-Ca}	0	0	1	–1

Matrix $\mathbf{E}_{gyp-anh}$ (gypsum and anhydrite saturated)

	u_W	u_H	u_{SO_4}	u_{Ca}
u_{SO_4-Ca}	0	0	1	–1
u_H	0	1	0	0

The basic system (no minerals in equilibrium) in the gypsum-anhydrite example is obtained by multiplying mass balance equation (2-4) times $\mathbf{U}$ (Table 2-1), which yields:

$$\frac{\Delta(\eta\mathbf{u})}{\Delta t}=\frac{\Delta}{\Delta t}\left(\eta\begin{pmatrix} m_{H_2O}+m_{OH^-}+2m_{gypsum} \\ m_{H^+}-m_{OH^-} \\ m_{SO_4^{2-}}+m_{anhydrite}+m_{gypsum} \\ m_{Ca^{2+}}+m_{anhydrite}+m_{gypsum}\end{pmatrix}\right)=\begin{pmatrix} f_{H_2O} \\ 0 \\ 0 \\ 0\end{pmatrix} \tag{2-10}$$

Where components **u** are defined implicitly as total water (u_{H_2O}), acidity (u_H), sulphate (u_{So_4}) and calcium (u_{Ca}). In general, mineral concentrations in equation (2-10) are zero, when the system is sub saturated with respect to minerals. If mineral equilibrium is assumed this equation needs to be multiplied times the corresponding E matrix in Table 1. Specifically, when the system is saturated in gypsum we multiply equation (2-10) times $\mathbf{E}_{gyp}$ (Table 2-1) which eliminates anhydrite

$$\frac{\Delta}{\Delta t}\left(\eta\mathbf{u}_{gyp}\right)=\frac{\Delta}{\Delta t}\left(\eta\begin{pmatrix} m_{H_2O}+m_{OH^-} \\ m_{H^+}-m_{OH^-} \\ m_{SO_4^{2-}}-m_{Ca^{2+}}\end{pmatrix}\right)=\begin{pmatrix} f_{H_2O} \\ 0 \\ 0\end{pmatrix} \tag{2-11}$$

Where sulphate and calcium components have been substituted, $u_{So_4-Ca}=u_{So_4}-u_{Ca}$.

On the other hand, if the system is saturated in both minerals, we multiply equation (2-10) times $\mathbf{E}_{gyp-anhy}$ (Table 2-1) giving:

$$\Delta\left(\eta\mathbf{u}_{gyp-anh}\right)\frac{1}{\Delta t}=\Delta\left(\eta\begin{pmatrix} m_{SO_4^{2-}}-m_{Ca^{2+}} \\ m_{H^+}-m_{OH^-}\end{pmatrix}\right)\frac{1}{\Delta t}=\begin{pmatrix}0\\0\end{pmatrix} \tag{2-12}$$

Where the water component has been eliminated, which explains why the liquid water source-sink term f_{H_2O} has disappeared. As a result, evaporation does not affect the evolution of the system, when the two minerals are in equilibrium. This holds for any invariant point and will be exhaustively discussed in section 2.2.5

2.2.4. Step 3 – Defining solution variables, speciation

According to Gibbs phase rule, for fixed pressure and temperature, the number of independent intensive variables is:

$$N_{iiv}=N_s-N_e-N_{phases} \tag{2-13}$$

For a complete description of the system the mass of each phase is also required. Mineral masses can be eliminated from component mass balance multiplying by matrix $\mathbf{E}$, but liquid

water mass η still remains (see equations (2-11)and (2-12)). As unknowns, we choose liquid water mass and the concentrations of a subset of species, which are termed primary.

In the above example, one set of primary species for system (2-10) (no mineral phases) could be: H^+, SO_4^{2-}, Ca^{2+}. If the system is saturated in gypsum (2-11)one set of primary species could be: H^+, SO_4^{2-}. Finally, only one primary specie (H^+) is needed when both minerals are present (2-12). The remaining aqueous species, secondary species, are obtained by solving mass action equations (2-3).

We treat mineral species as ideal, so that their activity value is one. Therefore, their masses do not affect chemical speciation. They are obtained from mass balance. Reaction rates are first calculated from the mass balance of aqueous species. These rates are introduced in the mineral mass balances to update mineral mass during each time step.

Evaporation of a liquid sample can be seen as a loss of liquid water. Without any chemical reaction, $\eta\mathbf{m}$ remains constant (except for the liquid water specie). Therefore a reduction of η has to be compensated by an increase in the molality of most species. Equilibrium reactions may force a decrease in some species, to maintain the equilibrium constraints. This leads to what is known as geochemical divide (Hardie and Eugster, 1980, Risacher et al., 2003). An example is provided by the acidity component ($u_H = m_H - m_{OH}$) in Equation(2-10). Evaporation causes u_H to increase in absolute value, so that pH will tend to increase if initially above 7 or to drop, otherwise. As salinity increases, minerals become saturated and new divides emerge. For example, when gypsum starts precipitating, Equation (2-11) becomes active and $\eta\left(m_{SO_4} - m_{Ca}\right)$ must remain constant. Therefore, $\left|m_{SO_4} - m_{Ca}\right|$ must increase to compensate evaporation (decrease in η). Together with $(SO_4)(Ca)\cdot a_w^2 = K_{gyp}$, this implies that the most concentrated of these two species will become enriched and the other will tend to zero. The problem arises when Equation (2-12) becomes active and evaporation rate disappears. This situation is addressed below.

2.2.5. The Invariant point during evaporation: an avoidable difficulty

Invariant points occur when mineral paragenesis fixes water activity, as given by Eq. (2-2) in the example of gypsum and anhydrite. In that case gypsum is transformed into anhydrite releasing

exactly the liquid water that has evaporated, so that molalities of all species molalities remain constant.

To the best of our knowledge, the only code that can handle invariant points without minimizing Gibss free energy is EQL/EVP (Risacher and Clement, 2001) .This code devotes a significant effort to detect mineral paragenesis that fixes water activity and adopts a special treatment for this scenario, because one mineral mass action law is a linear combination of the others, as illustrated by equation (2-2). Actually, this is true only if water activity is imposed and not calculated. Alternatively, if water activity is computed from species concentrations, then the mass action laws for gypsum and anhydrite are no longer identical. Calculations will naturally yield the value of a_W equation (2-2).In short, the concept proposed here is just to treat liquid water as a secondary species.

When the gypsum-anhydrite invariant point is reached, the reduced component mass balance (Eq.(2-12)) does not include either liquid water or its sink, which are naturally removed from the equation. The solution of equation (2-12) is trivial. The mass of liquid water and the component concentrations do not change. As a result species concentration values remain constant. As discussed before, reaction rates are derived from the mass balance (Eq. (2-4)), which reads:

$$\begin{pmatrix} 0 \\ 0 \\ 0 \\ 0 \\ 0 \\ \Delta\left(\eta m_{gyp}\right)/\Delta t \\ \Delta\left(\eta m_{anh}\right)/\Delta t \end{pmatrix} = \begin{pmatrix} f_{H_2O} \\ 0 \\ 0 \\ 0 \\ 0 \\ 0 \\ 0 \end{pmatrix} + \eta \begin{pmatrix} -r_{H_2O} - 2r_{gypsum} \\ r_{H_2O} \\ -r_{gypsum} - r_{anhydrite} \\ -r_{gypsum} - r_{anhydrite} \\ r_{H_2O} \\ r_{gypsum} \\ r_{anhydrite} \end{pmatrix} \tag{2-14}$$

The 2nd or 5th row yield $r_{H_2O} = 0$. This, together with the first row, yield $r_{gypsum} = f_{H_2O}/2$. The 3rd row yields $r_{gypsum} = -r_{anhydrite}$. Therefore, system (2-14) can be simplified to:

$$\frac{\Delta\left(m_{gyp}\right)}{\Delta t} = -\frac{\Delta\left(m_{anh}\right)}{\Delta t} = \frac{f_{H_2O}}{2\eta} \tag{2-15}$$

This equation makes it clear that the dissolution rate of gypsum equals the precipitation rate of anhydrite, which is exactly half of the evaporation rate. Thus, evaporated water solely comes from the water molecules released by gypsum as it transforms into anhydrite.

2.2.6. Step 4 – Numerical formulation implementation

This formulation has been implemented following the object oriented (OO) paradigm in a FORTRAN 95 code merging and expanding two existing OO frameworks PROOST (Slooten, 2008) and CHEPROO (Bea et al., 2009). PROOST is a general purpose hydrological modeling tool that can solve a large variety of conservation equations expressed as partial differential equations. It has been built and used to simulate flow and transport problems over large domains. For this implementation, the balance is local. Therefore, conservation is written as a set of ordinary differential equations and only a part of the framework functionality is used. CHEPROO is an OO tool specialized in geochemical processes. It can calculate the chemical composition of a geochemical system from component or primary species. For the calculations described here, the Pitzer model has been used as described by Bea et al. (2010a)

2.3. Numerical modeling of an evaporation experiment in a climatic chamber

2.3.1. Description of the experiment and modeling consideration

Sánchez-Moral et al., (2002) evaporated brine from Lake Quero (central Spain) in a climate chamber for 20 days. Liquid and mineral samples from the brine were analyzed during the experiment. Air temperature and relative humidity were controlled with a day-night cycle variation. We modeled the experiment assuming a constant temperature of 25 ºC and a relative humidity of 0.4. Equilibrium with atmospheric CO_2 was considered for the simulation. Initial water composition was set equal to the maximum dilution state of Quero Lake reported by Sánchez-Moral et al., (1998) (Table 2-2). The minerals considered by the model are listed in Table 2-3.

The evaporation rate was calculated using Dalton's equation (2-1) and the mass transfer coefficient was chosen to fit best the water activity with the one calculated by Sánchez-Moral et al. (2002) Figure 2-1 a). The simulation was carried out until no more water could evaporate from the system; when water activity value reached the value of relative humidity of 0,4 imposed in the chamber.

Table 2-2 – Initial composition of the evaporation experiment in a climate chamber. Concentration in meq/l

SO_4	Cl	Mg	Na	K	Ca	Alkalinity
939.6	1006.5	1348.4	568.2	12.9	4.2	17.9

Table 2-3 - List of the minerals, chemical formulas and equilibrium constants considered in this work and in Sanchez-Moral et al. (1998)

Mineral name	Mineral formula	log K 25ºC
Anhydrite	$CaSO_4$	-4.362
Bischofite	$MgCl_2{\cdot}6H_2O$	4.455
Bloedite	$Na_2Mg(SO_4)_2{\cdot}4H_2O$	-2.347
Calcite	$CaCO_3$	-8.406
Carnallite	$KMgCl_3{\cdot}6H_2O$	4.330
Dolomite	$CaMg(CO_3)_2$	-17.083
Epsomite	$MgSO_4{\cdot}7H_2O$	-1.881
Glauberite	$Na_2Ca(SO_4)_2$	-5.254
Gypsum	$CaSO_4{\cdot}2H_2O$	-4.581
Halite	NaCl	1.570
Hexahydrite	$MgSO_4{\cdot}6H_2O$	-1.635
Kainite	$KMgClSO_4{\cdot}3H_2O$	-0.193
Kieserite	$MgSO_4{\cdot}H_2O$	-0.123
Magnesite	$MgCO_3$	-7.834
Pentahydrite	$MgSO_4{\cdot}5H_2O$	-1.285
Polyhalite	$K_2Ca_2Mg(SO_4)_4{\cdot}2H_2O$	-13.744

2.3.2. Water activity and mineral evolution

Water activity values given by Sanchez-Moral et al. (Figure 2-1 a) show a clear plateau around day 16. Another one is suggested around day 14 though less clearly. The model can help to interpret the experimental results. Three water activity plateaus are predicted by the model; one around day 16 which correspond to the one observed, a brief one between day 17 and 18, and the last one from day 19 till 24. No plateau is predicted around day 14.

Constant water activity periods may appear under two possible scenarios. The first one corresponds to “invariant” points. As discussed earlier, the mineral paragenesis imposes water activity and evaporation comes from mineral dissolution, which ensures that the amount of liquid water, its activity and the molality of all aqueous species remain constant (hence the name “invariant”). Mineral paragenesies that fixes water activity found in the example are summarized in Table 2-4. The first one is so brief that can hardly be distinguished in Figure 2-1 a).

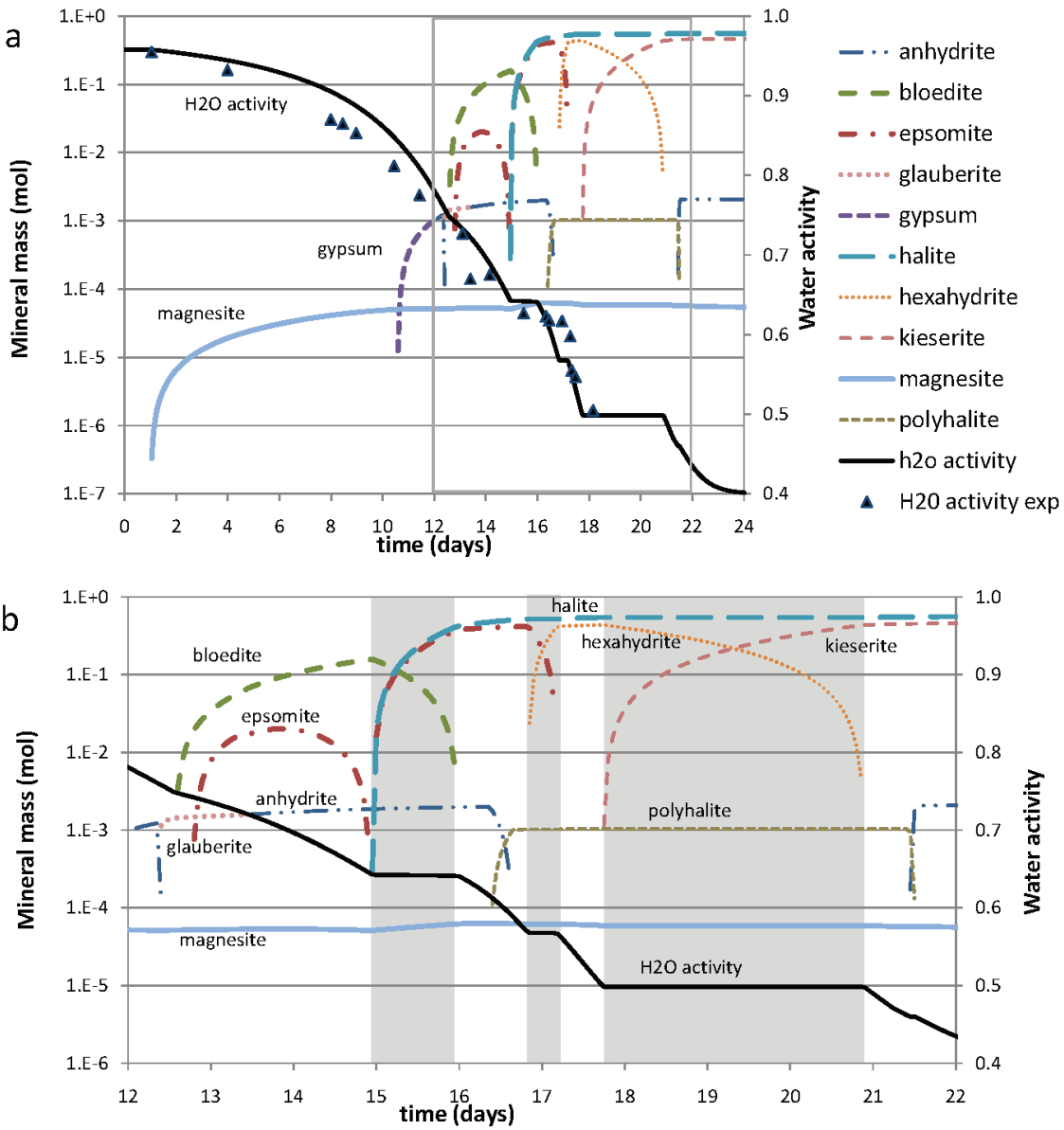

Figure 2-1 – a) Evolution of modeled water activity, mineral mass and experimental water activity. b) Detail of modeled water activity and mineral mass form day 12 to 22. Water activity plateaus can be appreciated between days 15 and 16, around day 17, and between day 18 and 21

Table 2-4 – Mineral paragenesies of invariant points with their value of fixed water activity obtained on the simulation.

Mineral paragenesis	water activity
Gypsum-Anhydrite	0.78
Epsomite-Hexahydrite	0.57
Hexahydrite-Kieserite	0.50

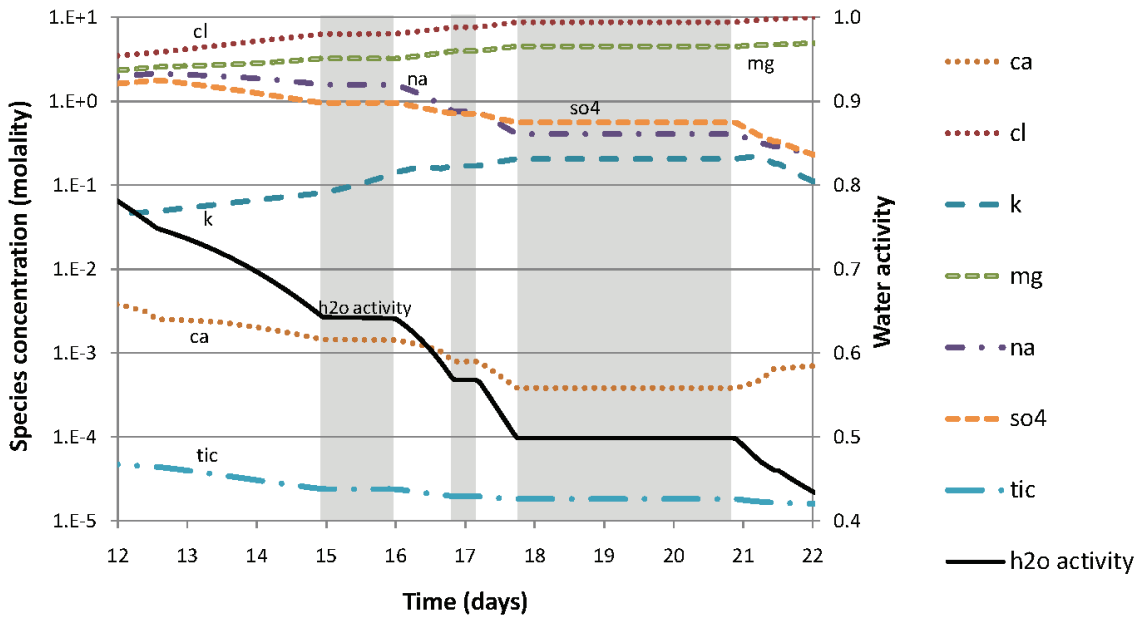

Figure 2-2 – water activity and aqueous concentrations form day 12 to 22. Note that during the first water activity plateau concentrations are almost constant, and are exactly constant during the second and third.

The other scenario in which water activity remains constant is when the number of minerals coexisting is the maximum allowed by Gibbs phase rule. The system has only one degree of freedom, which is the liquid water mass. When all these minerals are precipitating simultaneously this invariant point is known as "eutectic point". If there is mineral dissolution and precipitation the invariant point is called "peritectic point".

The first plateau (between day 15 and 16) is neither of the above, but can be considered as a "quasi-peritectic point". No significant changes occur on species concentrations except for K (see Figure 2-2). Moreover, the amount of liquid water is reduced significantly (Figure 2-3). Mineral paragenesis (Bloedite, Epsomite, Halite, Magnesite and Anhydrite) and equilibrium with atmospheric CO_2 reduces the degrees of freedom of the system to 3 (η, m_K, and m_{Cl}). Epsomite and halite precipitate during this period. So chemical divides would cause an increase of Cl and Mg and a decrease of SO_4 and Na. As it turns out, bloedite is dissolved during this period. Bloedite dissolution releases twice SO_4 and Na as Mg, and no Cl, which tends to compensate the effect of epsomite and halite precipitation. This mechanism explains why the concentration of most concentrated species remains nearly constant, so that changes on water activity are small.

The 2nd and 3rd plateaus are due to "invariant points" from magnesium sulfate minerals. All aqueous species concentrations and mineral mass, except for epsomite and hexaydrite, are fixed

between day 17 and 18 (Figure 2-1 and Figure 2-2). During this invariant point evaporation water came from the dissolution of epsomite and precipitation of hexaydrite.

$$MgSO_4 \cdot 7H_2O \rightarrow MgSO_4 \cdot 6H_2O + H_2O \quad (2\text{-}16)$$

The last "invariant point" occurs during dissolution of hexaydrite which supplies evaporation water and precipitation of kieserite

$$MgSO_4 \cdot 6H_2O \rightarrow MgSO_4 \cdot H_2O + 5H_2O \quad (2\text{-}17)$$

A gypsum-anhydrite invariant point occurs around day 12, but can hardly be seen in (Figure 2-1) because the mass of gypsum in the system is very small.

2.3.3. Water distribution

The evolution of the distribution of water in mineral and liquid forms is plotted in Figure 2-3. Until day 12, all water is liquid was and its loss is due to evaporation. Thereafter, hydrated minerals begin to precipitate. From day 12 to 17 almost 20% of the remaining liquid water precipitates as mineral and 60% evaporates. In fact, between days 15 and 16, more liquid water is lost to hydration than to evaporation (Figure 2-3 and Figure 2-4). This causes a sudden decrease in available liquid water with little change in water activity (first water activity plateau, called "quasi-peritectic"). As a result, the amount of mineral water is comparable to the amount of liquid water by day 17. The opposite behavior takes place during the following water activity plateaus, which are invariant points, so that liquid water mass does not change and mineral water release rate is maximum.

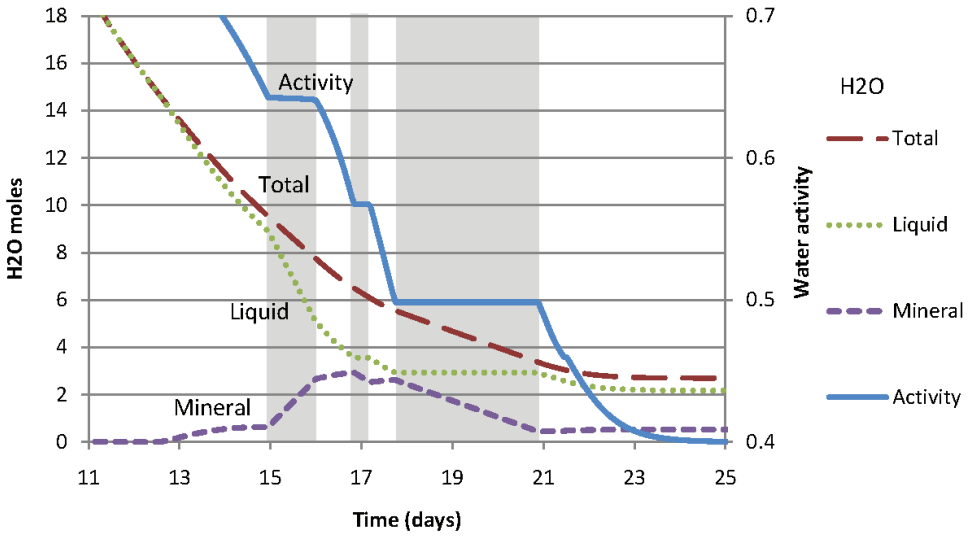

Figure 2-3 – Distribution of water in the system and water activity

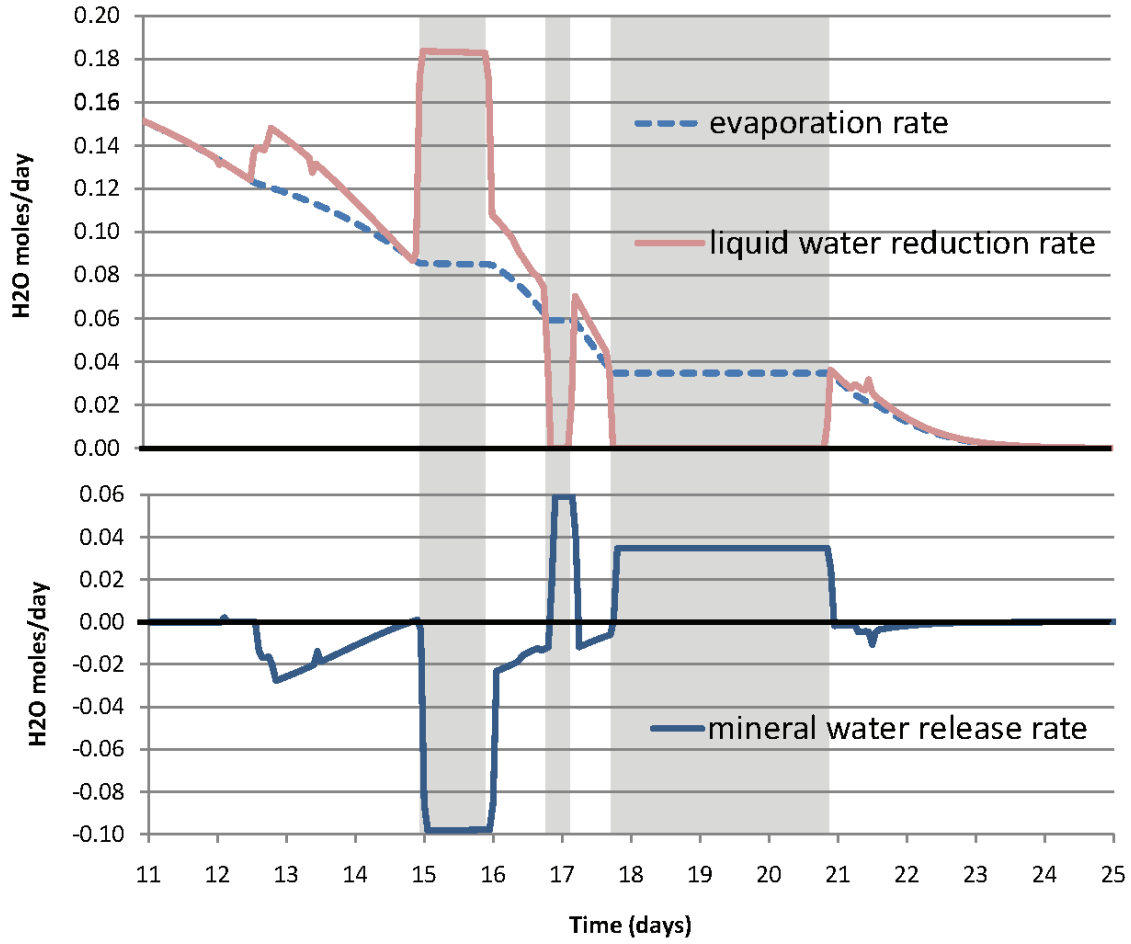

Figure 2-4 – Water consumption rates from evaporation and liquid water reduction (above) and from mineral release (below). Note that on day 17 and between 18 and 21 the evaporation rate is equal to the mineral release rate, while the amount of liquid water remains invariant. Note also that more liquid water is lost to mineral hydration than to evaporation in day 15.

2.4. Mineral paragenesis as a control mechanism of salt lake evolution

2.4.1. Conceptual model

The results of the previous section suggest that mineral paragenesis may control water activity and, thus, evaporation rate in shallow salt lakes, which can be assumed well mixed and in equilibrium with soluble minerals. This section is devoted to exploring such conjecture. To this end, we consider a well mixed lake, similar to the one of Wood and Sandford (1990), and Sandford and Wood (1991), except that outflow is proportional to water level and evaporation occurs according to Dalton's law with a periodic variation of atmospheric vapor pressure. Assuming constant water activity, density and surface, the water mass balance can be written as:

$$\frac{\partial h}{\partial t} = q_{in} - \alpha h - r_w - f_w\left(pv_{sat}a_w - pv_{air,amp}\sin\left(2\pi/P\, t\right) - pv_{air,mean}\right) \qquad (2\text{-}18)$$

where h [m] is the lake level, q_{in} [m/year] is the influx, α [years-1] is out flux coefficient, and r_w [m/year] is the mineral source sink term. f_w [m/Pa/years] is the mass transfer coefficient, a_w is he water activity, P is the time period and $pv_{air,amp}$ and $pv_{air,mean}$ [Pa] are, respectively, amplitude and mean value of atmospheric vapor pressure. The solution to this equation is.

$$h(t) = h_0^{'}e^{-\alpha t} + h_{mean} + h_{amp}\sin\left(\frac{2\pi t}{P} - \psi\right) \qquad (2\text{-}19)$$

Where $h_{mean} = \left(q_{in} - r_w - f_w\left(pv_{sat}a_w - pv_{air,mean}\right)\right)/\alpha$, $h_{amp} = f_w pv_{air,amp}\Big/\sqrt{\left(2\pi/P\right)^2 + \alpha^2}$, $\psi = \cos^{-1}\left(\alpha\Big/\sqrt{\left(2\pi/P\right)^2 + \alpha^2}\right)$, $h_o^{'} = \left(h_o - h_{mean} + h_{amp}\sin\psi\right)$, and h_o is the initial water level.

The first term represents the perturbation of the initial condition with respect to the long term behavior, and turns negligible for $t >> \alpha^{-1}$. Thus, lake level is expected to reach a cyclical steady state, oscillating with constant amplitude around h_{mean} (see Figure 2-5).

The evolution of concentrations obeys:

$$\frac{\partial hc}{\partial t} = q_{in}c_{in} - \alpha hc - r_m \qquad (2\text{-}20)$$

where c_{in} is the incoming concentration, c is the lake concentration and r_{m} is mineral precipitation rate, taken here as constant. The solution of (2-20)is:

$$c(t) = \frac{\left(c_0 h_0 - \frac{q_{in}c_{in} + r_m}{\alpha}\right)e^{-\alpha t} + \frac{q_{in}c_{in} - r_m}{\alpha}}{h(t)} \qquad (2\text{-}21)$$

where c_0 is the initial concentration. Again, the first term turns negligible for $t >> \alpha^{-1}$.

Therefore, lake concentration will also reach a cyclical steady state (see Figure 2-5). The main point of Eq. (2-21) is that concentration only depends on the lake level, so that the total mass of salts in solution (hc) is constant. Therefore, the volume average of outflow concentration (that is the mean concentration of outflow, not the time average of concentration in the lake) is given by:

$$c_{mean} = \frac{q_{in}c_{in} - r_{\mathrm{m}}}{q_{in} - r_w - f_w\left(pv_{sat}a_w - pv_{air,mean}\right)} \qquad (2\text{-}22)$$

Note that c_{mean} does not depend on out flux coefficient α . This surprising result reflects the simplifications of the model. In reality, concentrations will be largely dependent of the presence of soluble salts, so that concentration fluctuations are buffered by r_m. To acknowledge the variability of r_m, we discuss below a more realistic geochemical model.

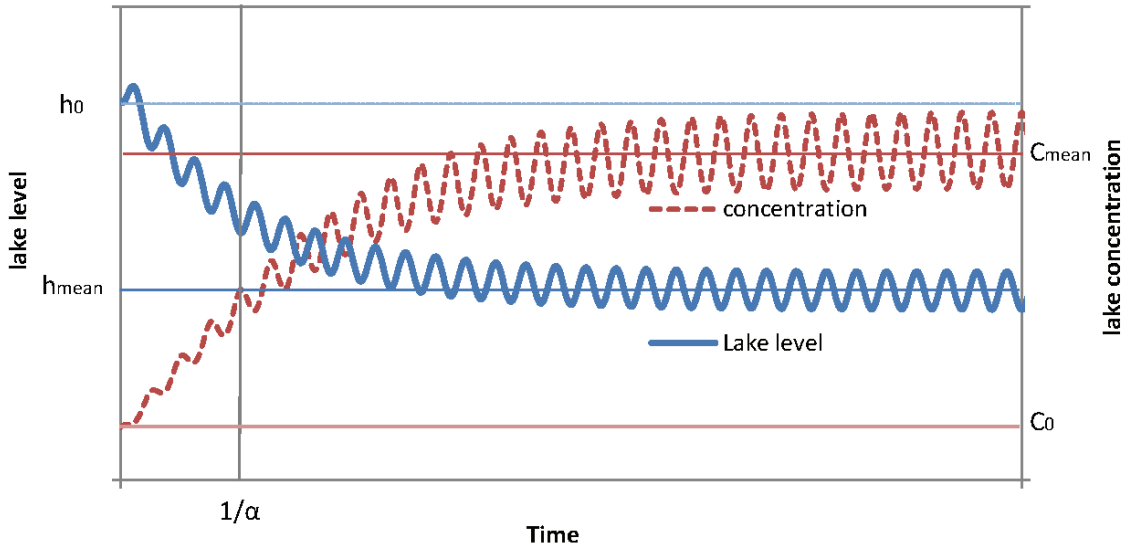

Figure 2-5 – Analytical solution for lake level and single specie concentration

2.4.2. Hydro-chemical model

The hydrological model of equation (2-18) is complemented with the geochemistry of section 2.3. Atmospheric relative humidity fluctuates between 0.45 and 0.55, around the hexahydrite-kieserite water activity (0.50). The mass transfer coefficient for Dalton's law, f_w , was set to 1.3 Kg/year/Pa/m^2 which correspond to a pan evaporation of 2000 Kg/year (typical value of semi-arid region, Weiß and Menzel, (2008)). A constant liquid density of 1300 kg/m^3 was used together with an influx, q_{in} of 58.5 Kg/year/m^2, and an out flux coefficient α of 0.01 year^{-1}. Sensitivity analyses to these parameters are discussed in the next section. Equilibrium with atmospheric CO_2 and a temperature of 25º C were used for the simulation.

The chemical system goes through an evaporation path similar to the one of the evaporation chamber and then, as suggested by the analytical solution, it reaches a cyclical steady state for both level and chemistry. Figure 2-6 illustrates several interesting points. First, as suggested by equation(2-21), water activity fluctuates quite like water level (water activity can be seen as the molar concentration of water in the liquid, so its variation is opposite to that of salinity). Second, as conjectured, water activity remains fixed due to the hexahydrite-kieserite invariant point for a

sizeable portion of time (around 50 %). Third, during this stage, the lake level remains constant despite of the incoming and outgoing fluxes. That is, mineral dissolution and precipitation suffice to offset inflow-outflow imbalances. Notice that, in this case, species concentrations need not be constant because contrary to the pure evaporation case, liquid inflow and outflows imply sink-source terms for all species. Still, these are small and barely affect water level.

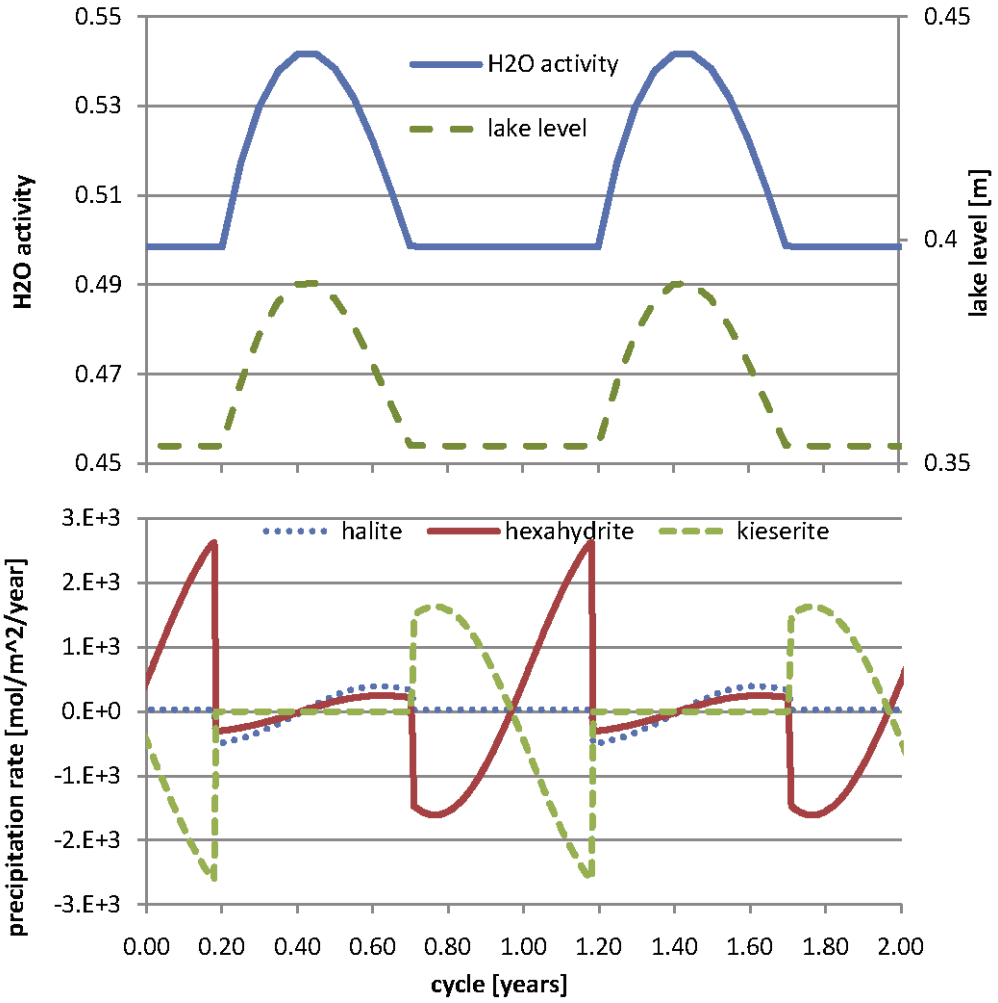

Figure 2-6 – Water activity, lake level and mineral precipitation. Note that during periods of fixed water activity the lake level remains practically constant. During this period hexahydrite and kieserite have the same precipitation rate value but with opposites sings, becoming a source or sink of water (see equation (2-17)).

The lake annual cycle can be divided into four different stages of approximately the same duration, 0.25 year. The point with maximum water activity value is considered as the beginning of the first stage. During the first stage (approximately between 0.4 and 0.7 year), water evaporates causing a little precipitation of hexahydrite and halite. Also water activity reduces due to an increase in solute concentration.

During the second stage (approximately between 0.7 and 1.0 year), hexahydrite dissolves and kieserite precipitates (reaction(2-17)). This reaction keeps water activity constant and provides

liquid water for evaporation. Actually, the water released by this reaction does not match evaporation as in the evaporation chamber case. In this case the released water matches evaporation plus outflow minus inflow.

The third and fourth stages reverse the second and first ones respectively. The third stage starts when net inflow of dilute water promotes kieserite dissolution and hexahydrite precipitation, still keeping water activity and lake level constant. The final stage starts when kieserite is exhausted. As the net inflow of diluted water still exceeds evaporation, the lake level and water activity increase.

The mean mass balance is shown in Table 5. Note that there is no net accumulation of kieserite. c_{mean}/c_{in} can be compared with the analytical results (2-22)

Table 2-5 – Lake mean values after reaching cyclical steady state

mean level [m]	H2O liquid [Kg/m^2]	C_{mean}/C_{in} (conservative)	H2O balance [Kg/year/m^2]			
			q in	q out	Evap	mineral
0.366	321	18.3	58.5	-3.2	-52.6	-2.7

mean precipitation rate [mol/year/m^2]				
Halite	hexahydrite	Polyhalite	magnesite	kieserite
31.740	25.365	0.061	0.004	0.000

2.4.3. Parameter sensitivity

We analyze here the dependence of the cyclical behavior of the system on influx value q_{in} and out flux coefficient α .

Sensitivity of incoming flux (q_{in})

The role of incoming flux is illustrated in Figure 2-7. A low influx implies a long portion of time on the hexahydrite-kieserite invariant point, and a low peak of water activity. Note that when the influx is increased to 292.6 Kg/y/m^2, water activity increases and reaches the epsomite-hexahydrite invariant point. This behavior is also reflected by the conservative concentration factor in

Table 2-6. However, while the water mass balance varies proportionally to the influx, the concentration factor changes little. That is, the lake accommodates to the presence of soluble salts.

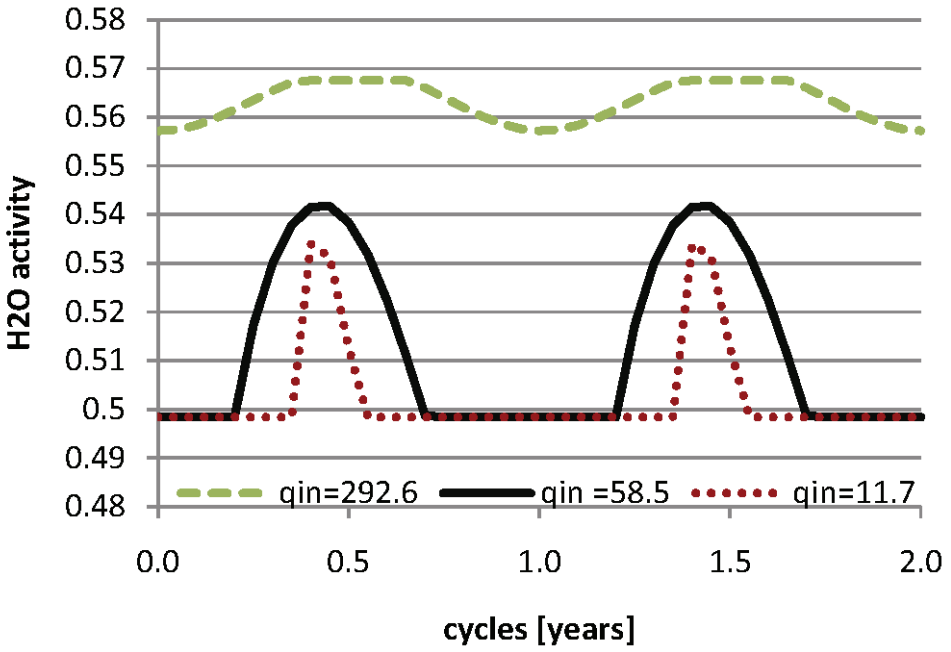

Figure 2-7 – Sensitivity of water activity to incoming flux (q_{in} [m/y]). For lower values the system reaches the hexaydrite-kiserite invariant point, and for the high value that of epsomite-hexahydrite

Table 2-6 - Lake mean values for different incoming flux after reaching cyclical steady state

qin [Kg/year/m^2]	Mean level [m]	C_{mean}/C_{in} (conservative)	Water balance [Kg/year/m^2]			
			q in	q out	evap	mineral
292.6	2.075	15.82	292.6	-18.5	-260.7	-13.3
58.5	0.365	18.31	58.5	-3.2	-52.6	-2.7
11.7	0.071	18.75	11.7	-0.6	-10.5	-0.6

Note also that the lake water activity can oscillate around the epsomite-hexahydrite invariant point with an activity of 0.57, despite the fact that relative humidity is varying between 0.45 and 0.55. This implies that the lake vapor partial pressure is never in equilibrium with the atmospheric vapor pressure. That is, it evaporates water continuously, which is what normal lakes do. The point is that, the system can stay on fixed water activity values outside the atmospheric relative humidity range.

Sensitivity of out flux coefficient (α)

In Figure 2-8 water activity is plotted for different out flux coefficient α. The water activity amplitude is sensitive to the out flux coefficient. For higher values of α the water activity amplitude increases. The analytical solution to h_{mean} (2-19) predicts a linearly inverse dependence of lake level with α, which fully agrees with the model results of Table 2-7. This effect of α on h_{mean} may be responsible for changes in the water activity amplitude. Small values

of h_{mean} mean smaller amount of water in the lake, so relative changes in lake water are larger for a given exchange with the outside. So changes in lake concentration and water activity will also be larger.

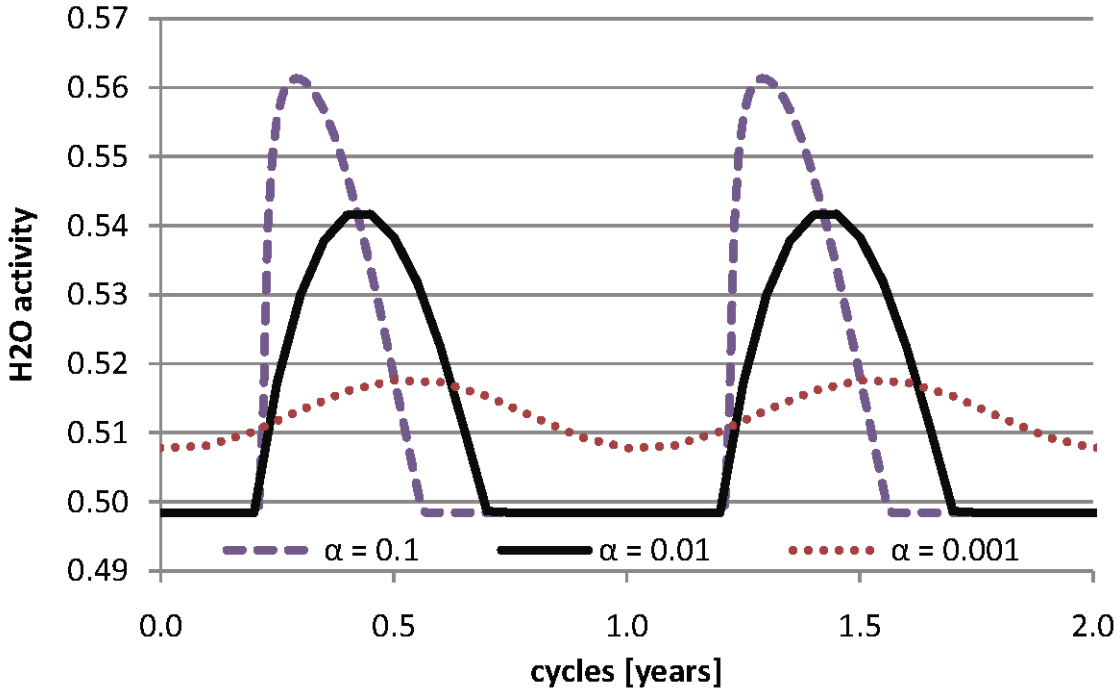

Figure 2-8 – Water activity sensitivity to out flux coefficient. For the α higher value water activity remains more time on hexahydrite-kiserite fixed value. For the lower out flux coefficient no fixed activity values are reached.

As the analytical solution suggest, α does not affect the conservative concentration factor C_{mean}/C_{in}(2-22). So water activity is expected to have similar mean values for different α values. In Table 2-7 it can be seen that mean water balance remains indifferent to α.

Table 2-7 - Lake mean values for different out flux coefficient after reaching cyclical steady state

α [year^{-1}]	mean level [m]	C_{mean}/C_{in} (conservative)	Water balance [Kg/year/m^2]			
			q in	q out	evap	Mineral
0.1	0.037	18.27	58.5	-3.2	-52.6	-2.7
0.01	0.365	18.31	58.5	-3.2	-52.6	-2.7
0.001	3.632	18.36	58.5	-3.2	-52.6	-2.7

So basically out flux coefficient α controls mean level of the lake and has no influence the mean chemistry. However, it does affect the amplitudes of the oscillation.

2.5. Conclusions

We have presented numerical formulation for modeling brine evaporation that can deal with invariant points naturally, without any special consideration. The key of this formulation is treating water activity as secondary variable, so that its value results from calculations and is never imposed. This lead to a much simpler algorithm than the one proposed by Risacher and Clement (2001).

The proposed formulation was used to simulate the evaporation experiment of Sánchez-Moral et al., (2002) in which a SO_4Mg rich natural brine was subject to evaporation. The model predicts one interval in which water activity remains almost constant ("quasi-peritectic point"), and two intervals in which water activity and the concentrations of all species remain constant; ("invariant points"). The two types of intervals are completely different regarding liquid water consumption by mineral phases, even though water activity remains fixed in both. During the "quasi-peritectic point" interval, liquid water decreases dramatically due to precipitation of hydrated minerals. On the other hand, during "invariant point" intervals liquid water remains constant, despite of evaporation. In fact, evaporation water comes from the dissolution of hydrated minerals. According to the model results, water activity was controlled by the mineral paragenesis for almost 20 % of the simulation time. This suggests that mineral paragenesis can have a considerable influence on shallow salt lake evolution by fixing chemical composition for a significant portion of time.

This conjecture was also tested by means of a simple model of a perennial saline playa lake. A simplified analytical solution was developed to illustrate the evolution of the proposed system. According to this solution, the system tends to a cyclical steady state for both lake level and chemical composition, where the total amount of salts in solution remains constant (salinity is inversely proportional to level). These results were approximately confirmed by the numerical model considering a complex geochemistry. Different simulations show that the lake can periodically remain at a fixed water activity. While water activity is fixed, lake level and chemical composition remain constant, despite of the evaporation and the incoming and outgoing fluxes. Fixed water activity paragenesis involves two or more minerals but, due to the periodicity of the system, not all these minerals need to accumulate. The relationship between lake level and outflow does not seem to affect annual balances, but it controls oscillations amplitudes. That is

the presence of minerals exerts a strong control on the lake behavior. The simulations suggest that natural systems, with similar characteristics to the one modeled, are prone to remain on fixed water activity values. The simulations also show that hydrated minerals can act as an important liquid water source and by controlling water activity it can affect the evolution of natural systems where evaporation is an important process.

3. A consistent compositional formulation for multiphase reactive transport where chemistry affects hydrodynamics.

3.1. Introduction

The most common approach for solving reactive transport problems is to decouple the equations involved. Usually one first calculates the flow of fluid phases, and optionally energy transport, and then equations for component conservation, including chemical reactions, are solved. A number of saturated and unsaturated reactive transport codes uses this decoupled procedure (Clement et al. 1998, Parkhurst et al. 2004, van der Lee 2003, Mayer 2002). Although the MIN3P code (Molins and Mayer 2007) couples gas flow and component conservation, it decouples the aqueous phase flow.

A similar approach is used by multiphase reactive transport codes, such as CODEBRIGHT-RETRASO (Saaltink et al., 2004), TOUGHREACT (Xu and Pruess 1998), and PFLOTRAN (Mills et al. 2007). These codes, instead of solving an explicit phase conservation equations, consider only as many components as mobile phases (normally two: water and air or CO2) and formulate a compositional formulation. This formulation eliminates the phase change terms, due to equilibrium heterogeneous reactions, which is convenient since there are no explicit expression for them. Thus, in a first step phase pressures and optionally temperature are calculated considering as many components as mobile phases. Then, in a second step, the conservation equations of all involved species are solved.

This approach has been successfully applied to a wide range of multiphase reactive transport problems, but it may be unsuitable for some cases, such as vadose tailings. In such scenarios considerable consumption of oxygen might occur due to pyrite and Fe oxidation. The effect of the oxygen consumption on the gaseous flow cannot be evaluated considering only a vapor-air gaseous phase. Thus chemical processes can act as an important phase sink-source term that is difficult to represent by means of a decoupled approach. None of the codes mentioned above simulates this effect. Another example is the chemical evolution of soils with a high salt content

under dry conditions. In such an environment it is possible that the amount of liquid water is so small that both vapor and hydrated minerals become significant for the water balance. Wissmeier and Barry (2008) developed a code capable of modeling the effect of chemical sink-sources of water on liquid flow, but only for cases where transport is limited to unsaturated liquid phase. However, under these conditions gas transport can also be important and water activity, which controls vapor pressure, is affected by capillary and salinity. Moreover, certain mineral paragenesis (the ones that produce invariant points) can fix water activity, causing the geochemistry to control vapor pressure, which is a key flow variable (Risacher and Clement, 2001). Thus, a fully coupled solution of phase fluxes and reactive transport is necessary to resolve certain problems.

Compositional formulations have been developed for a fixed number of components (Abriola and Pinder, 1985, Forsyth and Shao, 1991, Pruess et al. 1999, Olivella et al. 1996), and for a general number (Corapcioglu and Gaehr, 1987, Sleep and Sykes, 1993, Unger et al., 1995) including linear sorption (Adenekan et al., 1993) and linear decay (Pruess and Battistelli 2002). However, codes using compositional formulation do not include key processes for reactive transport, such as reactions between species of the same phase (e.g., complexation and hydrolysis), biochemical processes (among others Brun and Engesgaard 2002, Molinero and Samper 2006), complex adsorption models or equilibrium with several mineral phases. All these formulations define components as the sum of species related through equilibrium heterogeneous reactions. If homogeneous equilibrium reactions are also considered, compositional formulations can become more than a convenient alternative to phase conservation equations and be used to solve the entire problem.

The aim of this paper is to present a novel general compositional formulation capable of adequately representing cases where geochemical processes significantly affect fluid flow. This formulation considers all the necessary processes to solve complex chemical and biochemical multiphase reactive transport problems.

Below we present the proposed mathematical formulation. Then, we discuss a solution strategy and present its implementation. Finally, we illustrate the quality of this formulation by simulating the evolution of the evaporation of a gypsum column. In this case, extreme dry conditions and high salinity contents are reached, and the influence of geochemical processes on hydrodynamic processes can be appreciated.

Notation

a_i Activity of species i

$\mathbf{a}$ Vector of the activities of all species $\mathbf{a}(i) = a_i$

aq Sub index for the aqueous phase

$c_{i,\alpha}$ Moles of the species i belonging to a phase α per phase volume

$\mathbf{c}$ Vector of the concentration of all species $\mathbf{c}(i) = c_i$

$\mathbf{c}_{aqueous}$ Vector of the concentration of aqueous species

$\mathbf{c}_{gaseous}$ Vector of the concentration of gaseous species

$\mathbf{c}_{imm,va}$ Vector of the concentration of immobile species with variable activity

$\mathbf{c}_{imm,ca}$ Vector of the concentration of immobile species with constant activity

d_l, d_t Longitudinal and transversal dispersion coefficients

df Degrees of freedom of the system

$\mathrm{df}_{ph,rule}$ Gibbs's phase rule degrees of freedom

$\mathrm{df}_{ph,dist}$ Degrees of freedom due to phase distribution

$\mathbf{D}_{\alpha}^{diff}$ Diffusion coefficient of phase α

$\mathbf{D}^{disp}$ Dispersion coefficient for phase α

$$\mathbf{D}^{disp} = d_t |\mathbf{q}_\alpha| \mathbf{I} + (d_l - d_t) \frac{\mathbf{q}_\alpha \cdot \mathbf{q}_\alpha^{tr}}{|\mathbf{q}_\alpha|}$$

f_{cap} Correction factor for water activity due to capillary effects

f_i Source sink term for species i

$\mathbf{f}$ Vector of source-sink terms $\mathbf{f}(i) = f_i$

$\mathbf{f}'$ External component source-sink term $\mathbf{f}' = \mathbf{U} \cdot \mathbf{f}$

g Sub index for the gaseous phase

$\mathbf{g}$ Gravity vector

i Sub index indicating a species

$\mathbf{j}_{D_\alpha,i}$ Diffusive-dispersive flux of species i in phase α calculated by Fick's law:

$$\mathbf{j}_{D_\alpha,i} = -\left(\mathbf{D}_\alpha^{diff} \phi \theta_\alpha \tau + \mathbf{D}^{disp}\right) \cdot \nabla\left(c_{i,\alpha}\right)$$

$k_{r\alpha}$ Relative permeability for phase α

K_j Equilibrium constant of reaction j

$\mathbf{k}'$ Component source-sink term due to kinetic reactions $\mathbf{k}' = \mathbf{U} \cdot \mathbf{S}_\mathbf{k}^{\mathbf{tr}} \cdot \mathbf{r}_\mathbf{k}$

K_j Equilibrium constant of reaction j

$\mathbf{K}$ Intrinsic permeability

$L_\alpha(c_{i,\alpha})$ Transport operator, null for immobile phases, for mobile phases:

$$L_\alpha\left(c_{i,\alpha}\right) = -\nabla \cdot \left(c_{i,\alpha} \mathbf{q}_\alpha\right) - \nabla \cdot \left(\mathbf{j}_{D_\alpha,i}\right)$$

$\mathbf{L}(\ )$ Vector of transport operators

m_i Molality of aqueous species i

n_i Moles of species i

M_i Molecular weight of species i

Na Number of aqueous species

Nc Number of components

Nc' Number of reduced components $Nc' = Nc - Nca$

Nca Number of constant activity species

Ne Number of equilibrium reactions

Ng Number of gaseous species

Nk Number of kinetic reactions

Nms Number of mineral species in mineral phase s

Ns Number of species

$N_{\mathbf{xp}}$ Number of primary species

$N'_{\mathbf{xp}}$ Corrected number of reduced primary species

$N_{\mathbf{xs}}$ Number of secondary species

p_i Partial pressure of gaseous species i

p_α Pressure of phase α

$\mathbf{q}_\alpha$ Flow of phase α, calculated by Darcy's law:

$$\mathbf{q}_\alpha = -\frac{\mathbf{K} k_{r\alpha}}{\mu_\alpha} \left(\nabla p_\alpha - \rho_\alpha \mathbf{g}\right)$$

re_j Reaction rate of equilibrium reaction j

$\mathbf{r}_\mathbf{e}$ Vector of equilibrium reaction rates $\mathbf{r}_\mathbf{e}(j) = re_j$

rk_j Reaction rate of kinetic reaction j

$\mathbf{r}_\mathbf{k}$ Vector of kinetic reaction rates $\mathbf{r}_\mathbf{k}(j) = rk_j$

R Universal gas constant

$Se_{j,i}$ Stoichiometric coefficient of equilibrium reaction j for species i

$\mathbf{S}_\mathbf{e}^{\mathbf{tr}}$ Transpose of the equilibrium stoichiometric matrix $\mathbf{S}_\mathbf{e}^{\mathbf{tr}}(i,j) = Se_{j,i}$

$Sk_{j,i}$ Stoichiometric coefficient of kinetic reaction j for species i

$\mathbf{S}_{\mathbf{k}}^{\mathbf{tr}}$	Transpose of the kinetic stoichiometric matrix $\mathbf{S}_{\mathbf{k}}^{\mathbf{tr}}(i,j) = Sk_{j,i}$
T	temperature
$\mathbf{u}_{aq}$	Vector of aqueous component
$\mathbf{u}_{g}$	Vector of gaseous component
$\mathbf{u}_{imm,va}$	Vector of immobile components with variable activity
$\mathbf{U}$	Component matrix
V_g	Volume of the gaseous phase
x_i	Chemical concentration of species i
$\mathbf{x}$	Vector of chemical concentrations of all species $\mathbf{x}(i) = x_i$
Z_i	Compressibility factor of gaseous species i
α	Sub index indicating a phase
γ_i	Activity coefficient for aqueous species i ,or fugacity coefficient for gaseous
$\boldsymbol{\gamma}$	Vector of activity coefficient of all species $\boldsymbol{\gamma}(i) = \gamma_i$
θ_α	Volumetric fraction of phase α
μ_α	Viscosity of phase α
ρ_α	Density of phase α
τ	Tortuosity factor
ϕ	Porosity
χ_s^i	Molar fraction of mineral species i in the solid phase
ω_α^i	Mass fraction of species i in phase α

3.2. Governing equation

Modeling multiphase reactive transport involves global and local equations. Global equations comprise partial differential equations expressing conservation principles (mass, energy, momentum) and local equations include constitutive and thermodynamic expressions. All reactive transport codes, to our knowledge, consider one set of equations to represent phase conservation (from which flows are calculated) and another to represent components conservation. This and the fact that these equations are solved separately increase the difficulty of modeling coupled effects. In what follows we present a formulation which is based only on species conservation, and optionally energy conservation. Phases conservation are implicitly considered since they are equal to the sum of all species conservation that composes them.

3.2.1. Global equation

Mass conservation equations of species i belonging to phase α can be written as:

$$\frac{\partial}{\partial t}\left(\theta_\alpha c_{i,\alpha}\right) = L_\alpha\left(c_{i,\alpha}\right) + \sum_{j=1}^{Ne} Se_{j,i}\cdot re_j + \sum_{j=1}^{Nk} Sk_{j,i}\cdot rk_j + f_i \qquad (3\text{-}1)$$

Where θ_α is the phase volumetric content, $c_{i,\alpha}$ is the specie i concentration, $Se_{j,i}$ is the stoichiometric coefficient of the equilibrium reaction j for the specie i and re_j is the reaction rate of the equilibrium reaction j. $Sk_{j,i}$ and rk_j are analogous to $Se_{j,i}$ and re_j but for kinetic reactions. f_i is an external sink-source term, and $L_\alpha(\ )$ is the mobile phase transport operator

that consider advective and diffusive-dispersive processes $L_\alpha\left(c_{i,\alpha}\right)=-\nabla\cdot\left(c_{i,\alpha}\mathbf{q}_\alpha\right)-\nabla\cdot\left(\mathbf{j}_{D_\alpha,i}\right)$. Mobile phases flow $\mathbf{q}_\alpha$ are calculated according to Darcy's law and diffusive-dispersive fluxes $\mathbf{j}_{D_\alpha,i}$ according to Fick's law.

Note that equation (3-1) applies to all species of the problem including liquid water. Thus, liquid water will be affected by advection and diffusion-dispersion.

In what follows conservation of all species in the system (equation (3-1)) are represented using a vector-matrix notation:

$$\frac{\partial}{\partial t}\left(\boldsymbol{\theta}\mathbf{c}\right)=\mathbf{L}\left(\mathbf{c}\right)+\mathbf{S}_\mathbf{e}^\mathbf{tr}\cdot\mathbf{r}_\mathbf{e}+\mathbf{S}_\mathbf{k}^\mathbf{tr}\cdot\mathbf{r}_\mathbf{k}+\mathbf{f} \tag{3-2}$$

Where $\mathbf{c}$ is a vector containing the concentration of all species $\mathbf{c}^\mathbf{tr}=\left(\mathbf{c}_{aqueous}^\mathbf{tr}\quad\mathbf{c}_{gaseous}^\mathbf{tr}\quad\mathbf{c}_{imm,va}^\mathbf{tr}\quad\mathbf{c}_{imm,ca}^\mathbf{tr}\right)$. We distinguish between aqueous $\mathbf{c}_{aqueous}$ and gaseous $\mathbf{c}_{gaseous}$ species because the transport operator $\mathbf{L}()$ will be different for each group. Immobile species with variable activity $\mathbf{c}_{imm,va}$ (like adsorbed species) are also distinguished from immobile constant activity species $\mathbf{c}_{imm,ca}$ (normally minerals) because, as shown by Saaltink et al. (1998), the last can be eliminated from component conservation equations. $\mathbf{S}_\mathbf{e}^\mathbf{tr}$ and $\mathbf{S}_\mathbf{k}^\mathbf{tr}$ are the transpose of the stoichiometric and kinetic matrix, respectively, $\mathbf{r}_\mathbf{e}$ and $\mathbf{r}_\mathbf{k}$ are vectors containing the equilibrium and kinetic reaction rates and $\mathbf{f}$ is a vector of external source-sink terms. All these variables are described in detail in the notation table.

Equilibrium reaction rates ($\mathbf{r}_\mathbf{e}$) lack explicit expression for their evaluation, hence their values are constrained also by transport processes (De Simoni et al. 2005). Transport processes may tend to apart the solution form equilibrium but equilibrium reaction will neutralize this effect. The lack of explicit expression is solved by re-formulating equation (3-2) in terms of components, as they are independent of equilibrium reactions (Rubin 1983). This does not imply any loss of information or simplification since all species can be represented as a combination of one or more components (Yeh and Tripathi, 1989). Components can be defined through a full ranked kernel matrix $\mathbf{U}$, termed component matrix, which has the property of eliminating equilibrium reaction rates when equation (3-2) is multiplied by it.

$$\mathbf{U}\cdot\mathbf{S}_\mathbf{e}^\mathbf{tr}=0\Rightarrow\mathbf{U}\cdot\mathbf{S}_\mathbf{e}^\mathbf{tr}\cdot\mathbf{r}_\mathbf{e}=0 \tag{3-3}$$

Molins et al. (2004) showed several ways of defining matrix $\mathbf{U}$. We will consider the component matrix introduced by Saaltink et al. (1998) in which constant activity species are eliminated. Details on how this matrix is calculated are given in Appendix I.

Dimensions of matrix $\mathbf{U}$ are $[Nc', Ns]$, considering

$$Nc' = Ns - Ne - Nca \tag{3-4}$$

where Ns is the number of species, Ne is the number of equilibrium reactions and Nca is the number of constant activity species. Note that the number of components Nc' defined by matriz $\mathbf{U}$ is smaller than the classic component number $Nc = Ns - Ne$ (Steefel and MacQuarrie, 1996).

By multiplying equation (3-2) by $\mathbf{U}$ we obtain:

$$\frac{\partial}{\partial t}\left(\mathbf{U}\cdot\boldsymbol{\theta}\cdot\mathbf{c}\right) = \mathbf{L}\left(\mathbf{U}\cdot\mathbf{c}\right) + \mathbf{U}\cdot\mathbf{S}_{\mathbf{k}}^{\mathbf{tr}}\cdot\mathbf{r}_{\mathbf{k}} + \mathbf{U}\cdot\mathbf{f} \tag{3-5}$$

By defining the aqueous, gaseous and immobile variable activity parts of the components

$$\mathbf{u}_{aq} = \mathbf{U}\cdot\begin{pmatrix}\mathbf{c}_{aqueous}\\0\\0\\0\end{pmatrix};\ \mathbf{u}_{g} = \mathbf{U}\cdot\begin{pmatrix}0\\\mathbf{c}_{gaseous}\\0\\0\end{pmatrix};\ \mathbf{u}_{imm,va} = \mathbf{U}\cdot\begin{pmatrix}0\\0\\\mathbf{c}_{imm,va}\\0\end{pmatrix}, \tag{3-6}$$

and their kinetic and external source-sink terms

$$\mathbf{k}' = \mathbf{U}\cdot\mathbf{S}_{\mathbf{k}}^{\mathbf{tr}}\cdot\mathbf{r}_{\mathbf{k}}\ ,\quad \mathbf{f}' = \mathbf{U}\cdot\mathbf{f}\ , \tag{3-7}$$

equation (3-5) can be written as:

$$\frac{\partial}{\partial t}\left(\theta_{aq}\mathbf{u}_{aq}\right) + \frac{\partial}{\partial t}\left(\theta_{g}\mathbf{u}_{g}\right) + \frac{\partial}{\partial t}\left(\mathbf{u}_{imm,va}\right) = \mathbf{L}_{aq}\left(\mathbf{u}_{aq}\right) + \mathbf{L}_{g}\left(\mathbf{u}_{g}\right) + \mathbf{k}' + \mathbf{f}' \tag{3-8}$$

This is the conservation equation in terms of components.

As dimensions of matrix $\mathbf{U}$ are $[Nc', Ns]$ the number of conservation equations is reduced from Ns to Nc'. Since constant activity species might appear or disappear (like complete dissolution or appearance of new mineral species) the number of components can change in time and space. This produces space sub domains with different $\mathbf{U}$ definition, making equation (3-5) to be valid over each single sub domain and not over the entire domain (Rubin 1983).

Temperature affects constitutive and thermodynamic relations. So, if the problem is not isotherm, the energy balance should be considered. This implies considering one extra partial

differential equation. Details about energy conservation equation have been discussed by a number of authors (Olivella et al. 1996, Pruess et al. 1999, Mills et al. 2007).

3.2.2. Local equations

Mobile phase properties and medium properties

The literature provides several models for density, viscosity and diffusion coefficients of mobile phases. All these parameters are expressed as an explicit function of phase composition, pressure and temperature.

Medium saturation is described by a retention curve. Several models (such as that of van Genuchten and Brooks-Corey) express saturation as an explicit function of capillary pressure and surface tension. These models also provide expressions for relative permeability of mobile phases.

Phase fluxes

Phase fluxes normally associated to a phase conservation equations. As in the proposed formulation no explicit phase conservation is considered, phase fluxes are considered as local equations and are calculated according to Darcy's law.

Equilibrium reactions

Several processes can be expressed by equilibrium reaction: complexation, adsorption, mineral precipitation-dissolution and heterogeneous relations, such as Henry's law. Such reactions are expressed by the mass action law, which relates the activities of the species (or fugacity for gases) involved in reaction j:

$$\sum_{i=1}^{Ns} Se_{j,i} \cdot \log a_i = \log K_j \tag{3-9}$$

where $Se_{j,i}$ is the stoichiometric coefficient for species i, a_i is the activity or fugacity of species i and K_j is the equilibrium constant of reaction j. K_j may depend on pressure and temperature. Equilibrium constants for adsorption reactions involving electrostatic models may also depend on surface potentials.

Activity, or fugacity for gases, represents the chemical availability of species. Given that these variables have a similar physical meaning, we will term them activity and refer to them as a. Activity of species i can be written in a general way as:

$$a_i = \gamma_i x_i \tag{3-10}$$

The meaning of γ_i and x_i depends on the phase to which the species belongs.

For aqueous species x_i represents molality [mol/KgH_20] and γ_i the activity coefficient. Depending on the ionic strength, aqueous species activities can be considered equal to one or calculated considering models such as Debye-Hückel (1923), or Pitzer (1973).

The psychrometric law is used to calculate the capillary effect on the water activity.

$$f_{cap} = \exp\left(\frac{\left(p_g - p_l\right)\cdot M_{H_2O}}{RT\rho_l}\right) \tag{3-11}$$

Where p_g and p_l are the gaseous and liquid pressure, M_{H_2O} is water molar weight, R is the universal gas constant, T is temperature and ρ_l is liquid density. Thus, the water activity value will be:

$$a_{h_2o_{(l)}} = f_{cap}\cdot a^{osmotic}_{h_2o_{(l)}} \tag{3-12}$$

where $a^{osmotic}_{h_2o_{(l)}}$ is the activity of liquid water given by the thermodynamic model considering only osmotic effects.

For gaseous species, x_i represents partial pressure and γ_i represents the fugacity coefficient. Depending on pressure and temperature gas γ_i can be considered equal to one or calculated considering models such as van der Waals or particular virial relations (Atkins and De Paula, 2006).

Despite the fact that interfaces cannot be regarded as thermodynamic phases, it is convenient to consider them as phases for formulation organization purposes. The activity of these species cannot be regarded as the product of two values (x_i and γ_i), such as the one for liquid or gaseous phases. However, in order to have a common notation for all phases, we will regard x_i as the activity of the adsorbed species i and γ_i equal to one.

For mineral species, x_i represents the solid molar fraction χ_s^i, and γ_i represents activity coefficient. When pure minerals are considered, χ_s^i and γ_i are equal to one and therefore mineral activity is equal to one.

Kinetic reaction

Several kinds of process can be represented by kinetic reactions: mineral precipitation-dissolution, redox processes and microbiological degradations. There are several expressions for kinetic reaction rates, such as Monod or Lasaga (Mayer et al. 2002). For minerals with a kinetic behavior, a constitutive expression for surface area must be considered.

3.2.3. Phase concentrations and constraints

Species conservation (equation(3-1)) is formulated considering phase volumetric concentration $c_{i,\alpha}$, but geochemical models use different concentration units, x_i, depending on the phase the species belong to. For each phase, there is a different relation between $c_{i,\alpha}$ and x_i. Moreover, each phase gives rise to an additional constraint that can be inferred from the units of x_i.

The concentration for species i belonging to the aqueous phase l is expressed as:

$$c_{i,l} = \rho_l \, \omega_l^{h_2o} m_i \tag{3-13}$$

where ρ_l is aqueous density, $\omega_l^{h_2o}$ is water mass fraction and m_i is molality of species i.

Thermodynamic models for aqueous solutions use molality as concentration unit (moles per solvent kilograms, in this case liquid water). Thus, the concentration of water is constant. The mass fraction of water, $\omega_l^{h_2o}$, can be calculated from the fact that the sum of mass fractions of all aqueous species equals 1:

$$1 = \sum_i^{Na} \omega_l^i = \sum_i^{Na} \omega_l^{h_2o} m_i M_i = \omega_l^{h_2o} \left(1 + \sum_{i \neq h_2o}^{Na} m_i M_i \right) \Rightarrow$$

$$\omega_l^{h_2o} = \left(1 + \sum_{i \neq h_2o}^{Na} m_i M_i \right)^{-1} \tag{3-14}$$

where ω_l^i is the mass fraction of species i in the aqueous phase and M_i its molar weight. Considering equations (3-13) and (3-14) it can be seen that the volumetric concentration of H_2O can be expressed as a function of all other aqueous species molality, and density. This will be considered below in section 3.3.3, when defining the solution variables.

The aquifer volumetric concentration for species i belonging to the gaseous phase g can be obtained from the general gas law:

$$p_i V_g = n_i Z_i RT \Rightarrow \frac{n}{V_g} = \frac{p_i}{Z_i RT}$$

$$c_i = \frac{p_i}{Z_i RT} \tag{3-15}$$

Where R is the universal gas constant, T is temperature, V_g is gas volume, p_i and Z_i are partial pressure and compressibility factor for gaseous species i, respectively. Z_i values can be calculated from virial relations or considered equal to one if the gas is assumed to be ideal.

Gas phase pressure can be expressed as a function of partial pressure of all gaseous species by Dalton's law:

$$p_g = \sum_{i=1}^{N_g} p_i \tag{3-16}$$

Where p_g is the gas phase pressure and N_g is the number of gaseous species.

Mineral species must satisfy:

$$\sum_{i}^{Nms} \chi_s^i = 1 \tag{3-17}$$

where χ_{solid}^i is the molar fraction of mineral species i in mineral phase s, and Nms is the total number of mineral species in mineral phase s. If only pure minerals are considered, each mineral phase is composed of only one mineral species and thus equation (3-17) becomes trivial.

3.3. Resolution

3.3.1. Numerical approach

There are two approaches to numerically solving reactive transport equations: the Sequential Iterative Approach (SIA) and the Direct Substitution Approach (DSA). The pros and cons of these methods have been discussed by a number of authors (Reeves and Kirkner 1988, Steefel and MacQuarrie 1996, Saaltink et al. 2001). Both approaches require the successive resolution of the global and the local equations.

We chose the DSA method because of its robustness and because it is suitable for the component reduction due to constant activity species. Chemical local equations produce a particularly complex non linear system and its solution is known as "speciation" in reactive transport argot. A general methodology to solve speciation is presented in section 3.3.3.

3.3.2. Degrees of freedom and resolution strategy

All constitutive equations and thermodynamic models that are normally used in reactive transport problems can be expressed as functions of the distribution of the phases and their chemical composition. For example, knowledge of phase composition and distribution (which implies knowing phase pressures) will enable variables such as densities, viscosities, saturations, and even flows (using Darcy's law) to be calculated. Thus, the minimum set of variables that allows representing phase composition and distribution is the solution variables of the problem. Gibbs's phase rule indicates the number of thermodynamic degrees of freedom $\mathrm{df}_{ph,rule}$ of a system:

$$\mathrm{df}_{ph,rule} = Nc - Nph + 2 \tag{3-18}$$

Where Nc is the number of components (equal to the number of species Ns minus the number of equilibrium reactions Ne), Nph is the number of phases, and 2 corresponds to pressure and temperature. The phase rule gives the minimum number of variables needed to calculate the composition of all phases, but does not provide information about the number or distribution of phases. Hence, the system has additional degrees of freedom that correspond to phase distribution (Pruess et al. 1999). As the sum of all phase volume fraction should be equal to one, the number of degrees of freedom due to phase distribution $\mathrm{df}_{ph,dist}$ is:

$$\mathrm{df}_{ph,dist} = Nph - 1 \tag{3-19}$$

So, the total number of degrees of freedom of the system df is:

$$\mathrm{df} = \mathrm{df}_{ph,rule} + \mathrm{df}_{ph,dist} = Nc + 1 \tag{3-20}$$

If the problem is isothermal the number of degrees of freedom would be equal to the number of components. Saaltink et al. (1998) have shown that constant activity species, can be eliminated from the system, reducing the number of components to

$$Nc' = Nc - Nca \tag{3-21}$$

Thus, the minimal number of variables needed to represent phase composition and distribution, and evaluate all constitutive relation is Nc'. This number is equal to the number of component conservation equations obtained in section 3.2.1. Thus, all variables in the problem can be

calculated by solving component conservation equations(3-8). Given that constant activity species, such as minerals, might appear or disappear, the number of components Nc' will change in time and space.

3.3.3. Solutions variables and Speciation

Speciation consists basically in calculating the chemical composition of all phases from, what may be termed, solution variables. Total concentrations of components or concentrations of primary species can be considered solution variables. Primary species are defined as a subgroup of species from which concentration of all other species can be calculated. We choose primary species as solution variables because this facilitates speciation calculations, especially when complex activity models are considered. It is easier to calculate derivatives of activity coefficient with respect to primary species than with respect to component concentration.

Speciation is done by formulating and solving the complete set of equilibrium reactions. According to equation (3-9) all equilibrium reactions can be written as:

$$\mathbf{S}_\mathbf{e} \cdot \log \mathbf{a} = \log \mathbf{K} \tag{3-22}$$

where $\mathbf{S}_\mathbf{e}^{\mathbf{tr}}(i,j) = Se_{j,i}$ and $\mathbf{S}_\mathbf{k}^{\mathbf{tr}}(i,j) = Sk_{j,i}$ are the transpose of the equilibrium and kinetic stoichiometric matrices respectively.

As stated above, concentration of constant activity species, such as minerals, are not unknowns of equation (3-22). However, the presence of such species does affect speciation, because their reaction must be considered.

Species activities a can be expressed as the product of two variables: x which represents some sort of chemical concentration, and γ which represents a correction coefficient for activity. As the γ coefficients are functions of concentrations, x, equations (3-22) can be considered a nonlinear system of equations with x as variables:

$$\mathbf{S}_\mathbf{e} \cdot \log \mathbf{x} + \mathbf{S}_\mathbf{e} \cdot \log \boldsymbol{\gamma}(\mathbf{x}) = \log \mathbf{K} - \mathbf{S}_\mathbf{e} \cdot \log \mathbf{a}_{imm,ca} \tag{3-23}$$

where $\mathbf{x}$ and $\boldsymbol{\gamma}$ are vectors containing chemical concentrations and activity coefficients of all species with variable activity. Constant activity values are normally considered equal to one, thus $\log \mathbf{a}_{imm,ca}$ is equal to zero.

Equations (3-23) are composed of Ne equations (number of equilibrium reactions, including those of equilibrium minerals). Thus, it enables us to calculate the concentration of N_{xs} species, termed secondary speciesas a function of the rest, termed primary. Note that the number of primary species $N_{x_p} = Ns - Nca - Ne = Nc'$ is equal to the number of degrees of freedom obtained in the previous section.

As mentioned in section 3.2.3, the chemical concentration of aqueous species is molality, which makes the liquid water concentration a constant and not an unknown. It is also stated in section 3.2.2 that the gas-liquid pressure difference (capillary pressure) can affect activities. Thus phase pressures are needed for speciation. Gas pressure can be calculated adding the partial pressures of all gaseous species (equation (3-16)). However, there is no expression that links the molalities of aqueous species to liquid pressure. Therefore, liquid pressure has to be known for speciation calculations.

The fact that water molality is constant reduces the number of primary species by one, $N'_{x_p} = Nc' - 1 = N_{x_p} - 1$. Thus, the primary variables for speciation will be the chemical concentration of N'_{x_p} primary species plus the liquid pressure. Phase distribution can also be calculated from these variables through retention curves. Therefore, the primary variables required for the entire multiphase reactive transport problem are the same as for speciation.

3.3.4. Solving the component conservation equations (discretization)

Several numerical techniques such as finite differences and finite volumes are suitable for discretizing the partial differential equations for component conservation (3-8). These techniques approximate the solution in discrete entities of the domain (like cells or nodes) and generate a nonlinear set of ordinary equations. The Newton-Raphson method is the most suitable for solving this nonlinear set of equations. This method demands the evaluation and derivation of the discretized equations with respect to the primary variables, requiring the solution of all local equations (speciation).

Thus, two kinds of nonlinear systems have to be solved: a large one for the global equations for component conservation and several small ones (one for each discrete entity) for the local equations (speciation). Note that for each iteration of the large system it is necessary to solve all the small systems in order to update secondary variables and their derivatives.

3.3.5. Calculation of constant activity species

Once the system was solved, concentrations of all species were calculated, except those of constant activity since these were eliminated by using the component matrix $\mathbf{U}$ (see section 3.2.1). These concentrations can be calculated subsequently from the equations for species conservation (3-2). The only unknowns of this system are the Nca constant activity species and the Ne equilibrium reaction rates. As the number of species Ns is greater than $Nca + Ne$, the system has more equations than unknowns. Least squares techniques may be used to solve the system. Alternatively, some equations can be ignored to match the number of unknowns and equations. If the conservation equations of primary species are ignored, the number of unknowns equals the number of remaining equations:

$$Ns - Nc' = Ns - \left(Ns - Ne - Nca \right) = Ne + Nca \tag{3-24}$$

3.3.6. Implementation

This formulation was implemented following the object oriented (OO) paradigm in a FORTRAN 95 code merging and expanding two existing OO codes PROOST (Slooten 2008) and CHEPROO (Bea et al. 2009). PROOST is a general purpose hydrological modeling tool that can solve a large variety of conservation equations expressed as partial differential equations. It was built and used to simulate flow and transport problems. CHEPROO is an OO tool specialized in complex geochemical processes. It can calculate the chemical composition of a geochemical system from concentrations of component or primary species. It can also calculate phase properties such as density, viscosity and their derivatives with respect to solution variables (concentrations of primary species, liquid pressure, temperature).

While component mass balances are formulated in PROOST, all chemical aspects are handled by CHEPROO. For a given value of primary species, CHEPROO calculates the speciation, checks whether the definition of components corresponds to the set of minerals, changing it if necessary, and calculates phase properties and component concentrations and their derivatives. PROOST uses these to solve the component mass balance equation by the Newton-Raphson method.

3.4. Application: Gypsum column evaporation

3.4.1. Model description

Evaporation of soils involves liquid and gaseous phase fluxes, diffusive fluxes and energy flux. These natural phenomena can provide evidence of interaction between hydrodynamics and geochemistry especially in arid or semiarid environments where extreme dry conditions and high salt contents might arise. In these conditions water activity, which is a key parameter for evaporation, is influenced by osmotic effects because of high solute concentrations and by capillary effects because of low saturations. The amount of liquid water can be so small that the water balance may be significantly influenced by precipitation or dissolution of hydrated minerals. The application that follows will illustrate several features of the proposed formulation.

We modeled the evolution of a 24 cm column of porous gypsum subjected to a constant source of heat. The column was considered to be initially saturated, with a temperature of 25^{o}C and open at the top, permitting vapor exchange with the atmosphere due to advective and diffusive processes. As extreme dry conditions are reached, we consider a retention curve capable of representing oven dry conditions (Silva and Grifoll 2007 and Massana 2005). The high ionic strength necessitates the use of the Pitzer ion interaction model to evaluate activities of aqueous species. Problem parameters, constitutive models and boundary conditions are shown in Table 3-1 and Table 3-2. We consider gypsum because it dehydrates forming anhydrite and acts as a chemical source term of water that can affect flow.

Table 3-1– Constitutive equations

Retention curve (modified van Genuchten model)	$S_l = S_i + (1-S_i)S_e$ $S_e = \left(1+\left(P_g - P_l/P_0\right)^{\frac{1}{1-\lambda}}\right)^{-\lambda}$ $S_i = S^0_{\min}\alpha \ln\left(P_c^{dry}/\left(P_g - P_l\right)\right)$	$P_0 = 25\text{x}10^{-4}\left[\text{MPa}\right]$ $\lambda = 0.93\ ;\ \alpha = 0.1$ $S^0_{\min} = 0.08$ $P_c^{dry} = 650\left[\text{MPa}\right]$
Relative permeability	$K_{rl} = \begin{cases} K^0_{rl} & S_l > S_{l,min} \\ K^0_{rl}\left(S_l/S_{l,min}\right)^{\gamma} & S_l < S_{l,min} \end{cases}$ $K^0_{rl} = \sqrt{S_e\left(1-\left(1-S_e^{1/\lambda}\right)^{\lambda}\right)^2}$	$S_{l,min} = 0.1$ $\gamma = 5$ $K_{rg} = 1 - K_{rl}$
Intrinsic permeability	$\mathbf{K} = \mathbf{K}_0\left(\frac{\phi}{\phi_0}\right)^3\left(\frac{1-\phi_0}{1-\phi}\right)^2$	$\mathbf{K}_0 = 2.8\text{x}10^{-11}\left[m^2\right]$ $\phi_0 = 0.4$
Phase density	$\rho_{liq} = P_0 \exp\left(\alpha T + \beta\left(P_l - P_0\right) + \gamma\left(\sum_{i\neq h_2o}\omega_l^i\right)\right)$ $\rho_{gas} = \frac{P_{g,vap}\cdot M_{vap} + P_{g,air}\cdot M_{air}}{R\left(T+273.15\right)}$	$P_0 = 1002.6\left[\text{MPa}\right]$ $\alpha = -3.4\text{x}10^{-4}\left[{}^{\circ}C^{-1}\right]$ $\beta = 4.5\text{x}10^{-4}\left[\text{MPa}^{-1}\right]$ $\gamma = 0.6923$ $M_{vap} = 0.018\left[Kg/mol\right]$ $M_{air} = 0.02895\left[Kg/mol\right]$
Phase viscosity	$\mu_{liq} = 2.1\text{x}10^{-12}\cdot\exp\left(\frac{1808.5}{T+273.15}\right)\left[\text{MPa}\cdot\text{s}\right]$ $\mu_{gas} = 1.48\text{x}10^{-12}\cdot\exp\left(\frac{119.4}{T+273.15}\right)\left[\text{MPa}\cdot\text{s}\right]$	
Phase diffusion	$D_{gas} = 5.9x10^{-6}\left(\frac{\left(T+273.15\right)^{2.3}}{P_g}\right)\left[m^2/s\right]$ $D_{liq} = 1.1x10^{-4}\exp\left(\frac{-24539}{R\cdot\left(T+273.15\right)}\right)\left[m^2/s\right]$	
Thermal conductivity	$\lambda = \lambda_{sat}^{S_l}\lambda_{dry}^{(1-S_l)}\left[\text{Wm/K}\right]$	$\lambda_{sat} = 1.44\,;\,\lambda_{dry} = 1.54$
Chemical reactions	$H_2O_{(l)} \Leftrightarrow H_2O_{(g)}$ $K_{vapour} = 1.36075\text{x}10^{11}\exp\left(\frac{-5239.7}{273.15+T}\right)\left[\frac{\text{Pa}\cdot Kgh_2o}{mol}\right]$ $air_{(l)} \Leftrightarrow air_{(g)}$ $\quad K_{air} = 2.9\text{x}10^{8}\left[\frac{\text{Pa}\cdot Kgh_2o}{mol}\right]$ $Ca^{2+} + SO_4^{2-} \Leftrightarrow anhydrite$ $Ca^{2+} + SO_4^{2-} + 2H_2O_{(l)} \Leftrightarrow gypsum$	$K_{anhydrite} = 10^{-4.362}$ $K_{gypsum} = 10^{-4.581}$

Table 3-2- Boundary and initial conditions

Initial conditions	$S_l = 1$; $T = 25^{o}C$;	
	Hydrostatic liquid pressure: $P_l^{top} = 101325\left[\text{Pa}\right]$	
Top boundary gas flow	$j_i^{top} = \alpha\left(P_g^{ext} - P_g^{top}\right)\cdot c_i^{*} + \beta\left(P_i^{ext} - P_i^{top}\right)$	$\alpha = 50\left[m/\left(\text{MPa}\cdot s\right)\right]$
		$\beta = 2\left[mol/\left(\text{MPa}\cdot s\cdot m^2\right)\right]$
	$c_i^{*} = \begin{cases} c_i^{ext} & P_g^{ext} > P_g^{top} \\ c_i^{top} & P_g^{ext} < P_g^{top} \end{cases}$	$P_{h_2o}^{ext} = 3172\left[\text{Pa}\right]$
		$P_{air}^{ext} = 98152\left[\text{Pa}\right]$
Top boundary heat flow	$j_{e,in} = 750\left[J/s\right]$	
Heat lose	$j_{e,lose} = \alpha\left(T_{ext} - T\right)$	$\alpha = 25\left[J/\left(K\cdot s\right)\right]$; $T_{ext} = 26\left[^{o}C\right]$
Initial concentrations	$H_2O_{(l)} = 5.551\text{x}10^{1}\left[m\right]$	$Cl^{-} = 5.700\text{x}10^{-3}\left[m\right]$
	$air_{(l)} = 5.453\text{x}10^{-4}\left[m\right]$	$H_2O_{(g)} = 3.173\text{x}10^{-3}\left[\text{MPa}\right]$
	$Ca^{2+} = 2.000\text{x}10^{-2}\left[m\right]$	$air_{(g)} = 9.815\text{x}10^{-2}\left[\text{MPa}\right]$
	$SO_4^{2+} = 1.720\text{x}10^{-2}\left[m\right]$	$\theta_{gypsum} = 0.6$
	$K^{+} = 1.000\text{x}10^{-4}\left[m\right]$	$\theta_{anhydrite} = 0$

3.4.2. Column evolution

Saturation, vapor partial pressure and temperature profiles are shown in Figure 3-1. The profile of the vapor partial pressure shows the formation and descent of an evaporation front. This front divides the domain into two zones: a dry zone above the front where oven dry saturations prevail and a humid zone below. The figure also shows a different temperature gradient for each zone. The reason of this difference is that a large amount of energy is consumed at the evaporation front.

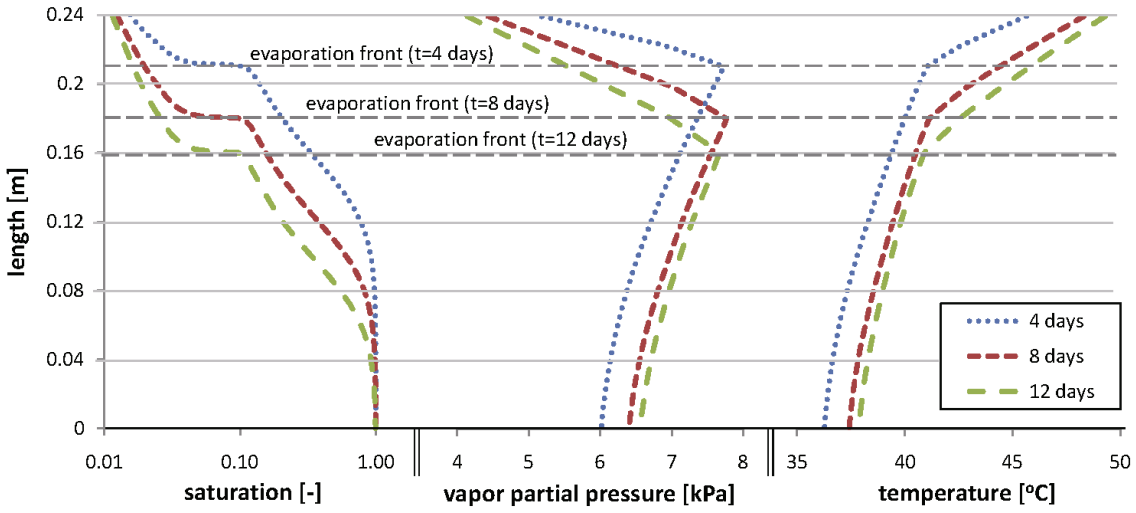

Figure 3-1 – Saturation, vapor partial pressure and temperature profiles. The position of the evaporation front position is marked by a horizontal line. Note that saturation attains oven dry values above the evaporation front and that temperature slopes change at this front.

Apart from an evaporation front, a mineral front of gypsum dissolution and anhydrite precipitation develops. As shown in Figure 3-2, this mineral front is situated above the evaporation front. This figure also shows that vapor partial pressure and temperature gradients change at the mineral front albeit to a lesser degree at the evaporation front. As the mineral front is very close to the evaporation front, this effect cannot be appreciated in Figure 3-1. At the mineral front, gypsum dehydrates forming anhydrite, releasing water that evaporates. This accounts for the changes in temperature gradient and vapor partial pressure.

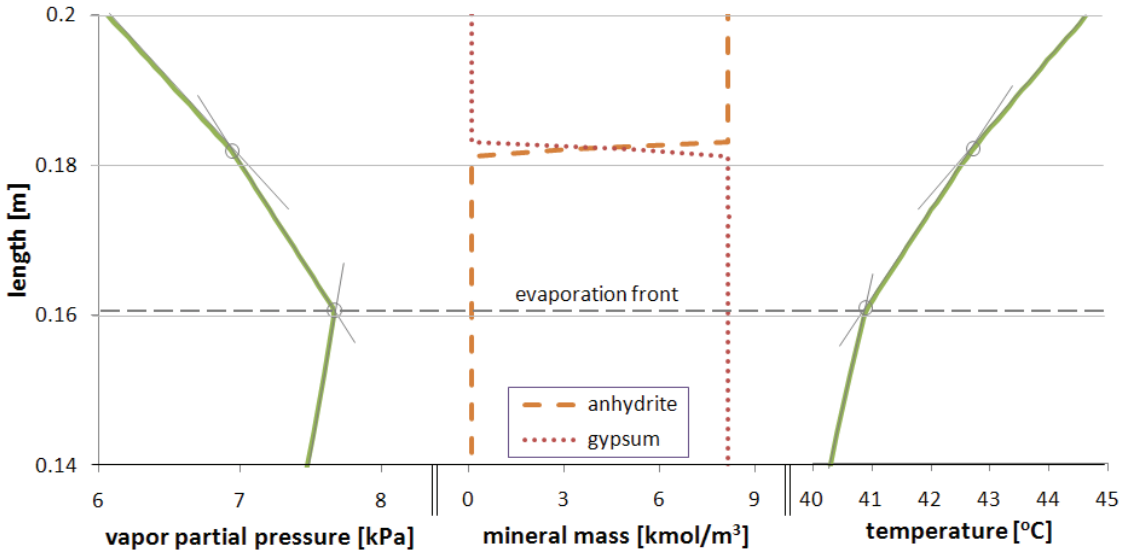

Figure 3-2 – Vapor partial pressure, mineral phases and temperature on day 12. Note that vapor partial pressure and temperature gradients not only change at evaporation front but also at a depth of around 0.181 m. At this point, gypsum is transformed into anhydrite releasing water.

3.4.3. Anhydrite-Gypsum invariant point

The coexistence of gypsum and anhydrite produces a singularity, known as "invariant point" (Risacher and Clement, 2001, Chapter 2 of this thesis), at which the water activity remains constant. This can be seen by combining the mass action laws for gypsum and anhydrite precipitation/dissolution:

$$\begin{aligned} \left(Ca^{2+}\right)\left(SO_4^{2-}\right)a_w^2 &= K_{gypsum} \\ \left(Ca^{2+}\right)\left(SO_4^{2-}\right) &= K_{anhydrite} \end{aligned} \Rightarrow a_w = \sqrt{\frac{K_{gypsum}}{K_{anhydrite}}} \tag{3-25}$$

If these two minerals coexist, water activity remains constant. Gypsum hydration or dehydration will provide the precise amount of water to maintain water activity constant, compensating for any effect induced by transport process. Thus, in zones where gypsum and anhydrite coexists, the water and vapor transport process does not affect the chemical composition. This effect is easily obtained in the proposed formulation. The component matrix $\mathbf{U}_{anh-gyp}$ for anhydrite and gypsum is:

$$\mathbf{U}_{anh-gyp} = \begin{bmatrix} & h_2o_{(l)} & air_{(l)} & ca^{2+} & so_4^{2-} & k^{+} & cl^{-} & h_2o_{(g)} & air_{(g)} & anh & gyp \\ u_k & 0 & 0 & 0 & 0 & 1 & 0 & 0 & 0 & 0 & 0 \\ u_{air} & 0 & 1 & 0 & 0 & 0 & 0 & 0 & 1 & 0 & 0 \\ u_{ca-so_4} & 0 & 0 & 1 & -1 & 0 & 0 & 0 & 0 & 0 & 0 \\ u_{cl} & 0 & 0 & 0 & 0 & 0 & 1 & 0 & 0 & 0 & 0 \end{bmatrix} \tag{3-26}$$

So the component conservation equation will be:

$$\frac{\partial}{\partial t}\begin{pmatrix} \theta_{aq}c_{k^+} \\ \theta_{aq}c_{air_{(l)}}+\theta_g c_{air_{(g)}} \\ \theta_{aq}c_{ca^{2+}}-\theta_{aq}c_{so_4^{2-}} \\ \theta_{aq}c_{cl^-} \end{pmatrix}=\mathbf{L}_{aq}\begin{pmatrix} c_{k^+} \\ c_{air_{(l)}} \\ c_{ca^{2+}}-c_{so_4^{2-}} \\ c_{cl^-} \end{pmatrix}+\mathbf{L}_g\begin{pmatrix} 0 \\ c_{air_{(g)}} \\ 0 \\ 0 \end{pmatrix} \tag{3-27}$$

As observed in equation (3-27), the liquid and the gaseous water concentrations do not appear in the component conservation equations, and, as water activity is fixed, they do not affect the chemical evolution while anhydrite and gypsum coexist. What these species do affect, is the gypsum and anhydrite precipitation dissolution rate (calculated from the mineral species concentration, see section 3.3.5). This can be seen by adding aqueous and gaseous conservation equations:

$$\frac{\partial}{\partial t}\left(\theta_{aq}c_{h_2o_{(l)}}+\theta_g c_{h_2o_{(g)}}\right)=L_{aq}\left(c_{h_2o_{(l)}}\right)+L_g\left(c_{h_2o_{(g)}}\right)-2r_{gyp} \tag{3-28}$$

Figure 3-3 shows the evolution of water activity and of concentrations of the mineral phases for the upper node of the domain. It may be seen that between 2.03 and 2.11 days (highlighted area) gypsum and anhydrite coexist, and water activity remains constant. Once all the gypsum is dissolved, water activity continues to decrease and then appears to reach another invariant value, which on closer inspection, show small variations. This peculiar behavior is due to the progress of the mineral front. At time 2.15 an invariant point is present at the node below. Given that external vapor pressure is fixed, the vapor pressure gradient remains constant when invariant points occur, and since vapor diffusion is the dominant process in the upper part of the column, transport becomes quasi stationary during these intervals.

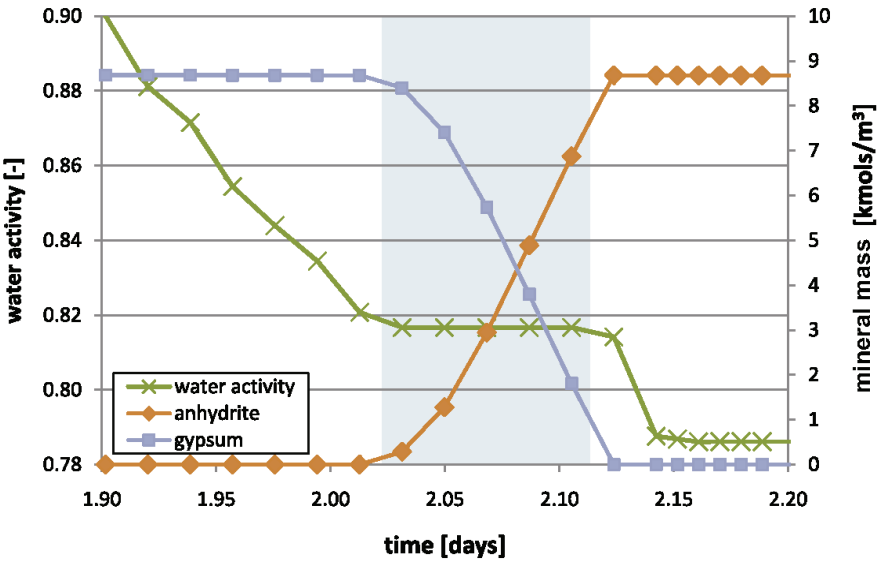

Figure 3-3 – Water activity and minerals mass for the domain top surface. An invariant point is reached when gypsum and anhydrite coexists (shaded area). Water activity remains constant during this interval

The influence of invariant points on adjacent nodes is shown in Figure 3-4. In this figure it can be seen that the constant vapor pressure gradient affects both superjacent and subjacent nodes where the invariant point appears. The influence of invariant points on superjacent nodes is more significant than on subjacent nodes as water activity of the former remains almost constant. This is because saturation is higher in subjacent nodes with the result that liquid flow is more significant. The stair-shaped water activity in Figure 3-4 is a consequence of the spatial discretization. The time that a node remains at an invariant point depends on the availability of the gypsum mass. For finer meshes, nodes will have less associated volume and hence less gypsum mass, leading to shorter intervals of invariant points. Figure 3-4 also shows the water activity at the upper node for a finer mesh (with twice the number of nodes). It can be observed that for the finer mesh the (semi-)constant water activity values are shorter but more frequent.

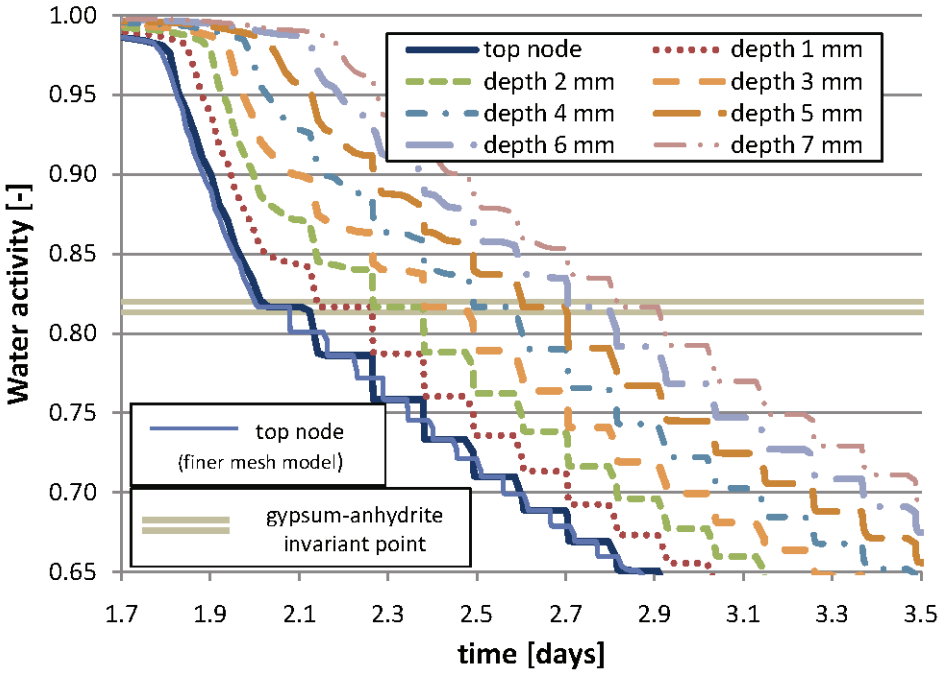

Figure 3-4 – Water activity evolution of the eight upper nodes. The occurrence of an invariant point significantly affects water activity adjacent nodes. The stair shape of the water activity is a consequence of the spatial discretization; a finer mesh produces a smaller stair-size

3.4.4. Mineral influence on column evolution

To evaluate the effect of invariant points and mineral hydration the same problem was simulated without considering anhydrite. Saturation profiles are compared in Figure 3-5. This figure shows that the evaporation front moves faster if anhydrite is not considered. Thus, ignoring water from mineral dissolution and the possible control of mineral phases over water activity could lead to appreciable differences in the evolution of the system.

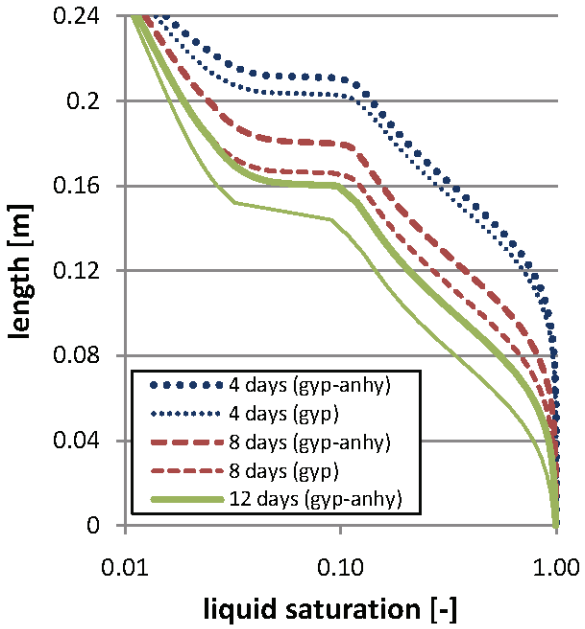

Figure 3-5 Saturation profiles considering gypsum and anhydrite (gyp-anhy) and only gypsum (gyp). If anhydrite is not considered the evaporation front moves faster.

3.5. Summary and conclusions

A generalized compositional formulation for modeling multiphase reactive transport problems is presented. The formulation avoids the classic approach of decoupling phases and component conservation, which does not adequately represent the influence of geochemical processes on phase flows. The formulation considers that constant activity species, such as minerals, do not affect speciation and can therefore be eliminated. This reduces the number of components and the size of the system to be solved.

The formulation is presented in a concise mathematical way that allows all the necessary chemical processes to solve complex chemical and biochemical problems, such as complexation, homogeneous and heterogeneous equilibrium reactions, kinetic reactions and adsorption (linear, cation exchange or electrostatic models).

An implementation of the formulation is used to model the evolution of a gypsum column subjected to a constant source of heat. The model shows the formation of a descending evaporation front, and also a gypsum-anhydrite front. Results show that the water released by gypsum dehydration to anhydrite affects both vapor partial pressure and temperature. The model can also represent gypsum-anhydrite coexistence (invariant point) which fixes water activity and, hence, controls evaporation.

Modeling these processes by decoupling phase flow and reactive transport is not viable, because several iterations between these two phenomena would be required and probably small time steps should be considered to ensure convergence. During an invariant point, mineral precipitation-dissolution acts as a water sink-source and provides the precise amount of water to keep water activity constant despite all the transport processes considered. This process in particular or any heterogeneous reaction produces a phase sink-source term that couples phase flow and reactive transport, which makes the use of a decoupled approach difficult.

In order to evaluate the influence of mineral dehydration, the results were compared with a simulation without anhydrite. The results show that the evaporation front moves faster if anhydrite is not considered. Thus, ignoring water from mineral dissolution and the possible control of mineral phases over water activity might lead to appreciable differences in the evolution of the system.

4. Object oriented concepts applied to multiphase reactive transport modeling in porous media

4.1. Introduction

Modeling multiphase reactive transport (MPRT) in porous media involves simulating several phenomena: multiphase flow, solute transport, and reactions. MPRT may also involve heat transport and porous media deformation (Steefel et al. 2005). These phenomena may be complex to model individually, but MPRT brings on new difficulties associated with coupled effects (Lichtner 1996). Which coupled effects have to be considered and the optimal solution strategy for the coupled equations depends on the nature of the problem to be solved and may vary significantly from case to case.

For example, most reactive transport codes decouple phase conservation(i.e. flow equation) from reactive transport calculations (Xu and Pruess 1998, Clement et al. 1998, Mayer 2002, van der Lee 2003, Saaltink et al. 2004, Parkhurst et al. 2004, Mills et al. 2007, Molins and Mayer 2007). This approach is convenient in most cases. However, a numerically coupled solution will generally be more suitable when the phenomena involved are highly physically coupled. Wissmeier and Barry (2008) showed that the consumption of water due to hydrated mineral precipitation can have impacts on flow and solute transport for unsaturated flow problems. These impacts can be even more important if gas transport is also considered because water activity, which controls vapor pressure, is affected by capillary and osmotic effects. Moreover, certain mineral paragenesis can fix water activity (producing an invariant point), causing the geochemistry to control vapor pressure, which is the key variable for vapor flow (Risacher and Clement, 2001). In such cases, decoupling is not appropriated and may require very small time steps to obtain a converging accurate solution.

The choice of coupling may be implicit in the adopted numerical scheme. For example, two board set of methods are used for reactive transport. On the one hand, sequential methods,

whether iterative (SIA) or not (SNIA) adopt operator splitting techniques that effectively decouple component transport equations. On the other hand, direct substitution approaches (DSA) solve all equations simultaneously. A number of authors have studied these methods (Steefel and MacQuarrie, 1996, Saaltink et al. 2001) and agreed that despite the fact the DSA is more robust, there are cases where the SIA is more convenient from an efficiency-accuracy point of view.

In short, the adopted coupling techniques for MPRT modeling may be problem dependent. Therefore, a MPRT code should include several solution approaches to be used in a broad range of problems. Moreover, in order to ensure its use for present and future problems, it must have an extensible design. A number of authors have pointed out that object oriented (OO) programming facilitates the implementation of these features (Fenvesm 1990, Filho and Devloo 1991, Khan et al. 1995, Commend and Zimmermann 2001).

The scientific community has been adopting OO techniques for problem solving since the end of the last century (Forde et al. 1990, Pidaparti and Hudli 1993, Budge and Peery 1993, Silva et al. 1994, Wang and Kolditz 2007, Slooten et al. 2010). But only in the last decade have OO codes been developed for reactive transport modeling. Meysman et al. (2003) developed an OO reactive transport code for a single fluid phase. Gandy and Younger (2007) developed an OO multiphase reactive transport code for pyrite oxidation and pollutant transport in tailing ponds. Shao et al. (2009) include reactive transport calculations into a Thermo-Hydro-Mechanic OO framework adopting a sequential non iterative approach (SNIA). Bea et al. (2009) developed an OO module capable of solving reactive transport for a single phase considering the SNIA, SIA or DSA approach. However, all of these codes, and most of the procedural reactive transport codes, have a predefined strategy for dealing with coupling effects. No MPRT code is capable of solving coupled phase conservation and reactive transport.

The objective of this paper is to present an OO structure for MPRT that can accommodate different level of coupling.

4.2. Equations to solve

MPRT modeling implies establishing several conservation principles (mass and energy) expressed as partial differential equations (PDE), and several constitutive and thermodynamic laws (such as

retention curve or mass actions laws) expressed as algebraic equations (AE). Darcy's law is used to represent momentum conservation. In this section we present a generic conservation equation to represent conservation principles in MPRT problems. We consider in detail the species and component conservation and we briefly go through the constitutive and thermodynamic laws.

4.2.1. General conservation equation

Conservation of a physical entity ε can be expressed as

$$\frac{\partial S_\varepsilon}{\partial t} = -\sum_\nu \nabla \mathbf{j}_{\varepsilon,\nu} + F_\varepsilon \tag{4-1}$$

Where S_ε is the amount of ε per unit volume of medium, $\mathbf{j}_{\varepsilon,\nu}$ is the flux of ε due to the driving force ν (e.g. advection or diffusion), and F_ε is a sink source term. Since time and spatial derivatives are involved, conservation equations usually take the form of a partial differential equation (PDE).

4.2.2. Species and component conservation equation

The conservation of a species i belonging to phase α, which is a particular case of equation (4-1), has the following expression:

$$\frac{\partial}{\partial t}\left(\theta_\alpha c_{i,\alpha}\right) = L_\alpha\left(c_{i,\alpha}\right) + \sum_{j=1}^{Ne} Se_{j,i}\cdot re_j + \sum_{j=1}^{Nk} Sk_{j,i}\cdot rk_j + f_i \tag{4-2}$$

Where θ_α is the volumetric content of phase α, $c_{i,\alpha}$ is the species i concentration, $Se_{j,i}$ is the stoichiometric coefficient of the equilibrium reaction j for the specie i, re_j is the reaction rate of the equilibrium reaction j, and Ne is the number of equilibrium reactions. $Sk_{j,i}$, rk_j and Nk are analogous to $Se_{j,i}$, re_j and Ne but for kinetic reactions. f_i is an external sink-source term, and $L_\alpha(\ )$ is the transport operator for mobile phase α, which consider advective and diffusive-dispersive processes $L_\alpha\left(c_{i,\alpha}\right) = -\nabla\cdot\left(c_{i,\alpha}\mathbf{q}_\alpha\right) - \nabla\cdot\left(\mathbf{j}_{D_\alpha,i}\right)$. Mobile phase fluxes $\mathbf{q}_\alpha$ are calculated according to Darcy's law $\mathbf{q}_\alpha = \mathbf{K}_\alpha\left(-\nabla p_\alpha + \rho_\alpha \mathbf{g}\right)$, where $\mathbf{K}_\alpha$, p_α and ρ_α are the conductivity tensor, pressure and density of the phase α respectively. Diffusive-dispersive fluxes $\mathbf{j}_{D_\alpha,i}$ are calculated according to Fick's law $\mathbf{j}_{D_\alpha,i} = -\left(\mathbf{D}_\alpha^{diff}\theta_\alpha\tau + \mathbf{D}^{disp}\right)\cdot\nabla\left(c_{i,\alpha}\right)$ where $\mathbf{D}_\alpha^{diff}$ and $\mathbf{D}^{disp}$ are the diffusion and dispersion tensor for phase α respectively and τ is the tortuosity.

Note that the general sink source term of equation (4-1) F_ε involves several different terms in equation (4-2):

$$F_\varepsilon = \sum_{j=1}^{Ne} Se_{j,i} \cdot re_j + \sum_{j=1}^{Nk} Sk_{j,i} \cdot rk_j + f_i \tag{4-3}$$

There is no explicit expression for the equilibrium reaction rates re_j, their value has to be such that the corresponding mass action law is satisfied. Therefore, re_j values can be written as a function of both transport and chemical processes (De Simoni et al. 2005). A common approach to avoid dealing with these terms is to formulate the conservation of components, which are a linear combination of species that remain unaffected by equilibrium reactions (Rubin 1983). As such, equilibrium reactive rates disappear from the conservation equations of components (Steefel and MacQuarrie 1996, Saaltink et al. 1998). However, components way involve species belonging to different phases, therefore conservation equation for components have to be written:

$$\sum_\alpha \frac{\partial}{\partial t}\left(\theta_\alpha u_{i,\alpha}\right) + \sum_\beta \frac{\partial}{\partial t}\left(\theta_\beta u_{i,\beta}\right) = \sum_\alpha L_\alpha\left(u_{i,\alpha}\right) + k_{u_i} + f_{u_i} \tag{4-4}$$

Where $u_{i,\alpha}$ and $u_{i,\beta}$ are the i component concentration in mobile phases α and immobile phases β respectively, and k_{u_i} is a linear combination of the kinetic terms that affect the species composing the component. There are several ways of defining components. Molins et al. (2004) generalized this definition to uncouple kinetic reactions. Saaltink et al. (1998) introduced a definition in to eliminate constant activity species. As minerals, often considered as constant activity species, might appear or disappear from portions of the domain, the component definition can change in time and space. This increases the difficulty of solving equation (4-4)since it will be valid over patches of the domain with the same mineral composition and fluxes between these zones would have to be evaluated.

Once all component conservation and geochemical equations have been solved, all species concentrations are known. Equilibrium reaction rates re_j are calculated form species conservation equation (4-2). If constant activity species have been eliminated from the component definition, their concentration had also to be calculated from equation (4-2).

4.2.3. Constitutive and thermodynamic laws

The literature provides several models for density, viscosity and diffusion coefficients of mobile phases, the parameters of which are expressed as an explicit function of phase composition, pressure and temperature. Several models (such as van Genuchten or Brooks-Corey) express saturation and relative permeability as an explicit function of capillary pressure and surface tension. All these relations produce a local system of equation which is valid at every point of the domain.

Thermodynamic relations also form part of this local system of equations. The most important of these are the chemical equilibrium reactions, which we express by means of mass action laws, as often done in reactive transport (e.g. Steefel and MacQuarrie 1996, Saaltink et al. 1998). Also required are activity models (such as Debye-Hückel (1923), or Pitzer (1973)) or kinetic reactions expressions (such as Monod or Lasaga (Mayer et al. 2002)).

Constitutive and thermodynamic relationships define a set of algebraic equations (AE) that need to be solved simultaneously with the conservation equations (PDE).

4.2.4. Numerical solution of the equations

Methods such as finite element or finite differences are used to approximate time or space derivative terms in PDEs. Application of such methods leads to a set of equations that represent the conservation principle for discrete points of the domain (representing nodes or cells). Contrary to constitutive or thermodynamic laws, these equations are not local, that is, equations at a discrete point are function of variables at other discrete points. As constitutive and thermodynamic models (AEs) involve variables that appear in the PDE, both AES and PDEs may have to be solved simultaneously. Different approaches can be adopted for solving these coupled sets of equation.

4.3. OO analysis of MPRT modeling and PROOST class organization

According to the OO philosophy, the numerical solution of MPRT can be represented by a group of interacting objects. These objects belong to classes which define common types of data and functionality. According to Filho and Devloo (1991), defining suitable classes is the first and perhaps the most important step in software design under OO.

Our analysis was based on the idea that a model is a set of equations (PDEs and AEs) that need to be solved. These equations involve several fields (such as concentrations, density or porosity) which are also defined over portions of the same domain. The domain is discretized and fields are defined on the discretized elements (nodes or cells). Using discretization techniques such as finite element or finite differences methods, PDE are turned into a set of ordinary differential equations (ODEs). This set of equations are solved together with the AE, simultaneously or using operator splitting techniques, for every discrete time interval.

The above description points to a natural class structure for our problems. The PDEs share attributes such as definitions domain, state variables or terms in the equation and functionalities such as computing the balance or the matrices for the ODE. Therefore, we find it natural to define a class, termed *Phenomenon*, to identify PDEs. In the same fashion, we define *Process* as the class whose instances will be specific terms in the PDE (e.g. advection, dispersion, etc). The class *Meshfields* defines objects representing space (and time) various properties. For chemical systems we use the class *CHEPROO* (Bea et al. 2009). All of these produce the terms for the (non-linear) ODEs, which are solved with the functions of the class *Solver*. The structure is shown in Figure 4-1 and specific details about these classes are given below.

4.3.1. Phenomenon class

PDEs are central ingredient of MPRT modeling. All PDEs represent a conservation principle. All of them consist of different terms, like storage, flux divergence or source terms. All of them are subject to initial and boundary conditions. Therefore, we define a class for representing PDEs. We term this class *Phenomenon*. A number of authors have defined similar classes in their analysis (Meysman et al. 2003, Boivin and Ollivier-Gooch 2004, Kolditz and Bauer 2004). The main attributes of the *Phenomenon* class are the terms that define the PDE and the initial and boundary conditions. Methods include the computations of balances or the contribution to matrices comprising the ODEs (discrete version of the PDE). The values of the solution variables will be obtained from the solution of this matrix system.

A *Phenomenon* object can be used to represent a single conservation principle, such as energy or a species mass, or several conservation principles with similar equations, like components concentrations. For this latter case, *Phenomenon* class makes use of the fact that the same conservation equation applies to all components, and therefore only one PDE has to be defined which applies to all components.

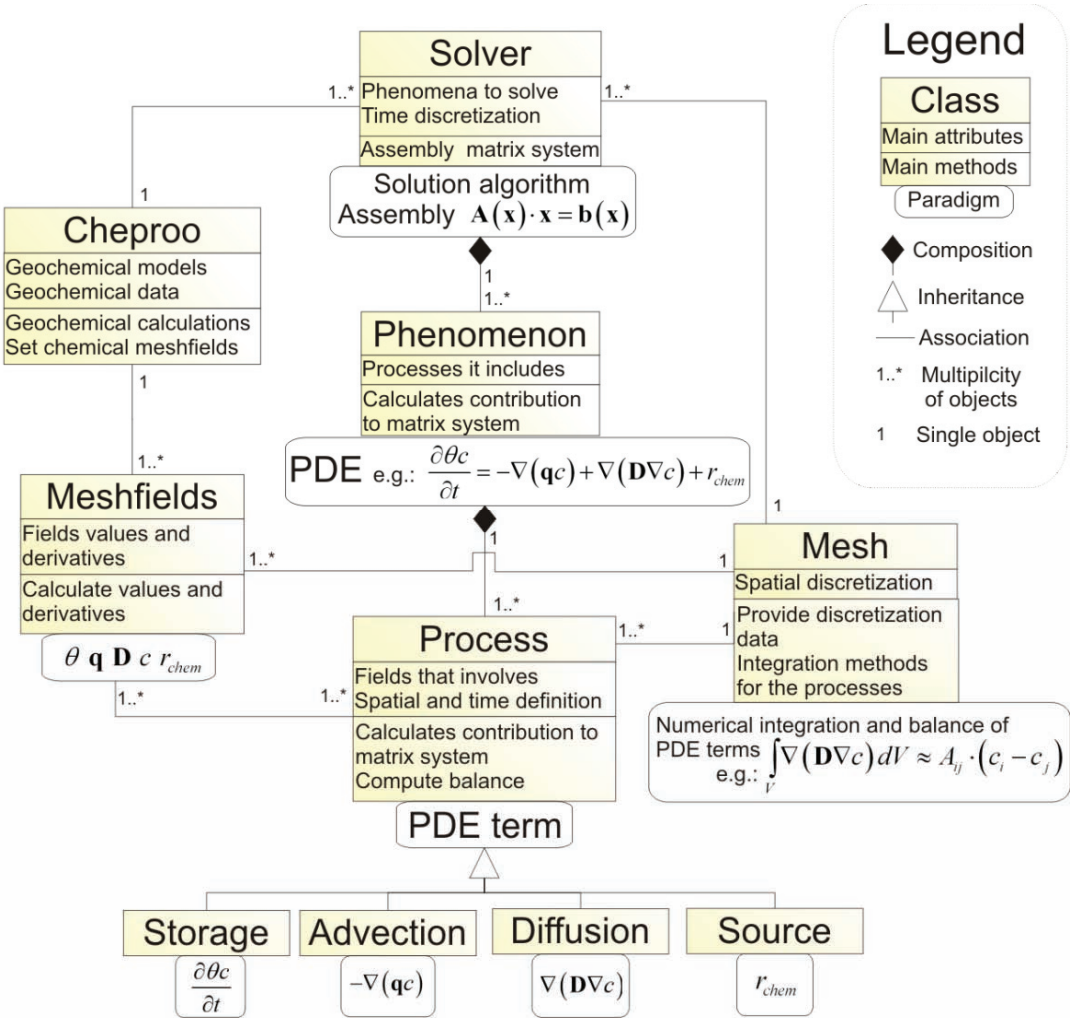

Figure 4-1 – Organization of main classes in PROOST. Each box represents a class with its attributes and methods. A paradigm is show below each class.

4.3.2. Process class

The terms that compose the PDE (e.g., storage or advection) and the boundary conditions that constrain it (eg leakage) are represented by the *Process* class. The actual nature of the term is defined via inheritance by specialization classes (Figure 4-1).

The main attributes of this class are the time and space where the *Process* is acting (for example the location of a pumping well for a sink-source *Process*) and the fields it involves (the pumping rate in this example). Methods include the computation of the process contribution to the matrix system or to the global balance. All these are performed by calling methods of the class *Mesh*, where all discretization-integration information and methods are encapsulated.

The *Processes* objects are the "basic bricks" to build conservation equations. A *Phenomenon* can be formulated by combining different *Processes*. This class facilitates the extensibility of the code because only the new terms (new specialization of the class *Process*) have to be programmed to extend the set of equations that can be solved. It also allows reusing code, since *Processes* of different conservation equation are different objects of the same class.

4.3.3. Mesh class

There are different techniques to solve PDEs numerically. All these techniques share a domain discretization approach (such as nodes, elements or cells) and methods to integrate (or differentiate) the terms (*Process*) of a PDE (*Phenomenon*) to produce a matrix system from which the discrete solution of the PDE can be obtained.

Thus, all the data and functionality regarding spatial discretization and the discretization-integration methods for solving PDE (such as finite element or finite differences) define a class that we term *Mesh*. A number of authors have defined similar classes in their analysis. However, most of them separate the domain discretization from the integration methods in different classes (Dubois-Pelerin and Pegon 1997, Masters et al. 1997, Zimmermann et al. 1998, Commend and Zimmermann 2001 ,Wang and Kolditz 2007).

The main attributes of the *Mesh* class are the domain discretization information (such as nodes or cell coordinates and connectivity between these discrete elements). Methods include yielding information of space discretization (such as the number of discrete elements and their geometrical information), integrating the different terms of the conservation equation (*Processes*) over the domain, and evaluating spatial properties of variables such as gradients.

The *Mesh* class allows incorporating new discretization-integration numerical methods by adding new specializations of the class. Two specializations of the class Mesh are currently implemented in PROOST: the Finite Elements and the Mixed Finite Elements.

4.3.4. Meshfield class

Another important element of MPRT modeling are the AEs that represent constitutive and thermodynamic laws. Constitutive laws express one field as a function of others.

Thus a class termed *Meshfield* is defined to represent the projection of different scalar, vector or tensor fields (such as pressure, flux or conductivity) in the discrete domain. The main attributes of this class are the values and derivatives of a field for the discrete entities (nodes, elements or cells) and the parameters of the function, or constitutive laws they represent. The main methods of the class are to calculate its values and derivatives, and to interpolate its values over any point of the domain.

For example a flux *Meshfield* object defined as $\mathbf{q} = -\mathbf{T}\nabla h$, can calculate its values and its derivatives to transmissivity $\mathbf{T}$ and head h fields. If the *Meshfield* represents one of the solution variables of the problems its values must be set to the *meshfield*, which cannot calculate them.

This class facilitates code expansion since new constitutive laws can be easily added to the code by creating new specializations.

4.3.5. CHEPROO class

Many geochemical variables affect the evolution of the system but do not appear explicitly in any PDE (e.g. the activity of aqueous species). For this reason and also because of the complexity of some geochemical calculations, all geochemical models and computations are encapsulated into a class termed *CHEPROO*. Only the chemical variables that appear in PDE (such as component concentration or density) are stored by a specialization of the *Meshfield* class termed *Chemical Meshfield*.

The *CHEPROO* class uses a module with the same named (Bea et al.2009), with an internal class hierarchy including classes like species, phase and reaction.

CHEPROO attributes include the geochemical models, such as those for activity coefficients, density or kinetic rates laws, and the chemical data associated to each discrete point of the problem, such as concentrations or components definition. *CHEPROO* includes methods for calculating the values and derivatives of chemical variables (like component concentration) from the solution variables of the PDE, and for storing them into *chemical meshfield* objects.

CHEPROO objects also control the number of chemical components. For some formulations, like the one of Saaltink et al. (1998), the number of components may change in time and space.

Thus, *CHEPROO* has to provide information about the components in order to establish the dimension of the final matrix system to be solved.

4.3.6. Solver class

A coupling strategy (coupled or decoupled) needs to be chosen when solving several PDE. A solution technique for nonlinear systems (Newton-Raphson or Picard) is also needed. An object of the *Solver* class will be in charge of solving a number of PDEs with a chosen solution strategy.

Solver attributes include the set of *Phenomena*, the coupling strategy, the time discretization parameters or the convergence criteria. Methods are required for assembling and solving the ODE system, for time integration. To address these, *Solver* needs other class. For instances, matrix systems are handled by a class termed *Matrix* that encapsulates matrix data and solution techniques.

Solver is the class that contributes most to the flexibility of the code since it can be set to solve several conservation equations following different strategies. For example, it might be set to solve first a steady state phase conservation equation (for phase flow calculation) and then a transient component conservation. Or it can be set to solve coupled the component and energy conservation.

4.3.7. Component conservation Phenomenon for the SIA and DSA approach

Despite the fact that the SIA and DSA are two approaches for solving the same *Phenomenon*, (the component conservation equation), the way this *Phenomenon* is formulated in PROOST depends on the chosen approach.

When solving component conservation equations with the DSA approach the input Phenomenon for PROOST should be the same as in equation (4-4). But for the SIA approach immobile species storage and kinetic reactions are treated as a sink-source term (Saaltink et al. 2001):

$$f_{SIA_i} = -\sum_{\beta} \frac{\partial}{\partial t}\left(\theta_\beta u_{i,\beta}\right) + k_{u_i} + f_{u_i} \tag{4-5}$$

Thus the component conservation equation is written only in terms of mobile component conservation:

$$\sum_{\alpha} \frac{\partial}{\partial t}\left(\theta_\alpha u_{i,\alpha}\right) = \sum_{\alpha} L_\alpha\left(u_{i,\alpha}\right) + f_{SIA_i} + f_{u_i} \tag{4-6}$$

The SIA sink source term values are calculated by *CHEPROO* and stored into a *Chemical Meshfield* that will be used by a sink-source *Process*.

4.4. Solution procedure for a time step

The interaction between PROOST objects can be illustrated by the solution of a time interval for a reactive transport problem. The flow diagram is shown in Figure 4-2, from were 15 relevant points have been identified.

1. *Solver* establishes the size of the matrix system to be solved. This size depends on the number of coupled phenomena and their dimension recall that component conservation dimension can be different for each discrete point and may change among the iterative process.
2. *Solver* assembles the matrix system to be solved. To this end, *Solver* requests each *Phenomenon* for its contribution.
3. *Phenomena* asks for the contribution of all its *Processes.*
4. *Proceses* ask the values of all the *Meshfields* they contain.
5. *Meshfield* computes its values.
6. *CHEPROO* calculates c*hemical meshfield* values*.*
7. *Mesh* computes the contribution of the process to the matrix system.
8. *Matrix* solves the matrix system.
9. *Solver* updates the calculated solution variables (concentrations, temperature or pressures) in *CHEPROO.*
10. *CHEPROO* calculates the concentration of all species from these values (speciation). If there are important changes on chemical composition, geochemical calculation might not converge. If that is the case, the length of time interval is reduced and the resolution procedure is restarted.

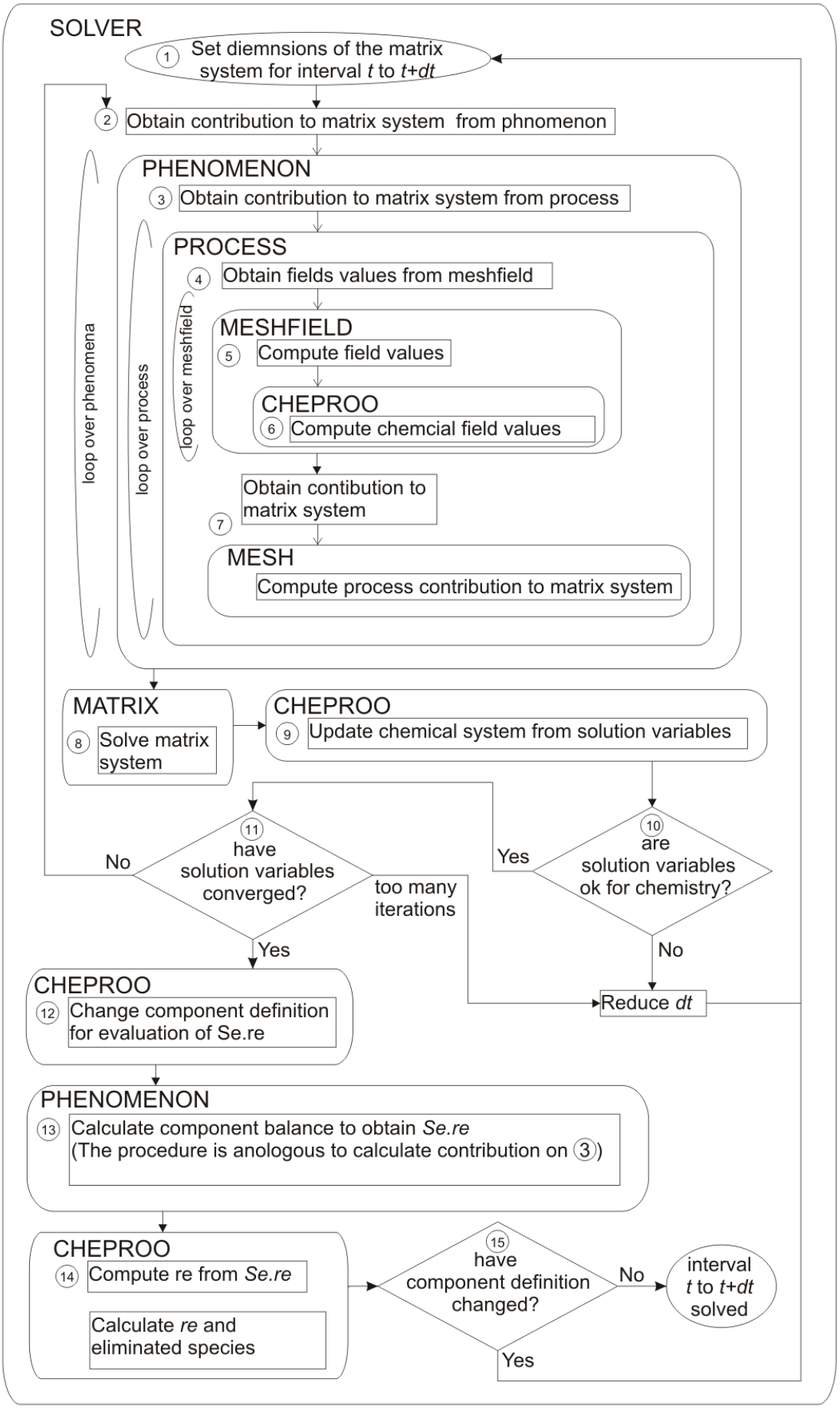

Figure 4-2 – Flow diagram of the resolution of a time interval for a reactive transport problem in PROOST both for SIA and for DSA

11. *Solver* controls convergence.

    When convergence is reached all variables involved in the *phenomena* are known, except equilibrium reactions rates that were eliminated when solving component conservation (equation (4-4)). These rates can be calculated from the species conservation equations (equation (4-2)). In order to avoid the formality of formulating both components and species *Phenomenon*, this is done by considering an alternative component definition; each species is considered a component. Therefore, the result of the balance of the new component conservation will be the product of the stoichiometric coefficient and the equilibrium reaction rates.
12. *CHEPROO* changes component definition (each species is considered a component)
13. *Phenomenon* computes balance (similar to step 3)
14. *CHEPROO* calculates equilibrium reaction rates from *Phenomenon* balance. Some reactive transport formulations, like the one of Saaltink et al. (1998), eliminate constant activity species, like minerals, from component composition. These species concentration can be calculated once the equilibrium reaction rates are known.
15. If the formulation considered eliminates constant activity species, the number of component is affected by the disappearance or appearance of minerals. Therefore, component definition has to be controlled after the eliminated species were calculated. If component definition changes the resolution procedure has to be started for the new definition, if not then resolution procedure for the time step is finished.

4.5. Code implementation

4.5.1. Implementation language

The code was programmed in FORTRAN 95 following the OO paradigm. This language was chosen for its high popularity among hydrogeologists and its excellent performance reputation. Even though FORTRAN is not a full object-oriented language it can directly support many of the important concepts of OO programming. Details about OOP concepts in FORTRAN can be found in Maley et al. (1996), Decyk et al. (1998), Norton et al. (1998), Akin (1999), Carr (1999) and Gorelik (2004).

4.5.2. PROOST and CHEPROO expansion and merge

The code presented results from merging and expanding two existing codes: PROOST and CHEPROO. The original design of PROOST was already capable of solving different Phenomenon,

in a coupled or decoupled way, considering different techniques for the resolution of nonlinear system (such as Newton-Raphson or Picard) (Slooten 2010). However, such a design only allowed solving Phenomenon objects that had one scalar field unknown. Also Phenomenon Processes had to be written explicitly as a function of the unknown variable. These featured clashed with the resolution of component conservation, especially when the DSA approach is considered.

The solution of component conservation equations involves considering the conservation equation of several components. As the number of components and its definition might change in time and space (because of complete dissolution or appearance of new mineral species), the number of *Phenomenon* considered would also have to vary. In order to avoid this difficulty, and as the same *Processes* affect all component concentration, only one *Phenomenon* is considered which applies to a vector variable: the component concentration vector. Therefore, *Phenomenon* and *Process* classes were expanded to handle a vector variable whose dimension may change in time and space.

Processes where originally designed to represent terms of PDE that directly involve the unknowns of the problem (i.e. main state variables of the phenomenon). For example, all *Processes* in a conservative transport problem involve the solute concentration variable which is also the unknown of this problem. When solving reactive transport by the DSA method *Processes* are formulated in terms of components but the unknowns of the problem are the primary species concentrations (Saaltink, 1998). Therefore, *Phenomenon* and *Process* classes were expanded so they can be formulated in terms of any variable and not necessarily the unknown.

Originally, CHEPROO was capable of solving single phase reactive transport problems. CHEPROO uses a matrix system calculated by another conservative transport code to formulate and solve the reactive transport problem (Bea et al. 2009). In order to take advantage of PROOST flexibility we choose to formulate and solve the multiphase reactive transport equations in PROOST instead of CHEPROO. Therefore, CHEPROO was added to PROOST structure with the only purpose of performing the chemical calculations (speciation) and provide geochemical variables values and derivatives.

Besides adding new services to make chemical variables available outside its module, several improvements were made in CHEPROO. Phase properties like density, viscosity and enthalpy, and capillary effect over water activity were added. Also a new speciation algorithm that uses the Newton-Raphson method had to be programmed due to the high nonlinearity of concentrated solutions.

4.6. Application: Evaporation of a sand column saturated with a rich $MgSO_4$ solution

4.6.1. Experiment description

Gran et al. (2009) preformed a laboratory experiment where a 24 cm sand column, initially saturated with a $MgSO_4$ solution, was subject to a constant source of heat on the top. The column was isolated except at the top, allowing vapor exchange with the atmosphere due to advection and diffusion. This experiment involves liquid and gas phase flow, advective and diffusive mass fluxes, and energy flux. In this kind of problems the interaction between different phenomena is important, especially when dry conditions and high salt contents arise. Evaporation is the main process in this kind of problems and reflects the coupling between hydrodynamics and geochemistry. Evaporation affects liquid and gas fluxes. It affects also the chemistry of the system by increasing solute concentration. Water activity, which is a key parameter for evaporation, highlights the coupled nature of the problem because its value can be influenced by osmotic effects for high solute concentrations and by capillarity effects at low saturations degrees.

As extreme dry conditions are reached, we consider a retention curve capable of representing oven dry conditions (Silva and Grifoll 2007 and and Massana 2005). Due to the high ionic strength we use of the Pitzer ion interaction model, as described by Bea et al. 2010a, to evaluate activities of aqueous species. The psychometric law was considered to include capillary effect in water activity. The problem was solved using the DSA approach and the finite element specialization of the class *Mesh*. Problem parameters and constitutive models are shown in Table 4-1, chemical reaction considered are summarized in Table 4-2 boundary and initial conditions are shown in Table 4-3 (modified from Gran et al. 2009).

Table 4-1 - Constitutive equations

Retention curve (modified van Genuchten model)	$S_l = S_i + (1-S_i)S_e$ $S_e = \left(1+\left(P_g - P_l/P_0\right)^{\frac{1}{1-\lambda}}\right)^{-\lambda}$ $S_i = S^0_{\min}\alpha \ln\left(P_c^{dry}/\left(P_g - P_l\right)\right)$	$P_0 = 25\text{x}10^{-4}\left[\text{MPa}\right]$ $\lambda = 0.93\ ;\ \alpha = 0.1$ $S^0_{\min} = 0.08$ $P_c^{dry} = 650\left[\text{MPa}\right]$
Relative permeability	$K_{rl} = \begin{cases} K^0_{rl} & S_l > S_{l,min} \\ K^0_{rl}\left(S_l/S_{l,min}\right)^{\gamma} & S_l < S_{l,min} \end{cases}$ $K^0_{rl} = \sqrt{S_e^{'}\left(1-\left(1-S_e^{'1/\lambda}\right)^{\lambda}\right)^2}$ $K_{rg} = 1 - K_{rl}$	$S_e^{'} = \frac{S_l - S^0_{\min}}{1-S^0_{\min}}$ $S_{l,min} = 0.1$ $\gamma = 5$
Intrinsic permeability	$\mathbf{K} = \mathbf{K}_0\left(\frac{\phi}{\phi_0}\right)^3\left(\frac{1-\phi_0}{1-\phi}\right)^2$	$\mathbf{K}_0 = 2.8\text{x}10^{-11}\left[m^2\right]$ $\phi_0 = 0.4$
Phase density	$\rho_{liq} = P_0 \exp\left(\alpha T + \beta\left(P_l - P_0\right) + \gamma\left(\sum_{i\neq h_2o}\omega_l^i\right)\right)$ $\rho_{gas} = \frac{P_{g,vap}\cdot M_{vap} + P_{g,air}\cdot M_{air}}{R\left(T+273.15\right)}$	$P_0 = 1002.6\left[\text{MPa}\right]$ $\alpha = -3.4\text{x}10^{-4}\left[{}^{\text{o}}C^{-1}\right]$ $\beta = 4.5\text{x}10^{-4}\left[\text{MPa}^{-1}\right]$ $\gamma = 0.6923$ $M_{vap} = 0.018\left[Kg/mol\right]$ $M_{air} = 0.02895\left[Kg/mol\right]$
Phase viscosity	$\mu_{\text{liq}} = 2.1\text{x}10^{-12}\cdot\exp\left(\frac{1808.5}{T+273.15}\right)\left[\text{MPa}\cdot\text{s}\right]$ $\mu_{\text{gas}} = 1.48\text{x}10^{-12}\cdot\exp\left(\frac{119.4}{T+273.15}\right)\left[\text{MPa}\cdot\text{s}\right]$	
Phase diffusion	$D^{diff}_{gas} = 5.9x10^{-6}\left(\frac{\left(T+273.15\right)^{2.3}}{P_g}\right)\left[m^2/s\right]$ $D^{diff}_{liq} = 1.1x10^{-4}\exp\left(\frac{-24539}{R\cdot\left(T+273.15\right)}\right)\left[m^2/s\right]$	
Vapor enhancement factor	$\theta_{gas}\tau = 1$	
Thermal conductivity	$\lambda = \lambda_{sat}^{S_l}\lambda_{dry}^{(1-S_l)}\left[\text{Wm/K}\right]$	$\lambda_{sat} = 1.44\ ;\ \lambda_{dry} = 1.54$

Table 4-2 – Chemical reactions considered

$H_2O_{(l)} \Leftrightarrow H_2O_{(g)}$	$K_{vapour} = 1.36075\text{x}10^{11} \exp\left(\frac{-5239.7}{273.15+T}\right)\left[\frac{\text{Pa}\cdot Kgh_2o}{mol}\right]$
$air_{(l)} \Leftrightarrow air_{(g)}$	$K_{air} = 2.9\text{x}10^{8}\left[\frac{\text{Pa}\cdot Kgh_2o}{mol}\right]$
$H_2O_{(l)} \Leftrightarrow H^+ + OH^-$	$K_{oh} = 10^{-14}$
$Mg^{2+} + OH^- \Leftrightarrow Mg(OH)^+$	$K_{mg(oh)} = 10^{2.19}$
$SO_4^{2+} + H^+ \Leftrightarrow H(SO_4)^-$	$K_{h(so4)} = 10^{1.98}$
$Mg^{2+} + SO_4^{2-} + 7H_2O_{(l)} \Leftrightarrow epsomite$	$K_{epsomite} = 10^{1.8881}$
$Mg^{2+} + SO_4^{2-} + 6H_2O_{(l)} \Leftrightarrow hexahydrite$	$K_{hexahydrite} = 10^{1.7268}$
$Mg^{2+} + SO_4^{2-} + 5H_2O_{(l)} \Leftrightarrow pentahydrite$	$K_{pentahydrite} = 10^{1.285}$
$Mg^{2+} + SO_4^{2-} + 4H_2O_{(l)} \Leftrightarrow leonhardite$	$K_{leonhardite} = 10^{0.887}$
$Mg^{2+} + SO_4^{2-} + H_2O_{(l)} \Leftrightarrow kieserite$	$K_{kieserite} = 10^{0.123}$

Table 4-3- Boundary and initial conditions

Initial conditions	$S_l = 1$; $T = 25^{\circ}C$;	
	Hydrostatic liquid pressure: $P_l^{top} = 101325\left[\text{Pa}\right]$	
Top boundary gas flow	$j_i^{top} = \alpha\left(P_g^{ext} - P_g^{top}\right)\cdot c_i^* + \beta\left(P_i^{ext} - P_i^{top}\right)$	$\alpha = 43\left[m/\left(\text{MPa}\cdot s\right)\right]$
		$\beta = 1.5\left[mol/\left(\text{MPa}\cdot s\cdot m^2\right)\right.$
	$c_i^* = \begin{matrix} c_i^{ext} & P_g^{ext} > P_g^{top} \\ c_i^{top} & P_g^{ext} < P_g^{top} \end{matrix}$	$P_{h_2o}^{ext} = 3172\left[\text{Pa}\right]$
		$P_{air}^{ext} = 98152\left[\text{Pa}\right]$
Top boundary heat flow	$j_{e,in} = 750\left[J/s\right]$	
Heat lose	$j_{e,lose} = \alpha\left(T_{ext} - T\right)$	$\alpha = 25\left[J/\left(K\cdot s\right)\right]$; $T_{ext} = 26\left[^{\circ}C\right]$
Initial concentrations	$H_2O_{(l)} = 5.551\text{x}10^{1}\left[m\right]$	
	$air_{(l)} = 5.453\text{x}10^{-4}\left[m\right]$	$Cl^- = 5.700\text{x}10^{-3}\left[m\right]$
	$Ca^{2+} = 2.000\text{x}10^{-2}\left[m\right]$	$H_2O_{(g)} = 3.173\text{x}10^{-3}\left[\text{MPa}\right]$
	$SO_4^{2+} = 1.720\text{x}10^{-2}\left[m\right]$	$air_{(g)} = 9.815\text{x}10^{-2}\left[\text{MPa}\right]$
	$K^+ = 1.000\text{x}10^{-4}\left[m\right]$	$\phi = 0.4$

4.6.2. Column evolution

Saturation, temperature, Mg concentration and vapor partial pressure profiles are shown in Figure 4-3. From the partial pressure profile it can be seen that a descending evaporation front is produced which divides the column in two zones: a dry zone where the concentrations are higher and a wet zone with lower concentrations. The temperature curve shows a change in its slope at the evaporation front due to the energy required for evaporation.

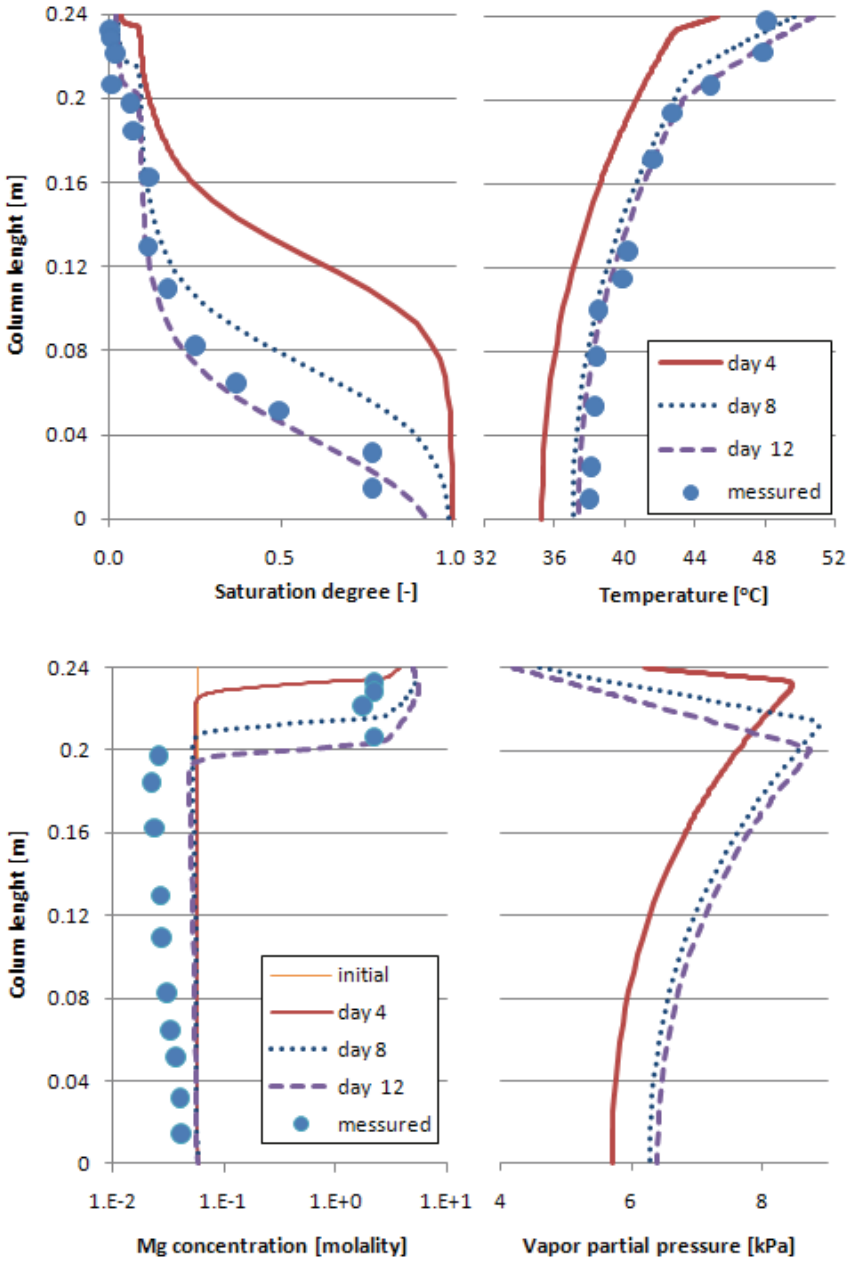

Figure 4-3 Saturation and temperature (above), Mg concentration and vapor partial pressure (below) modeled for day 4, 8 and 12, and experimental data for day 12.

The model fits well saturation and temperature data. Mg concentration evolution is only qualitatively reproduced. Below the evaporation front concentration is reduced below initial values. This is due to the condensation of vapor that diffuses from the evaporation front (Figure 4-4). The evaporation front produces an ascent vapor flux above its peak and a descend flux below.

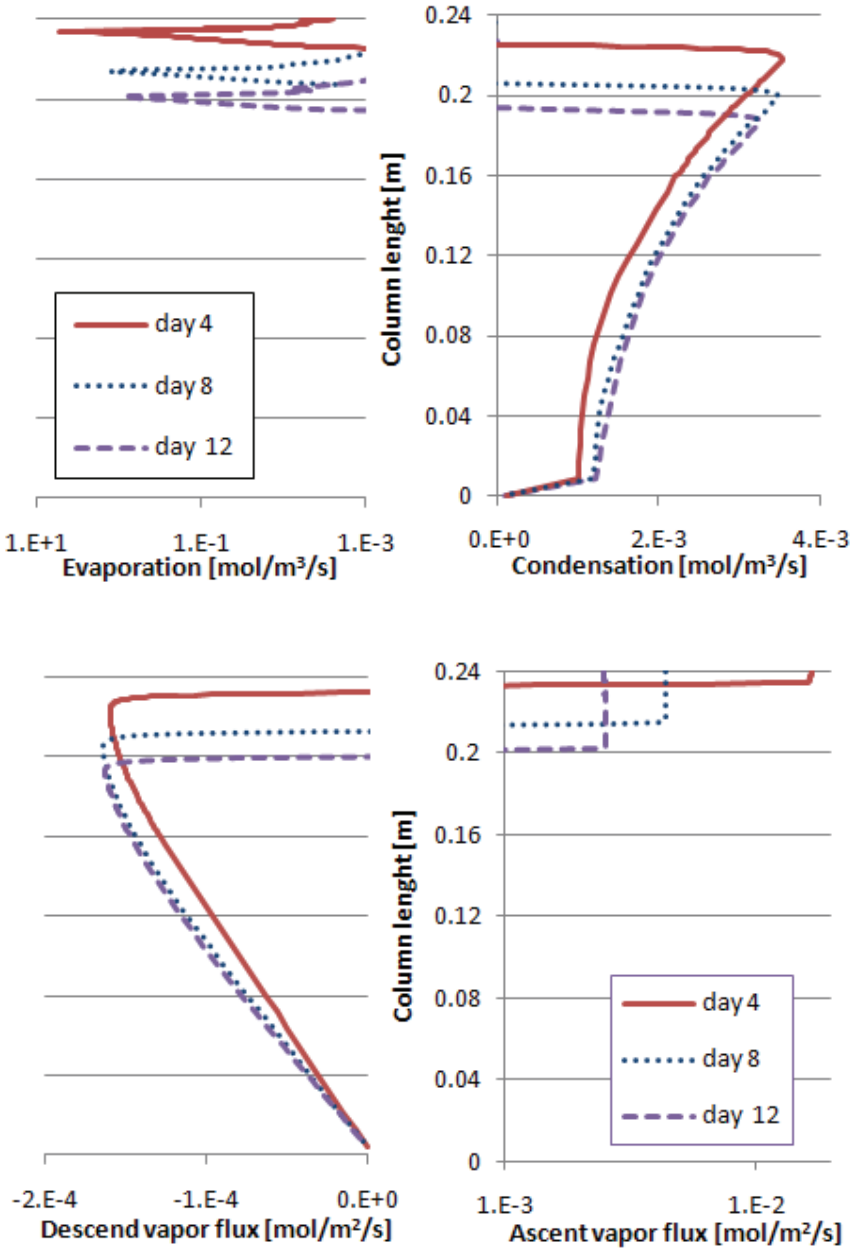

Figure 4-4 – Evaporation-condensation and vapor transport evolution. The evaporation front produces an ascent vapor flux above its peak and a descend flux below.

When a rich $MgSO_4$ water is evaporated a sequence of hydrated $MgSO_4$ minerals (epsomite, hexahydrite and kieserite) is expected. The coexistence of epsomite-hexahydrite or hexahydrite-

kieserite produces an invariant point which fixes water activity (Risacher and Clement 2001) Indeed, expressing mass action law for both mineral yields water activity as:

$$\begin{aligned} a_{Mg^{2+}} a_{SO_4^{2-}} a_{H_2O}^7 &= K_{epsomite} \\ a_{Mg^{2+}} a_{SO_4^{2-}} a_{H_2O}^6 &= K_{hexahydrite} \end{aligned} \quad \Rightarrow a_{H_2O} = \frac{K_{epsomite}}{K_{hexahydrite}} \tag{4-7}$$

Water activities are calculated considering osmotic effects (Pitzer model) and capillary effects (Psychometric law). Therefore, when minerals fix water activity not only geochemical variables are affected but also phase pressures. A fix water activity influences the evolution of the system, as can be noticed in Figure 4-5, which displays mineral mass, water activity and vapor boundary fluxes at uppermost node. It can be seen that water activity remains constant during two intervals, a small one for the epsomite-hexaydrite invariant point (before day 4), and another for the hexahydrite-kieserite (between day 5 and 6).

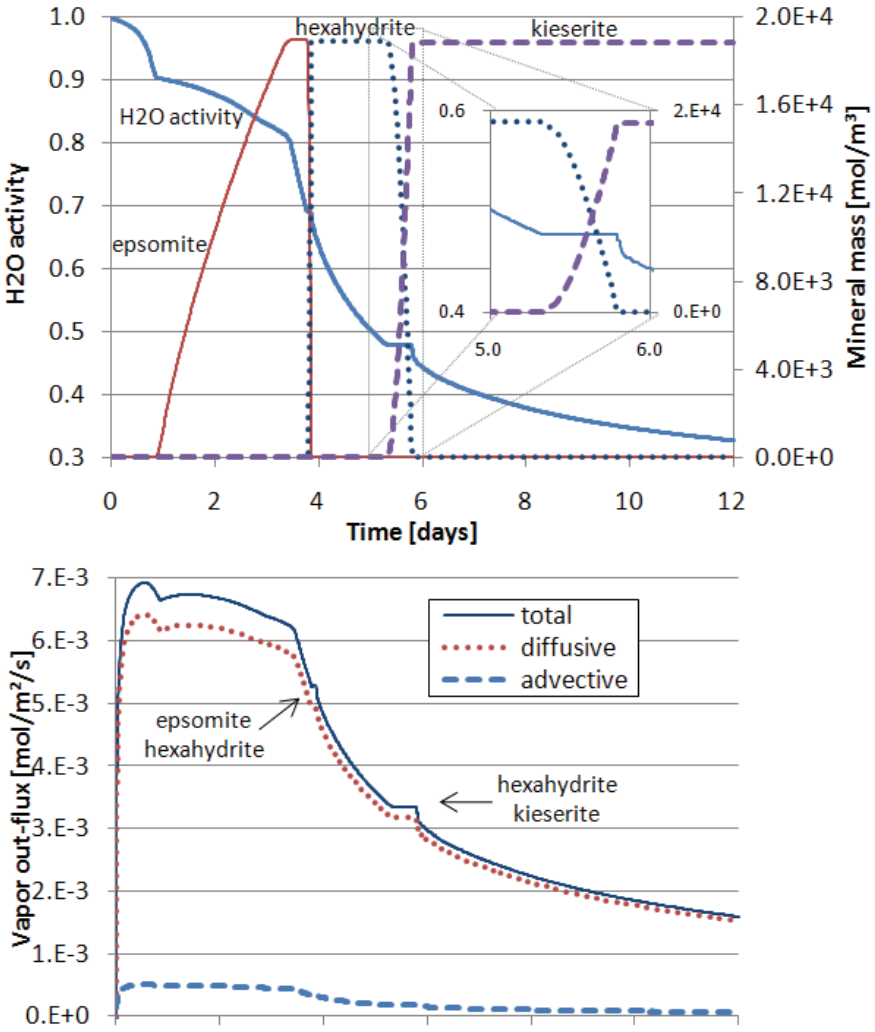

Figure 4-5 – Mineral mass and water activity (above) and vapor fluxes (below) for the uppermost node. An invariant point produced by the coexistence of epsomite and hexahydrite occurs at day 4 and another on , associated to hexahydrite and kieserite between day 5 and 6. By fixing water activity value the invariant point controls de mass of vapor that leaves the column during these periods.

Vapor flux leaving the column also stays constant during these intervals. During invariant points mineral precipitation-dissolution acts as a source term of water, releasing as many water as necessary to keep the water activity constant. As the external vapor pressure is fixed and the boundary node vapor partial pressure at the boundary is controlled by water activity, the vapor out-flux remains constant. Therefore, during these intervals the mineral paragenesis is controlling the amount of vapor that leaves the column.

The second interval is longer than the first because the passage from hexahydrite to kieserite releases more water (5 moles of water per mol of mineral) than the passage from epsomite to hexahydrite (1 mol of water per mol of mineral)

The first mineral to precipitate is epsomite (Figure 4-6-a). An epsomite precipitation front, like the evaporation front, descends through the column. The reduction in the liquid saturation increases capillary suction which reduces water activity further and, together with the increases in temperature, produces hexahydrite precipitation. Thus, there is a second precipitation front in which epsomite is turned into hexahydrite (Figure 4-6 -b). As water activity reaches lower values, a third precipitation front appears in which hexahydrite is replaced by kieserite (Figure 4-6-d).

Right after an invariant point occurs on the top of the column the amount of precipitated epsomite at the mineral front changes. The positions of the mineral front when an invariant point takes place in the top of the column are highlighted in Figure 4-6. It can be seen that after an invariant point occurs in the top of the column the amount of precipitated epsomite increases (Figure 4-6-b and Figure 4-6-d). As the precipitation front moves downwards precipitation decreases and then an almost constant precipitation is obtained.

This behavior is due to the fact that when an invariant point takes place on the top of the column the dynamic of all processes is affected. In this scenario vapor partial pressure in the top of the domain remains constant due to the water coming from mineral dehydration. This slows down the descent of the evaporation front. Meanwhile, the upwards liquid flux keeps bringing salt to the evaporation front, which causes an increase in the amount of salt precipitated at the evaporation front. This explains the peaks of mineral mass obtained in Figure 4-6.

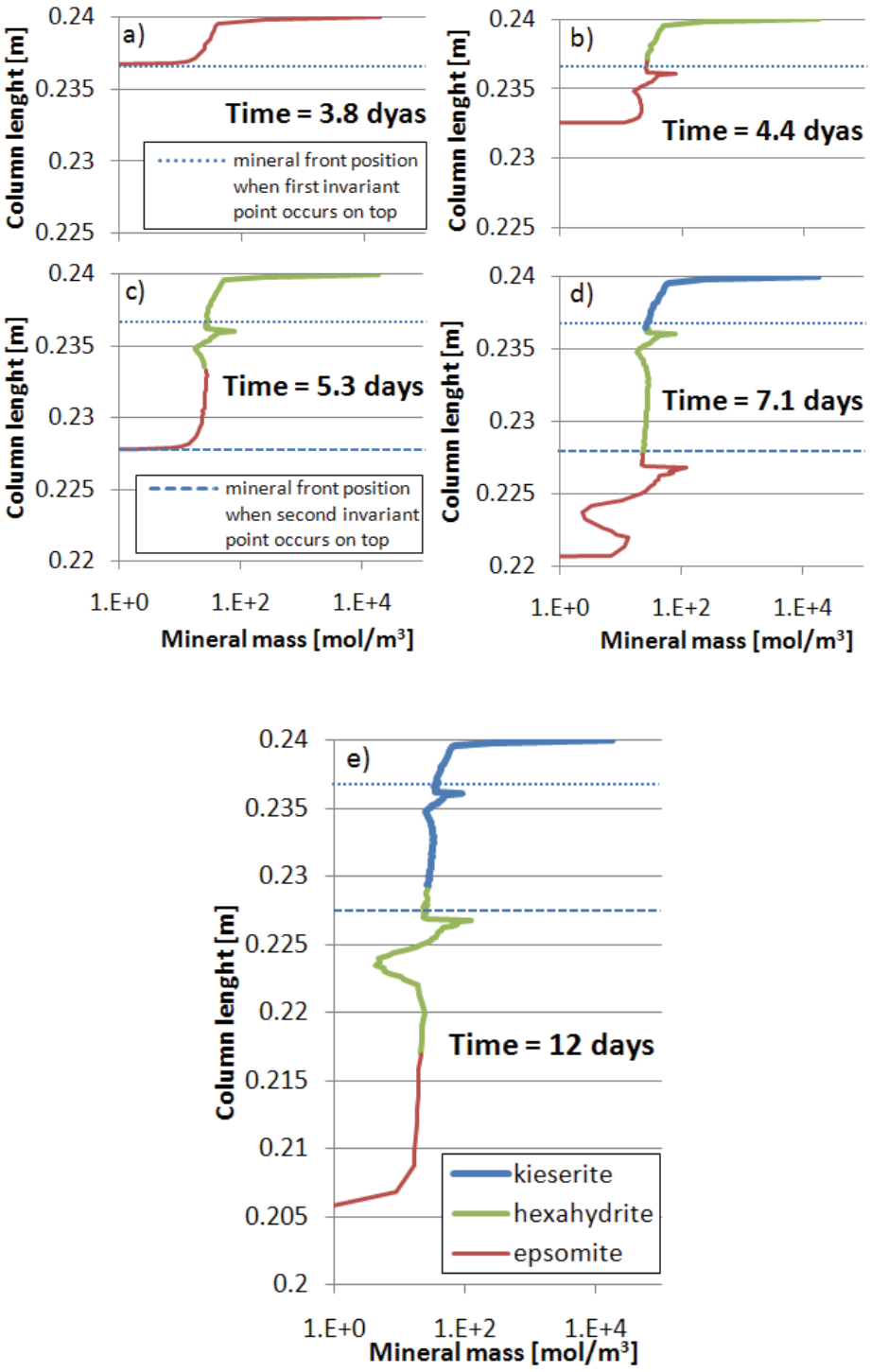

Figure 4-6 – Evolution of mineral species. The first mineral to precipitate is epsomite. As water activity diminish epsomite is replaced by hexahydrite and finally epsomite. After an invariant occurs at the top of the column, an increase followed by a decrease in the amount of precipitated mineral occurs in the mineral front.

The accumulation of water below the evaporation front produces a sharp saturation profile (Figure 4-7), and an almost uniform liquid saturation zone is obtained. In this zone the saturation gradient decreases reducing the liquid flow and also the advective and dispersive transport of

solute. Therefore, there is less solute accumulation in this zone and that is way the mineral precipitation is smaller than in the rest of the column.

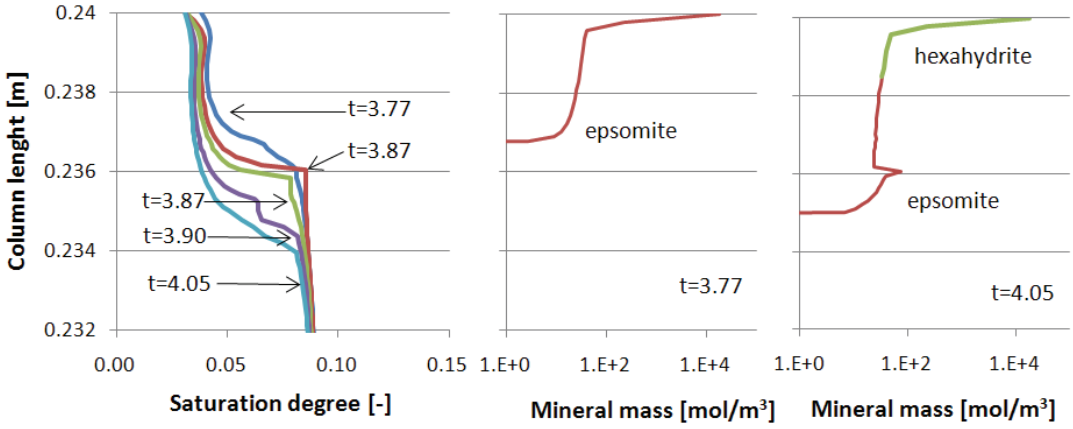

Figure 4-7 – Saturation degree and mineral mass before (t=3.77 days) an invariant point occurs at the top of the column and after (t=3.87 days).

This behavior is observed only when invariant points are occurring in the top of the domain, because this is the place where more mineral mass precipitates. The occurrence of invariant points on the rest of the column does not release enough water to affect the vapor flow because little mineral mass is available to dehydrate.

4.7. Summary and conclusions

An object oriented multiphase reactive transport structure has been presented. Its object oriented structure was designed to ensure extensibility and flexibility. Its main classes are: *Mesh* (contains all the discretization information and integration methods, such as finite elements or finite differences), *Meshfield* (represent spatial fields and the constitutive laws that relate them, like saturation or concentrations), *Phenomenon* (represents the conservation of a physical magnitude expressed as a partial differential equation (PDE), such as mass or energy conservation), *Process* (represents a ters of a *Phenomenon* PDE, like advection or storage), *Solver* (controls the coupling strategy for solving all *Phenomena* and assembles the matrix system to solve) and *CHEPROO* (encapsulates all thermodynamic date and perform chemical calculations).

The flexibility and extensibility of PROOST come from the following particularities of its design. Several *Phenomenon* can be formulated by combining the available *Process*. In order to solve a new kind of *Phenomenon,* only new *Processes* have to be programmed. The *Solver* class can be

set to solve all *Phenomena* in a coupled or decoupled way. New constitutive laws can be easily added to the code by creating new specialization of the *Meshfield* class, and new numerical methods for discretization-integration of PDE can be added by implementing new specializations of the *Mesh* class.

PROOST was used to model a laboratory experiment where a sand column saturated with a rich $MgSO_4$ solution was subjected to a source of heat. The experiment involves oven dry conditions, high salinity and hydrated mineral precipitation. A reactive transport compositional formulation was adopted for the model and several coupling effects between hydrodynamic and geochemical process were considered, like sink source of water due to evaporation-condensation and hydrated mineral precipitation-dissolution, and capillary and osmotic effects over water activity. The model was capable of representing the occurrence of several invariant points associated to the precipitation of $MgSO_4$ hydrated minerals. Model results shows that the occurrence of invariant points on the top of the domain can have an appreciable effect on the outlet of vapor from de column and on the distribution of salt precipitates along the column. In fact, invariant points explain spatial fluctuation on salt precipitates.

5. General conclusions

This thesis has been focused on several difficulties related with the modeling of geochemical processes and their interaction with the rest of multiphase reactive transport (MPRT) processes.

A novel generalized compositional formulation for modeling MPRT problems is presented. The formulation avoids the classic approach of decoupling phases and component conservation, which does not adequately represent the influence of geochemical processes on phase flows. It is based on compositional formulations that express conservation of components made of species from the different phases reacting to each other only through heterogeneous reactions (Abriola and Pinder, 1985, Forsyth and Shao, 1991, Pruess et al. 1999, Olivella et al. 1996). The compositional formulation was extended to include all sorts of geochemical processes including homogeneous reactions. In this way, geochemical and hydrodynamic processes are fully coupled. The formulation also considers the capillary and salinity effects on water activity, which makes it suitable for calculating the evolution of concentrated solutions under dry conditions. The formulation is very convenient to treating invariant points, at which water activity (and thus vapor pressure) is fixed by a set of precipitated minerals. The key of treating invariant points is to treat water as a secondary species. This leads to a much simpler algorithm than presented in previous works (Risacher and Clement, 2001). The formulation assumes that constant activity species, such as minerals, do not affect speciation and can therefore be eliminated. This reduces the number of components and the size of the system to be solved (Saaltink et al. 1998).

There are different approaches to deal with coupling effects in reactive transport problems. First, the coupling between phase flow and reactive transport can be neglected or not. Second, the reactive transport equation can be solved by means of the Direct Substitution Approach or Sequential Iterative Approach. Of course, the optimal solution strategy depends on the nature of the problem to be solved. Therefore, reactive transport code should be able to adopt different coupling techniques. A code is presented, capable of adopting these techniques, including the generalized compositional formulation. The object oriented paradigm was chosen, because it allows representing the numerical solution of MPRT as a group of interacting objects than can be

recombined easily in different ways. This facilitates flexibility and extensibility (Fenvesm 1990, Filho and Devloo 1991, Khan et al. 1995, Commend and Zimmermann 2001).

The code was used to model several batch problems including the evolution of a water sample in an evaporation chamber and the interaction between geochemistry and evaporation in shallow salt lakes. The results show that hydrated minerals can act as an important liquid water source and by controlling water activity and, hence, vapor pressure, they affect important processes such as evaporation. The code was also used to model the evaporation from several columns which involves oven dry conditions, high salinity and hydrated minerals. Results show that the occurrence of invariant points has an appreciable effect in the outlet of vapor from the column and in the distribution of salt precipitation along the column. During an invariant point, mineral precipitation-dissolution provides the exact amount of water to keep water activity constant and compensates for all the transport processes. This particular process (or any heterogeneous reaction) produces a phase sink-source term that couples phase flow and reactive transport, and makes the use of a decoupled approach more difficult.

Appendices

I. U matrix calculation

We divide the stoichiometric matrix ($\mathbf{S}_e^{tr}$) into two sub matrices:

$$\mathbf{S}_e^{tr} = \begin{pmatrix} \mathbf{S}_1^{tr} \\ \mathbf{S}_2^{tr} \end{pmatrix} \tag{5-1}$$

A component matrix $\mathbf{U}'$ can be calculated by means of the Gauss-Jordan elimination (Steefel and MacQuarrie, 1996), which leads to the following expression:

$$\mathbf{U}' = \left(\mathbf{I} \middle| -\mathbf{S}_1^{tr} \cdot \left(\mathbf{S}_2^{tr} \right)^{-1} \right) \tag{5-2}$$

Where $\mathbf{I}$ is the identity matrix of dimension $Ns - Ne$. Matrix $\mathbf{S}_2$ must be invertible.

We will consider the component matrix introduced by Saaltink et al. (1998) that also eliminates constant activity species. To do so we divide the vector of concentrations of all species into two:

$$\mathbf{c} = \begin{pmatrix} \mathbf{c}_{va} \\ \mathbf{c}_{ca} \end{pmatrix} \tag{5-3}$$

Where $\mathbf{c}_{va}$ and $\mathbf{c}_{ca}$ are vectors containing the concentration of species with variable and constant activity, respectively.

Likewise, matrix $\mathbf{U}'$ can be divided into two:

$$\mathbf{U}' = \left(\mathbf{U}'_{va} \middle| \mathbf{U}'_{ca} \right) \tag{5-4}$$

Also by means of the Gauss-Jordan elimination a matrix $\mathbf{E}$ can be obtained that satisfies:

$$\mathbf{E} \cdot \mathbf{U}'_{ca} = 0 \tag{5-5}$$

Matrix $\mathbf{U}'_{ca}$ can be divided into two:

$$\mathbf{U}'_{ca} = \begin{pmatrix} \mathbf{U}'_{ca1} \\ \mathbf{U}'_{ca2} \end{pmatrix} \tag{5-6}$$

Thus **E** is defined as:

$$\mathbf{E} = \left(\mathbf{I} \middle| -\mathbf{U}'_{ca1} \cdot \left(\mathbf{U}'_{ca2} \right)^{-1} \right) \tag{5-7}$$

Where $\mathbf{I}$ is the identity matrix of dimension $Ns - Ne - Nm$. Matrix $\mathbf{U}'_{ca2}$ must be invertible.

The component matrix $\mathbf{U}$ that eliminates equilibrium reaction rates and constant activity species is defined as:

$$\mathbf{U} = \mathbf{E} \cdot \mathbf{U}' \tag{5-8}$$

II. Code Verification

A. Outline

In this appendix PROOST is used to solve several problems. Results are compared to the ones from other codes and experimental data when available. A complete description of every problem is given or can be found in the references.

B. Numerical modeling of seawater evaporation path

McCaffrey et al. (1987) analyzed samples of brines and salts from a solar salt production facility. Data are available up to a degree of evaporation of 100. The evolution of this evaporation path was modeled following the same procedure used for the evaporation chamber experiment discussed on section 2.3. For the modeling a temperature of 25 ºC and a relative humidity of 0.4 were considered. The evaporation rate was calculated using Dalton's equation with a mass transfer coefficient mentioned in section 2.3. Mineral species considered in the chemical system are shown in Table II-1.

Table II-1 – Mineral species considered on the chemical system for seawater evaporation path

Mineral name	Mineral formula
Anhydrite	$CaSO_4$
Bischofite	$MgCl_2 \cdot 6H_2O$
Bloedite	$Na_2Mg(SO_4)_2 \cdot 4H_2O$
Calcite	$CaCO_3$
Carnallite	$KMgCl_3 \cdot 6H_2O$
Epsomite	$MgSO_4 \cdot 7H_2O$
Glauberite	$Na_2Ca(SO_4)_2$
Gypsum	$CaSO_4 \cdot 2H_2O$
Halite	NaCl
Hexahydrite	$MgSO_4 \cdot 6H_2O$
Kainite	$KMgClSO_4 \cdot 3H_2O$
Kieserite	$MgSO_4 \cdot H_2O$
Magnesite	$MgCO_3$
Pentahydrite	$MgSO_4 \cdot 5H_2O$
Polyhalite	$K_2Ca_2Mg(SO_4)_4 \cdot 2H_2O$

The simulation was carried out until no more water could evaporate from the system. Concentration values obtained are compared with the available data until a degree of evaporation of 100 (Figure II-1) The evolution of mineral species are plotted together with the EQL/EVP code results (Risacher and Clement, 2001) in Figure II-2. A significant agreement between both codes was found. In Figure II-3 invariant points of the problem are plotted in detail.

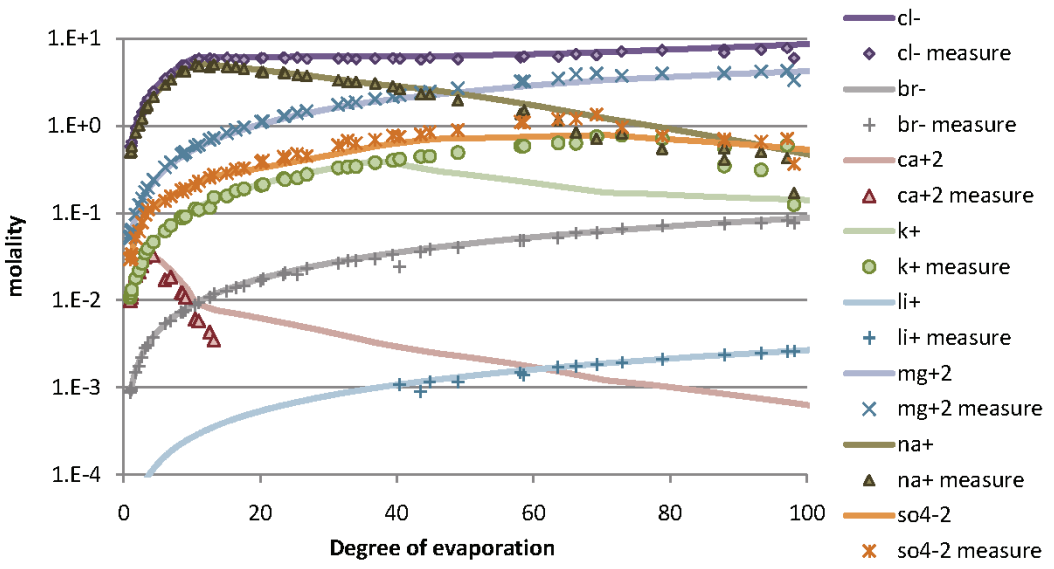

Figure II-1 – Simulated and measured concentration of evaporation path of seawater

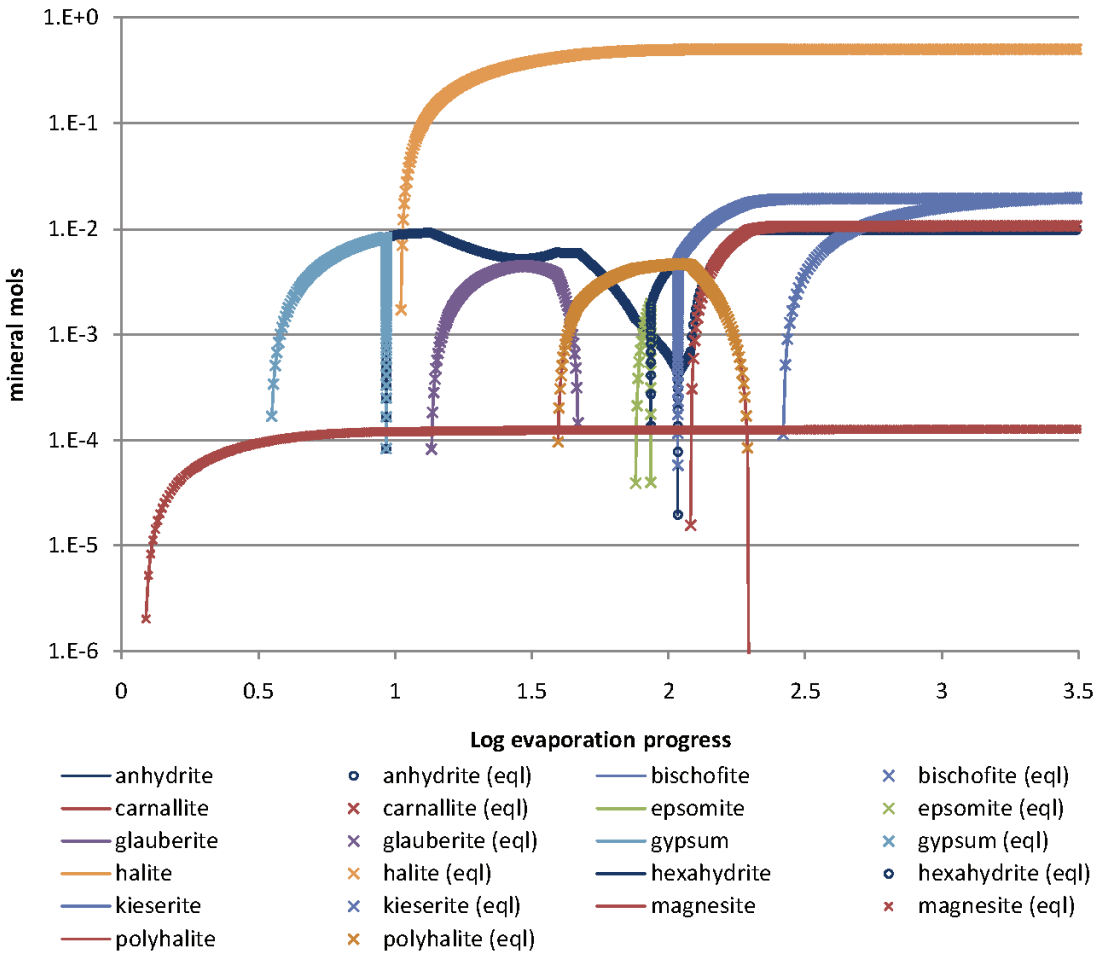

Figure II-2 – Obtained mineral precipitation of seawater evaporation path values are compared with results from the EQL/EVP code

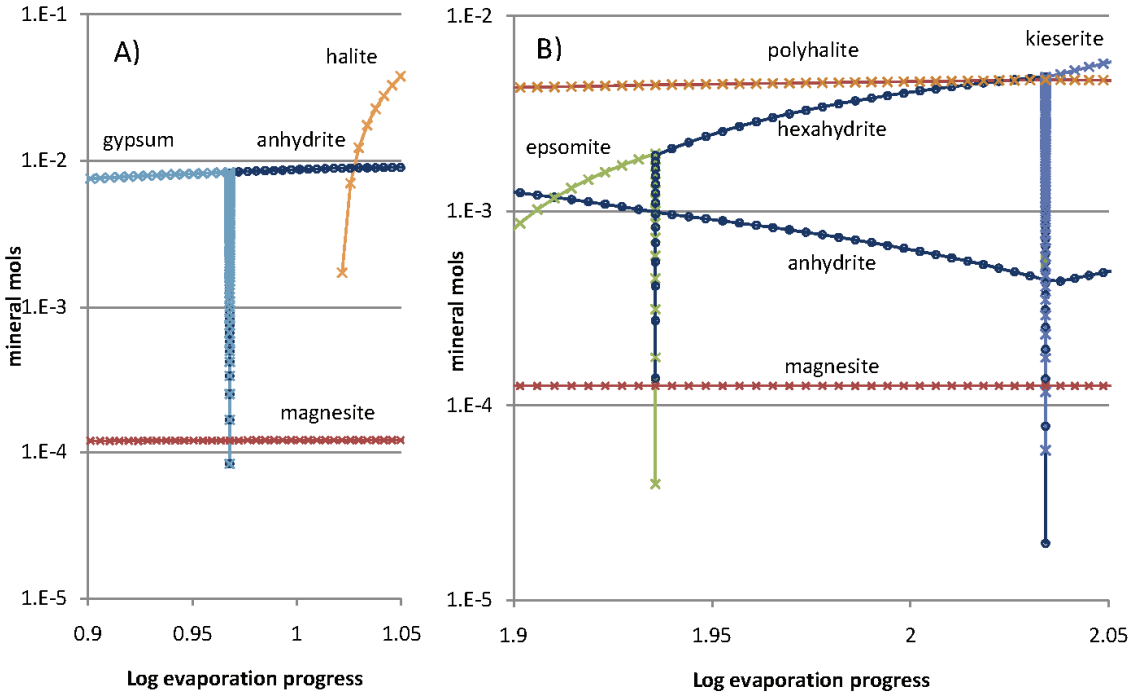

Figure II-3 – Details of invariant points shown on Figure II-2. A) Gypsum-Anhydrite invariant point. B) Epsomite-hexahydrite and hexahydrite-kieserite invariant points

C. Flushing of saline water by fresh water

Saaltink et al. (1998) modeled the flushing of saline water by fresh water, an example originally described by Appelo and Postma (1994, p.166). This one dimensional problem includes dissociation of water, carbonate reactions, cation exchange of Na, Mg, and Ca, and precipitation/dissolution of calcite. This problem was modeled using PROOST. Results from the proposed formulation, Saaltink and Appelo are plotted in Figure II-4. A significant agreement between codes results was found.

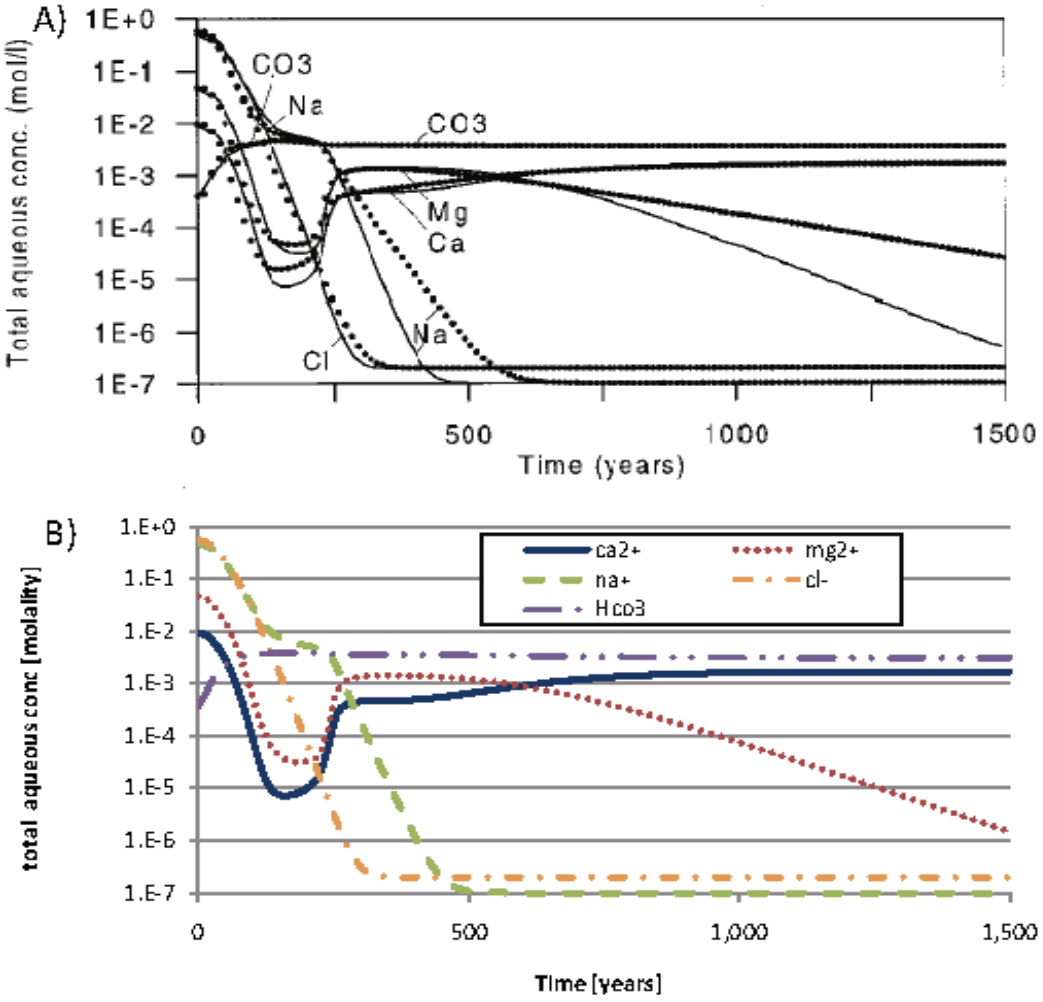

Figure II-4 – Results of modeling flushing of saline water by fresh water (B) are compared with results from RETRASO (A solid line) and PHREEQM (dotted line) codes

D. Natural attenuation of phenolic compounds

Mayer et al. (2001) modeled the natural attenuation of a plume of phenolic contaminant in the West Midlands, UK. For the sake of simplicity, only one phenolic compound was considered in our calculations. As a consequence, the effective reaction rates were slightly modified in order to reproduce result present by Mayer et al. (2001).

The following reactions and rate-limiting processes were considered:

1) aerobic respiration, limited by the substrate (phenol) and the electron acceptor (oxygen) availability:

$$\frac{1}{7}C_6H_6O + O_2 + \frac{3}{7}H2O \Rightarrow \frac{6}{7}HCO_3^- + \frac{6}{7}H^+ \quad (5\text{-}9)$$

2) denitrification: substrate and electron acceptor limitation, inhibited by the presence of oxygen:

$$\frac{5}{26}C_6H_6O + NO_3^- + \frac{1}{28}H_2O \Rightarrow \frac{15}{14}HCO_3^- + \frac{1}{2}N_2 + \frac{1}{14}H^+ \quad (5\text{-}10)$$

3) reductive dissolution of pyrolusite (MnO_2), substrate and electron acceptor limitation, inhibited by the presence of oxygen and nitrate:

$$\frac{1}{14}C_6H_6O + MnO_2 + \frac{11}{7}H^+ \Rightarrow \frac{3}{7}HCO_3^- + \frac{1}{2}Mn^{+2} + \frac{11}{14}H_2O \quad (5\text{-}11)$$

4) reductive dissolution of goethite (FeOOH), substrate and electron acceptor limitation, inhibited by the presence of oxygen and nitrate:

$$\frac{1}{28}C_6H_6O + FeOOH + \frac{25}{14}H^+ \Rightarrow \frac{3}{14}HCO_3^- + Fe^{+2} + \frac{39}{28}H_2O \quad (5\text{-}12)$$

5) sulfate-reduction: substrate and electron acceptor limitation, inhibited by the presence of oxygen and nitrate, and inhibited by the presence of high phenol concentrations due to toxic effects on the sulfate-reducing bacteria:

$$\frac{2}{7}C_6H_6O + SO_4^{-2} + \frac{6}{7}H_2O + \frac{2}{7}H^+ \Rightarrow \frac{12}{7}HCO_3^- + H_2S \quad (5\text{-}13)$$

6) methane fermentation, inhibited by the presence of oxygen and nitrate:

$$\frac{2}{7}C_6H_6O + \frac{13}{7}H_2O \Rightarrow \frac{5}{7}HCO_3^- + CH_{4(aq)} + \frac{5}{7}H^+ \quad (5\text{-}14)$$

These modifications were formulated by Bea (2008) in his PhD thesis, and are also used to compare the results with the ones from Mayer et al. (2001). A significant agreement between both codes was found. Results from Bea are indistinguishable from the ones obtained with the implementation of the proposed formulation as the same chemical system is considered. Results are compared with the ones from Mayer et al. in Figure II-5

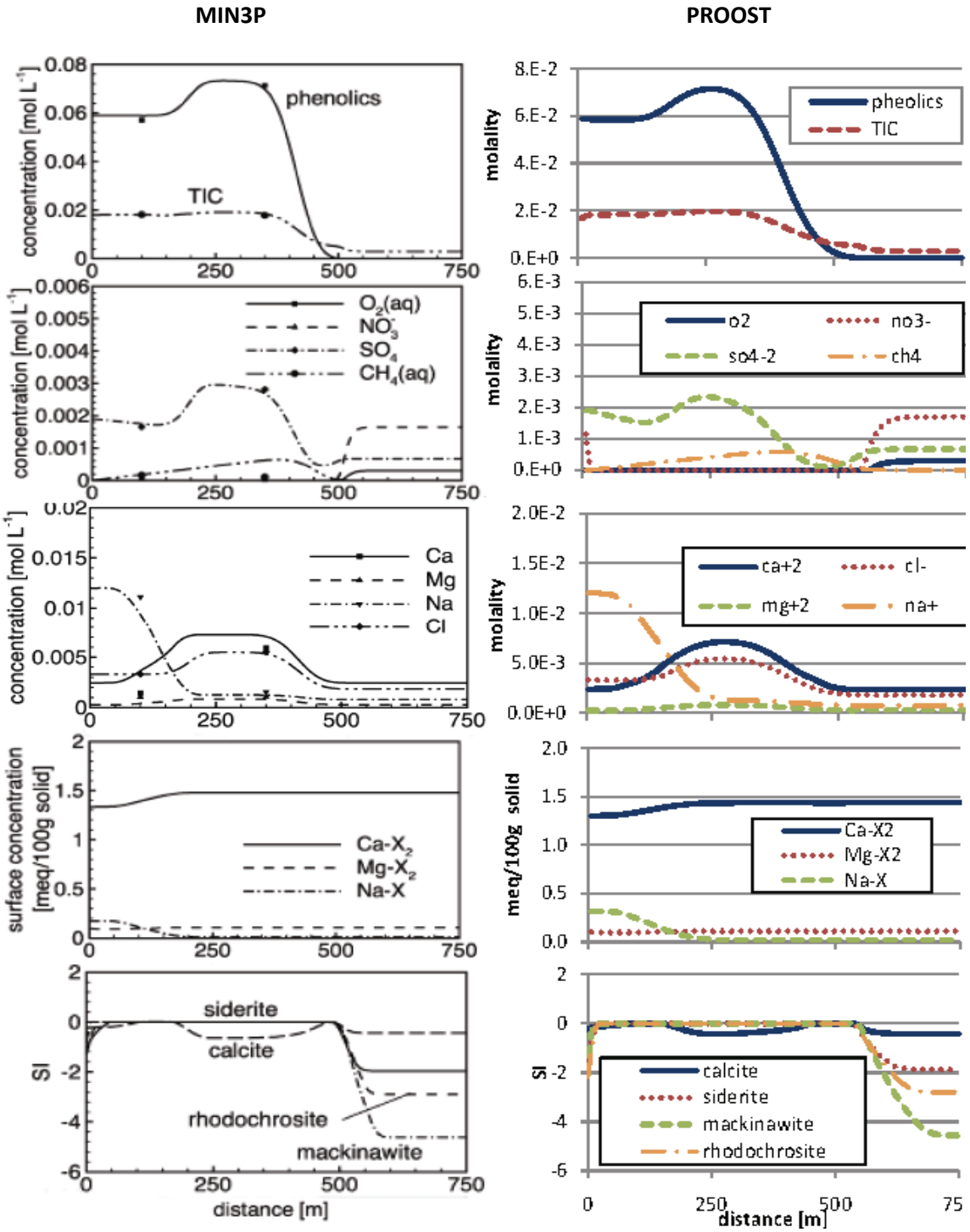

Figure II-5 – PROOST results (right) of modeling natural attenuation of phenolic compounds are compared with results from MIN3P (left)

E. Dry air flux in a sand column

In order to verify the implementation of multiphase reactive transport the code was compared to CODEBRIGHT (Olivella et al. 1996). A chemically simple problem was formulated so that it could be solved with CODEBRIGHT. A two meters length sand column in which a dry flux of air is injected. On the opposite side of the column temperature and air and vapor partial pressure are keep constant. A diagram of the proposed system is shown on Figure II-6. Constitutive laws and the conceptual model are summarized in Table II-2. Results after a simulation time of six days are shown in Figure II-7 for both codes.

Figure II-6 – Diagram of the system for the dry air flow of a sand column model

Table II-2 – Constitutive laws and conceptual model for the dry air flow on a sand column problem

Retention curve: van Genuchten	$S_l = \left(1 + \left(\frac{P_g - P_l}{P_0}\right)^{\frac{1}{1-\lambda}}\right)^{-\lambda}$	$P_0 = 0.1[\mathrm{MPa}]$ $\lambda = 0.072$
Phase permeability	$\frac{\mathbf{K} \cdot \mathrm{K}_{r\alpha}}{\mu_\alpha}\left[m^2 \cdot \mathrm{MPa}^{-1} \cdot \mathrm{s}^{-1}\right]$	$\mathbf{K} = 1\mathrm{x}10^{-11}\left[m^2\right];\ \mathrm{K}_{r\alpha} = S_\alpha^3$
Phase density	$\rho_{liq} = P_0 \exp\left(\alpha T + \beta\left(P_l - P_0\right)\right)$	$P_0 = 1002.6[\mathrm{MPa}]$ $\alpha = -3.4x10^{-4}\left[{}^{\circ}C^{-1}\right]$ $\beta = 4.5\mathrm{x}10^{-4}\left[\mathrm{MPa}^{-1}\right]$
	$\rho_{gas} = \frac{P_{g,vap} \cdot mw_{vap} + P_{g,air} \cdot mw_{air}}{R\left(T + 273.15\right)}$	$mw_{vap} = 0.018 Kg \cdot mol^{-1}$ $mw_{air} = 0.02895 Kg \cdot mol^{-1}$
Phase viscosity	$\mu_{\mathrm{liq}} = 2.1\mathrm{x}10^{-12} \cdot \exp\left(\frac{1808.5}{T + 273.15}\right)[\mathrm{MPa} \cdot \mathrm{s}]$	
	$\mu_{\mathrm{gas}} = 1.48\mathrm{x}10^{-12} \cdot \exp\left(\frac{119.4}{T + 273.15}\right)[\mathrm{MPa} \cdot \mathrm{s}]$	
Phase diffusion	$D_{gas} = 5.9x10^{-6}\left(\frac{\left(T + 273.15\right)^{2.3}}{P_g}\right)\left[m^2 \cdot s^{-1}\right]$	
	$D_{liq} = 1.1x10^{-4} \exp\left(\frac{-24539}{R \cdot \left(T + 273.15\right)}\right)\left[m^2 \cdot s^{-1}\right]$	
Thermal conductivity	$\lambda = \lambda_{sat}^{S_l} \lambda_{dry}^{(1-S_l)}\left[\mathrm{WmK}^{-1}\right]$	$\lambda_{sat} = 4.\left[\mathrm{WmK}^{-1}\right]$ $\lambda_{dry} = 0.4\left[\mathrm{WmK}^{-1}\right]$
Initial conditions	$S_l = 0.9\ ;\ P_l = -1\mathrm{MPa}\ ;\ T = 25^{\circ}C$	
Flow boundary	$j = 3.\mathrm{x}10^{-3} m^3 \cdot s^{-1}\ ;\ h_r = 0.4$	
Fixed value boundary	$S_l = 0.9\ ;\ P_l = -1\mathrm{MPa}\ ;\ T = 25^{\circ}C$	

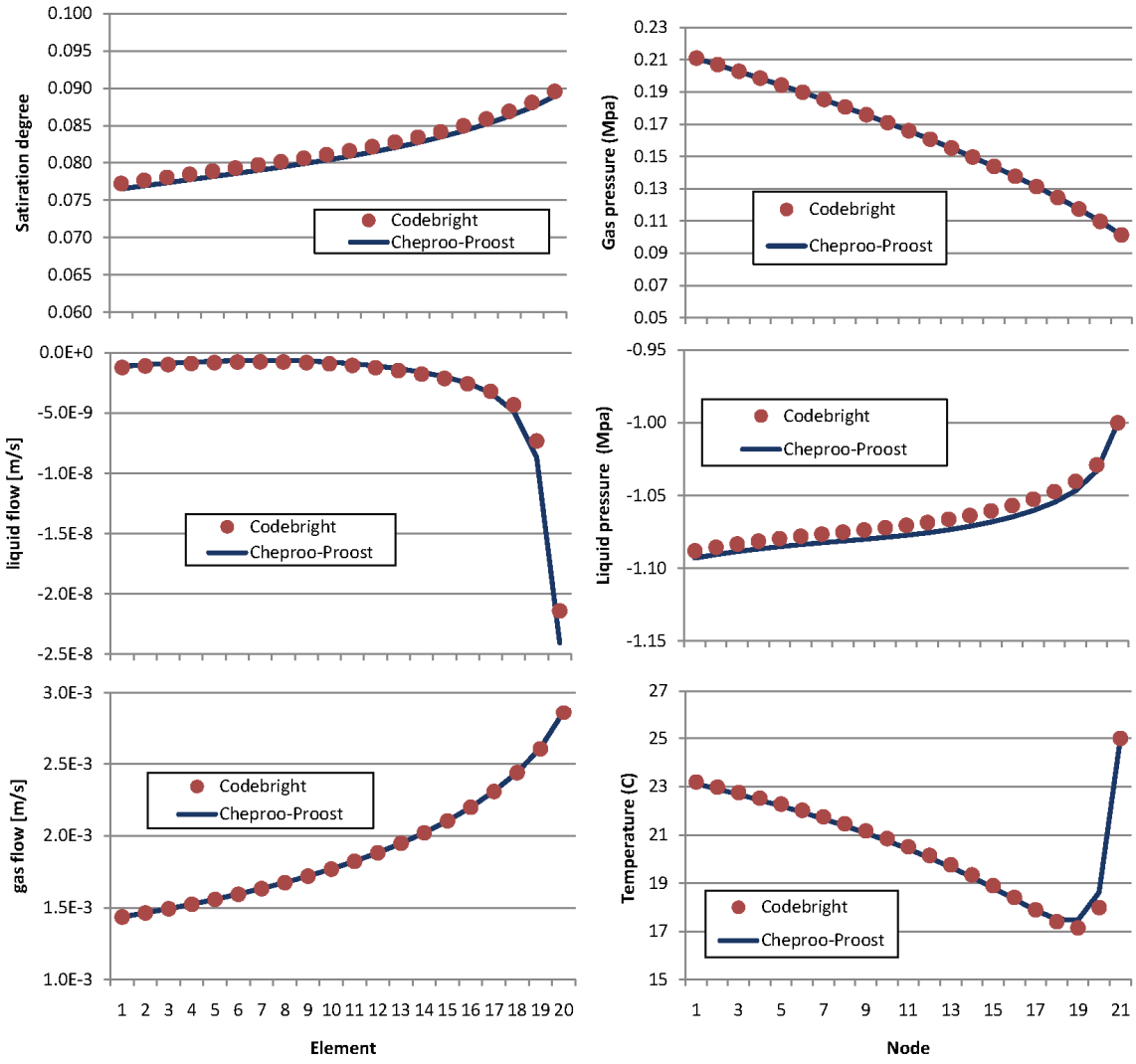

Figure II-7 – Results for the dry air flow on a sand column problem after a simulation time of six days for both codes

III. Input files example

Input files for solving the problem C "*Flushing of saline water by fresh water*" with the DSA approach

1. PrositIn.xml

```
<prosit >
  <direct_problem ndim = "1">
    <cheproohandler>
      <inputfile path="ChepInt.xml" format="XML" />
    </cheproohandler>
    <contfieldlist>
      <inputfile path="ContFieldList.xml" format="XML" />
    </contfieldlist>
    <meshfieldlist>
      <inputfile path="MeshFieldIn.xml" format="XML" />
    </meshfieldlist>
    <Phenlist>
      <inputfile path="Phenlist.xml" format="XML" />
    </Phenlist>
    <Solverlist>
      <inputfile path="solverlist_spa.xml" format="XML" />
    </Solverlist>
    <Etlist>
      <inputfile path="etListIn.xml" format="XML" />
    </Etlist>
    <meshlist>
      <inputfile path="mesh.xml" format="XML" />
    </meshlist>
    <modeloutput>
       <inputfile path="output.xml" format="XML" />
    </modeloutput>
    <tasks number = "1">
      <task order = "1"  regime = "transient">
        <temporal_definition lowbound = "inclusive"  lowboundval = "0" upbound =
          "inclusive" upboundval = "1036800"/>
        <solver name = "transp"/>
      </task>
    </tasks>
  </direct_problem>
</prosit>
```

2. ChepInt.xml

```
<?xml version="1.0" encoding="UTF-8" ?>
<che filename="wad_CHE.inp" format="dat" method="dsa"/>
<master25 filename="master25.dat" format="dat"/>
<path pathinfo = ""/>
```

3. ContFieldList.xml

```
<?xml version="1.0" encoding="UTF-8" ?>
<contfieldlist nrfields = "2">
  <field name = "conc_ext" >
    <basicpoints nr = "2" idim = "1">
      <basicpoint x ="0." type ="constant" value ="1.0" />
      <basicpoint x ="2." type ="constant" value ="2.0" />
    </basicpoints>
    <method name = "plane">
    </method>
  </field>
    <field name = "flowinout" >
      <basicpoints nr = "2" idim = "1">
        <basicpoint x ="0." type ="constant" value =".015" />
```

```
        <basicpoint x ="2." type ="constant" value ="-.015" />
        </basicpoints>
        <method name = "plane">
        </method>
      </field>
    </contfieldlist>
```

4. MeshfieldIn.xml

```
<?xml version="1.0" encoding="UTF-8" ?>
<meshfieldList>
  <!--Flow parameters-->
  <meshfield name = "velocity" use = "processatpoint" family = "" t_rank = "1" targetkind
    = "element" type = "by comp">
    <spatial_definition type = "everywhere" targetkind = "element"/>
    <components nrComp = "1">
      <component nr = "1" value = ".015" />
    </components>
  </meshfield>
  <meshfield name = "dispersion" targetkind = "element" use = "dispersion" family = ""
    t_rank = "2" type = "by comp" >
    <spatial_definition type = "everywhere" targetkind = "element"/>
      <components nrComp = "1" anis ="1">
        <component nr = "1" value = ".006" />
      </components>
  </meshfield>
  <meshfield name = "flowinout" use = "processbalance" family = "" t_rank = "0" targetkind
    = "node" type = "by comp" >
    <spatial_definition type = "et list">
      <ets number = "2"> left right</ets>
    </spatial_definition>
    <components nrComp = "1">
      <component nr = "1" >
        <contfield name = "flowinout" integration = "none"/>
      </component>
    </components>
  </meshfield>

  <!-- Density -->
  <meshfield name = "elemdensity" targetkind = "element" use = "density" family = ""
    t_rank = "0" type = "by comp" >
    <spatial_definition type = "everywhere" targetkind = "element"/>
    <components nrComp = "1">
      <component nr = "1" value = "1000" />
    </components>
  </meshfield>
  <meshfield name = "nodedensity" targetkind = "node" use = "density" family = "" t_rank
   ="0" type = "by comp" >
    <spatial_definition type = "everywhere" targetkind = "node"/>
    <components nrComp = "1">
      <component nr = "1" value = "1000" />
    </components>
  </meshfield>
  <meshfield name = "nodedensity" targetkind = "node" use = "externaldens" family = ""
    t_rank = "0" type = "by comp" >
    <spatial_definition type = "et list">
      <ets number = "2"> left right</ets>
    </spatial_definition>
    <components nrComp = "1">
      <component nr = "1" value = "1000" />
    </components>
  </meshfield>

  <!--Porosity-->
  <meshfield name = "porosity" use = "fluidvolume" family = "" t_rank = "0" targetkind =
    "element" type = "by comp" >
    <spatial_definition type = "everywhere" targetkind = "element"/>
    <components nrComp = "1">
      <component nr = "1" value = "0.3" />
    </components>
  </meshfield>

  <!--Node volume-->
  <meshfield name = "one" use = "one" family = "" t_rank = "0" targetkind = "element" type
    = "by comp" >
```

```
    <spatial_definition type = "everywhere" targetkind = "element"/>
    <components nrComp = "1">
      <component nr = "1" value = "1." />
    </components>
  </meshfield>
  <meshfield name = "node_volume" use = "node_volume" family = "" t_rank = "0" targetkind
    = "node" type = "meshfieldfunction" mesh = "default">
    <spatial_definition type = "everywhere" targetkind = "node"/>
    <referenced_meshfields nr = "1">
      <referenced_meshfield name = "one" use = "one" family= "" index = "1"/>
    </referenced_meshfields>
    <meshfieldfunction type = "linear">
      <inputparameters number = "2">
        <parameter type = "real" name = "scalar_factor" value = "1"/>
        <parameter type = "real" name = "scalar_term" value = "0.0"/>
      </inputparameters>
      <preprocessing> node_areal_average </preprocessing>
    </meshfieldfunction>
  </meshfield>

  <!--Initial water mass content-->
  <meshfield name = "initialKGH2o" use = "initialdeff" family = "" t_rank = "0" targetkind
    = "node" type = "meshfieldfunction" >
    <spatial_definition type = "everywhere" targetkind = "node"/>
    <referenced_meshfields nr = "2">
      <referenced_meshfield name = "node_volume" use = "node_volume" family = "" index =
        "1"/>
      <referenced_meshfield name = "nodedensity" use = "density" family = "" index = "2"/>
    </referenced_meshfields>
    <meshfieldfunction type = "multiplication">
      <inputparameters number = "3">
        <parameter type = "real" name = "scalar_factor" value = "0.3"/> <!--Porosity -->
        <parameter type = "real" name = "exponent_1" value = "1.0"/>
        <parameter type = "real" name = "exponent_2" value = "1.0"/>
      </inputparameters>
    </meshfieldfunction>
  </meshfield>

  <!--Chemical definition-->
  <meshfield name = "mineral_def" use = "mindeff" family = "" t_rank = "0" targetkind =
    "node" type = "by comp">
    <spatial_definition type = "everywhere" targetkind = "node"/>
    <components nrComp = "1">
      <component nr = "1" value = "1." />
    </components>
  </meshfield>
  <meshfield name = "min_sup_def" use = "supdeff" family = "" t_rank = "0" targetkind =
    "node" type = "by comp">
    <spatial_definition type = "everywhere" targetkind = "node"/>
    <components nrComp = "1">
      <component nr = "1" value = "1." />
    </components>
  </meshfield>
  <meshfield name = "initialConc" use = "initialdeff" family = "" t_rank = "0" targetkind
    = "node" type = "by comp" >
    <spatial_definition type = "everywhere" targetkind = "node"/>
    <components nrComp = "1">
      <component nr = "1" value = "2." />
    </components>
  </meshfield>

  <meshfield name = "uaext" use = "chemdeff" family = "" t_rank = "0" targetkind = "node"
    type = "by comp" >
    <spatial_definition type = "et list">
      <ets number = "2"> left right</ets>
    </spatial_definition>
    <components nrComp = "1">
      <component nr = "1" >
        <contfield name = "conc_ext" integration = "none"/>
      </component>
    </components>
  </meshfield>

<!--Mineral sink source term-->
<meshfield name = "Rumin" use = "flux" family = "" t_rank = "1" targetkind = "node"
  type = "chemical" multikind= "multiple non uniform" multidim="by cheproo">
  <chemicalinfo chemid = "RUmin"/>
```

```
  <spatial_definition type = "everywhere" targetkind = "node"/>
    <referenced_meshfields nr = "1">
      <referenced_meshfield name = "concentration" use = "nexttime" family= "" index =
        "1"/>
    </referenced_meshfields>
  </meshfield>
  <meshfield name = "ruminflux" use = "flux" family = "" t_rank = "1" targetkind = "node"
      type = "meshfieldfunction" multikind= "multiple non uniform" multidim="by cheproo" >
    <spatial_definition type = "everywhere" targetkind = "node"/>
    <referenced_meshfields nr = "2">
      <referenced_meshfield name = "Rumin" use = "flux" family = "" index = "1"/>
      <referenced_meshfield name = "initialKGH2o" use = "initialdeff" family = ""
       index = "2"/>
    </referenced_meshfields>
    <meshfieldfunction type = "multiplication">
      <inputparameters number = "3">
        <parameter type = "real" name = "scalar_factor" value = "1"/>
        <parameter type = "real" name = "exponent_1" value = "1.0"/>
        <parameter type = "real" name = "exponent_2" value = "1.0"/>
      </inputparameters>
    </meshfieldfunction>
  </meshfield>

  <!--External component concentration-->
  <meshfield name = "uaext" use = "externalstatevar" family = "" t_rank = "1" targetkind =
    "node" type = "chemical" multikind= "multiple non uniform" multidim="by cheproo">
    <chemicalinfo chemid = "Uaext"/>
    <spatial_definition type = "et list">
      <ets number = "2"> left right</ets>
    </spatial_definition>
    <referenced_meshfields nr = "1">
      <referenced_meshfield name = "uaext" use = "chemdeff" family= "" index = "1"/>
    </referenced_meshfields>
  </meshfield>
</meshfieldList>
```

5. PhenList.xml

```
<?xml version="1.0" encoding="UTF-8" ?>
<PhenList nrPhen = "1">
  <cheproo_plugin method="dsa" retraso_specia_method="newton-raphson" >
    <concentration name="concentration" initial_deff_name="initialConc"
      initial_deff_use="initialdeff"/>
    <surface_definition initial_deff_name="min_sup_def"
      initial_deff_use="supdeff"/>
    <mineral_definition initial_deff_name="mineral_def"
      initial_deff_use="mindeff"/>
    <target_vol name="node_volume" use="node_volume"/>
    <tagret_kgh2o initial_deff_name="initialKGH2o"
      initial_deff_use="initialdeff"/>
    <aqueous_component name="ua"/>
    <adsorbed_component name="uads"/>
    <units time_unit = "years" aqueous="mol/kgh2o" />
  </cheproo_plugin>
  <phenomenon name = "transport" mystatevariable = "concentration"
    nrpreviousssolutions ="1" multikind="multiple non uniform">
    <initialConditionID name = "concentration" use = "steady state" />
    <processes nr = "6">
      <process name = "storage_conc_aq" type = "Storage" >
        <temporal_definition lowbound = "minus_infinity" upbound =
          "infinity" />
        <timefraction type = "1 - theta"/>
        <spatial_definition type = "everywhere" targetkind ="element" />
        <FieldReferences category = "input" nrRef = "2">
          <meshfieldid name = "porosity" use = "fluidvolume" />
          <meshfieldid name = "elemdensity" use = "density"/>
        </FieldReferences>
        <Storage_specific>
          <parameter name = "mass scheme" value = "lumped"/>
      <statevar name = "ua" />
    </Storage_specific>
  </process>
  <process name = "storage_conc_ads" type = "Storage" >
    <temporal_definition lowbound="minus_infinity" upbound="infinity" />
    <timefraction type = "1 - theta"/>
    <spatial_definition type = "everywhere" targetkind = "element" />
```

```
    <FieldReferences category = "input" nrRef = "2">
      <meshfieldid name = "porosity" use = "fluidvolume" />
      <meshfieldid name = "elemdensity" use = "density"/>
    </FieldReferences>
    <Storage_specific>
      <parameter name = "mass scheme" value = "lumped"/>
      <statevar name = "uads" />
    </Storage_specific>
  </process>
  <process name = "diffusion" type = "dispersion">
    <timefraction type = "theta"/>
    <temporal_definition lowbound ="minus_infinity" upbound="infinity"/>
    <spatial_definition type = "everywhere" targetkind = "element">
    </spatial_definition>
    <FieldReferences category = "input" nrRef = "3">
      <meshfieldid name = "porosity" use = "fluidvolume" />
      <meshfieldid name = "dispersion" use = "dispersion" />
      <meshfieldid name = "elemdensity" use = "density"/>
    </FieldReferences>
    <Dispersion_specific>
      <statevar name = "ua"/>
      <parameter name = "multiply_by_density" value = "true"/>
      <parameter name = "mulitply_by_volume_fraction" value = "true"/>
    </Dispersion_specific>
  </process>
  <process name = "advection" type = "advection">
    <timefraction type = "theta"/>
    <temporal_definition lowbound="minus_infinity" upbound ="infinity"/>
    <spatial_definition type = "everywhere" targetkind = "element">
    </spatial_definition>
    <FieldReferences category = "input" nrRef = "2">
      <meshfieldid name = "velocity" use = "processatpoint" />
      <meshfieldid name = "elemdensity" use = "density"/>
    </FieldReferences>
    <advection_specific>
      <statevar name = "ua" />
      <parameter name = "conservation_scheme" value = "mass"/>
      <parameter name = "method" value = "divergenceform"/>
    </advection_specific>
  </process>
  <process name = "boundaryflow" type = "massflow">
    <temporal_definition lowbound="minus_infinity" upbound="infinity" />
    <spatial_definition type = "et list">
      <ets number = "2"> left right</ets>
    </spatial_definition>
    <timefraction type = "theta"/>
    <FieldReferences category = "input" nrRef = "5">
      <meshfieldid name = "uaext" use = "externalstatevar"/>
      <MeshfieldID name = "flowinout" use = "processbalance"/>
      <meshfieldid name = "nodedensity" use = "density"/>
      <meshfieldid name = "nodedensity" use = "externaldens" />
      <meshfieldid name = "ua" use = "lasttime"/>
    </FieldReferences>
    <massflow_specific>
      <statevar name = "ua"/>
      <parameter name = "multiply_flow_by_density" value = "true"/>
      <parameter name = "method" value = "divergenceform"/>
    </massflow_specific>
  </process>
  <process name = "mineral sink/source" type = "flux" >
    <temporal_definition lowbound="minus_infinity" upbound="infinity"/>
    <spatial_definition type = "everywhere" targetkind = "node">
    </spatial_definition>
    <timefraction type = "theta"/>
      <FieldReferences category = "input" nrRef = "1">
        <meshfieldid name = "ruminflux" use = "flux" />
      </FieldReferences>
    <flux_specific>
      <parameter name = "conservation_scheme" value = "volume"/>
    </flux_specific>
  </process>
</processes>
</phenomenon>
</PhenList>
```

6. SolverList_spa.xml

```
<?xml version="1.0" encoding="UTF-8" ?>
<solverlist nrSolvers = "1" >
  <solver name = "transp" type = "dsa">
    <solverDSA>
      <mesh name = "cuad"/>
      <temporal_discretization>
        <timesteps>
          <parameters>
            <parameter name = "ideal_timestep" type= "double" value= "15."/>
            <parameter name = "constant" value= "false"/>
            <parameter name = "increasefactor" value= "1.2"/>
            <parameter name = "decreasefactor" value= ".8"/>
            <parameter name = "nrconvforincrease" value= "10"/>
            <parameter name = "maxdelta" value= "15"/>
            <parameter name = "mindelta" value= "5"/>
          </parameters>
        </timesteps>
      </temporal_discretization>
      <phenomena number = "1" >
        <phenomenon Name = "transport" statevarname = "concentration" order = "1" >
          <temporal_discretization method = "finite differences">
            <parameters>
              <parameter name = "theta" type = "double " value = "1"/>
              <parameter name = "epsilon" type = "double " value = "1"/>
            </parameters>
          </temporal_discretization>
          <NonlinearProblem>
            <method name = "newton"/>
            <systemMatrix>
              <matrix type = "fullband">
              </matrix>
            </systemMatrix>
            <Convergencecriteria>
              <ConvergCrit name = "reldeltamax" value = "1e-5"/>
              <ConvergCrit name = "maxresid" value = "1e-8"/>
            </Convergencecriteria>
            <Stoppingcriteria>
              <StoppingCrit name = "maxiter" value = "50" />
            </Stoppingcriteria>
          </NonlinearProblem>
        </phenomenon>
      </phenomena>
    </solverDSA>
  </solver>
</solverlist>
```

7. EtListIn.xml

```
<?xml version="1.0" encoding="UTF-8" ?>
<ETlist Meshname = "transin-mesh" nrETs = "3">
  <ET name = "left" targetkind = "node" nrmeshes = "1" >
    <mesh name = "cuad">
      <vector type = "integer" dimension = "1" > 1</vector>
    </mesh>
  </ET>
  <ET name = "right" targetkind = "node" nrmeshes = "1" >
    <mesh name = "cuad">
      <vector type = "integer" dimension = "1" > 21</vector>
    </mesh>
  </ET>
  <ET name = "notbound" targetkind = "node" nrmeshes = "1" >
    <mesh name = "cuad">
      <vector type = "integer" dimension = "19" > 2 3 4 5 6 7 8 9 10 11 12 13 14 15 16
       17 18 19 20</vector>
    </mesh>
  </ET>
</ETlist>
```

8. Mesh.xml

```
<?xml version="1.0" encoding="UTF-8" ?>
<meshlist nrmeshes="1" ndim="1">
```

```
  <mesh type="fem" name="cuad" nband="2">
    <nodes nrnodes="21" ndim="1">0 .10 .20 .30 .40 .50 .60 .70 .80 .90 1.00 1.10 1.20
        1.30 1.40 1.50 1.60 1.70 1.80 1.90 2.00 </nodes>
    <elements nrelem="20"><elementTypes> 1 1 1 1 1 1 1 1 1 1 1 1 1 1 1 1 1 1 1 1
    </elementTypes>
    <connections lmxndl="2"> 1 2 2 3 3 4 4 5 5 6 6 7 7 8 8 9 9 10 10 11 11 12 12 13 13
        14 14 15 15 16 16 17 17 18 18 19 19 20 20 21 </connections></elements>
  </mesh>
</meshlist>
```

9. Output.xml

```
<?xml version="1.0" encoding="UTF-8" ?>
<modeloutput root = " ">
  <cheproo_outputs number= "2" write_initial="true" write_step_system="true">
    <cheproo_out OutputKind = "spatialout" >
      <frequency frequency = "1" />
    </cheproo_out>
    <cheproo_out OutputKind = "nodalchem" nodalchem ="21" file ="nodalchem21.dat">
      <frequency frequency = "1"/>
    </cheproo_out>
  </cheproo_outputs >
</modeloutput>
```

10. Wad_Chem.inp

```
'TITLE OF THE PROBLEM: Wad case for CHEPROO-PROSIT'
'-------------------------------------------------------------------------------'
'DEFINITION OF THE GEOCHEMICAL SYSTEM'
25.0          2    1               !initial temp. of the system
'PRIMARY AQUEOUS SPECIES'
'h+'
'na+'
'mg+2'
'ca+2'
'cl-'
'hco3-'
'*'
'AQUEOUS COMPLEXES'
'oh-'
'co3-2'
'co2(aq)'
'*'
'MINERALS'
'calcite'       0
'*'            0
'GASES'
'co2(g)'
'*'
'SURFACE COMPLEXES'
'EX'
'x2ca'
'xna'
'x2mg'
'*'
'-------------------------------------------------------------------------------'
'INITIAL AND BOUNDARY WATER TYPES'
2   0   0   !niwtype, nbwtype, nrwtype= number of ini, bound, rech waters
1     25.0                                          !
 '        icon        guess          ctot          constrain'
'h+'          3        1.00d-7    5.24807d-8         ''
'ca+2'        4        1.70d-3      1.70d-3        'calcite'
'mg+2'        1        1.00d-7      1.00d-7        ' '
'hco3-'       5        3.49d-3      0.01d0         'co2(g)'
'na+'         1        1.00d-7      1.0E-07         ' '
'cl-'         1        2.00d-7      2.00d-7          ' '
'*'       0          0.0            0.0            ' '
```

```
2      25.0
'        icon         guess          ctot           constrain'
'h+'           3          1.00d-8      8.07d-9          ''
'na+'          1          4.79d-1       4.79d-1          ' '
'mg+2'         1          4.75d-2       4.75d-2          ' '
'ca+2'         1          9.51d-3       9.51d-3          ' '
'cl-'          1          5.66d-1       5.66d-1          ' '
'hco3-'        4          3.70d-4       3.70d-4        'calcite'
'*'       0           0.0             0.0            ' '
'-------------------------------------------------------------------------------'
'INITIAL MINERAL ZONES'
1                                                 !nmtype= number of mineral zones
1                                               !imtype
'mineral          vol.frac.    area'
'calcite'           0.03       1.09d+5
'*'                 0.0          0.0
'INITIAL SURFACE ADSORPTION ZONES'
1
1
' '        0.0
' '        0.0
' '        0.0
' '        18.9
'-------------------------------------------------------------------------------'
'OUTPUT'
'cl-'
'ca+2'
'mg+2'
'na+'
'hco3-'
'co3-2'
'co2(aq)'
'h+'
'xna'
'x2ca'
'x2mg'
'calcite'
'*'
'end'
```

References

Abriola, L.M. and Pinder, G.F. 1985. A multiphase approach to the modeling of porous media contamination by organic compounds. 1. Equation development. Water Resources Research 21 (1), pp. 11-18.

Acero, P., Ayora, C., Carrera, J., Saaltink, M. W., & Olivella, S. 2009. Multiphase flow and reactive transport model in vadose tailings. *Applied Geochemistry*, 24(7), 1238–1250.

Adenekan, A. E., Patzek, T. W. and Pruess, K. 1993. Modeling of multiphase transport of multicomponent organic contaminants and heat in the subsurface - Numerical model formulation, Water Resources Research 29 (11), pp. 3727-3740.

Akin, J. E. 1999. Object oriented programming via Fortran 90. *Engineering Computations*, 16, 26–48.

Akridge, D. Glen. 2008. Methods for calculating brine evaporation rates during salt production. *Journal of Archaeological Science*, 35(6), 1453–1462.

Appelo, C. A. J., and Postma, D., 1994. Geochemistry, Groundwater and Pollution, A.A. Balkema, Brookfield, Vt.

Atkins, P. and De Paula, J. Atkin's Physical Chemistry, Oxford, New York 2006

Bea, S.A., 2008. *An object-oriented module for geochemical and reactive transport modeling*. Ph.D. thesis, Technical University of Catalonia (UPC).

Bea, S.A., Carrera, J., Ayora, C., Batlle, F., & Saaltink, M.W. 2009. CHEPROO: A Fortran 90 object-oriented module to solve chemical processes in Earth Science models. *Computers & Geosciences*, 35, Issue 6, 1098–1112.

Bea, S.A. and Carrera, J. and Ayora, C. and Batlle, F. 2010a Modeling of concentrated aqueous solutions: Efficient implementation of Pitzer equations in geochemical and reactive transport models. *Computers & Geosciences*, 36, 526–538.

Bea, S.A., Ayora, C., Carrera, J., Saaltink, M.W., & Dold, B. 2010b. Geochemical and environmental controls on the genesis of soluble efflorescent salts in Coastal Mine Tailings Deposits: A discussion based on reactive transport modeling. *Journal of Contaminant Hydrology*, 111(1-4), 65–82.

Boivin, C. and Ollivier-Gooch, C. 2004. A toolkit for numerical simulation of pdes. ii. solving generic multiphysics problems. *Computer Methods in Applied Mechanics and Engineering*, 193(36-38):3891–3918.

Budge, K.G., Peery, J.S. 1993. RHALE—a MMALE shock physics code written in c++. International Journal of Impact Engineering; 14:107–120.

Brun, A. and Engesgaard, P. 2002. Modelling of transport and biogeochemical processes in pollution plumes: literature review and model development. *Journal of Hydrology*, 256(3-4):211–227.

Carr, M. 1999. Using Fortran90 and object-oriented programming to accelerate code development, *IEEE Antennas and Propagation Magazine*, 41, 85–90.

Clement, T., Sun, Y., Hooker, B. and Petersen, J. 1998. Modeling multispecies reactive transport in ground water. *Ground Water Monitoring & Remediation*, 18(2):79–92.

Commend, S. and Zimmermann, T. 2001. Object-oriented nonlinear finite element programming: a pimer. Advances In Engineering Software, vol. 32, no. 8, pp. 611_628.

Corapcioglu, M. Y. and Gaehr, A. L. 1987. A compositional multiphase model for groundwater contamination by petroleum products. 1. Theoretical considerations. Water Resources Research 23 (1), pp. 191-200.

De Simoni, M., Carrera, J., Sanchez-Vila, X., and Guadagnini, A. 2005. A procedure for the solution of multicomponent reactive transport problems. *Water Resources Research*, 41(11):W11410.

Debye, P., Hückel, E.,.Thetheory of electrolytes, 1923. I .Lowering of freezing point and related phenomena. Physikalische Zeitschrift 24, 185–206.

Decyk, V. K., Norton, C. D. and Szymanski, B. K. 1998. How to support inheritance and run-time polymorphism in Fortran90, *Computer Physics Communications*, 115, 9–17.

Dold, B. 2006. Element Flows Associated with Marine Shore Mine Tailings Deposits. *Environmental Science & Technology*, 40(3), 752–758.

Donovan, J. J., & Rose, A. W. 1994. Geochemical evolution of lacustrine brines from variable-scale groundwater circulation. *Journal of Hydrology*, 154(1-4), 35–62.

Dubois-Pelerin Y. and Pegon, P. 1997. Improving modularity in object-oriented finite element Programming. Communications In Numerical Methods In Engineering, vol. 13, no. 3, pp. 193-198, Mar.

Eugster, H. P., Harvie, C. E., & Weare, J. H. 1980. Mineral equilibria in a six-component seawater system, Na-K-Mg-Ca-SO4-Cl-H2O, at 25°C. *Geochimica et Cosmochimica Acta*, 44(9), 1335–1347.

Fenvesm, GL. Object-oriented programming for engineering software development. *Engineering with Computers* 1990; 6:1–15.

Filho, J., Devloo, P. Object-oriented programming in scientific computations: the beginning of a new era. *Engineering Computations* 1991; 8:81–87.

Forde, B., Foschi, R.O., Stiemer, S.F. Object-oriented finite element analysis. Computers and Structures 1990;34(3):355–374.

Forsyth, P. A., and Shao, B. Y. 1991. Numerical simulation of gas venting for NAPL site remediation, Advances in Water Resources, 14 (6), 354-367.

Hardie, L. A., & Eugster, H. P. 1980. Evaporation of Seawater: calculated mineral sequence. *Science*, 208, 498–500.

Gandy, C. J. and Younger, P. L. 2007. An object-oriented particle tracking code for pyrite oxidation and pollutant transport in mine spoil heaps. *ournal of Hydroinformatics*, 9 (4):293–304.

Gorelik, A. M., 2004. Object-oriented programming in modern Fortran. *Programming and Computer Software*, 30, 173–179.

Gran, M, Carrera, J., Olivella, S., Massana, J., Saaltink, M. W., Ayora, C amd Lloret, A. 2009. Salinity is reduced below the evaporation front during soil salinization. Estudios de la zona no saturada del suelo Vol IX, 281-287.

Hardie, L.A., & Eugster, H.P. 1980. The evolution of closed basin brines. *Mineralogical Society of America*, Special Paper 3, 273–290.

Holzbecher, E. 2005. Groundwater flow pattern in the vicinity of a salt lake. *Hydrobiologia*, 532, 233–242.

Jankowski, J., & Jacobson, G. 1989. Hydrochemical evolution of regional groundwaters to playa brines in central Australia. *Journal of Hydrology*, 108, 123–173.

Jury, W. A., & Horton, R. 2004. *Soil Physics*. Wiley.

Khan, E. H. , Alaali, M. and Girgis, M. R. 1995. Object-oriented programming for structured procedural programmers. Computer, vol. 28, no. 10, pp. 48.

Kolditz, O. and Bauer, S. A process-oriented approach to computing multi-field problems in porous media. *Journal of Hydroinformatics*, 6:225–244, 2004.

Krumgalz, B. S., Hecht, A., Starinsky, A., & Katz, A., 2000. Thermodynamic constraints on Dead Sea evaporation: can the Dead Sea dry up? *Chemical Geology*, 165(1-2), 1–11.

Lichtner, P.C. Continuum formulation of multicomponent–multiphase reactive transport in: Lichtner, P.C., Steefel, C.I., Oelkers, E.H. (Eds.), *Reactive Transport in Porous Media, Reviews in Mineralogy,* vol. 34, 1996, pp. 1 –81.

Maley, D., Kilpatrick, P. L., Schreiner, E. W., Scott, N. S. and Diercksen, G. H. F. 1996. The formal specification of abstract data types and their implementation in fortran 90: Implementation issues concerning the use of pointers. *Computer Physics Communications*, vol. 98, no. 1-2, pp. 167-180.

Massana, J. 2005, Influència de la salinitat en el flux multifàsic en solumnes de sòl obertes i sota condicions d'evaporació. Master thesis, Technical University of Catalonia (UPC).

Masters, I., Usmani, A. S., Cross , J. T. and Lewis, R. W. 1997. Finite element analysis of solidification using object-oriented and parallel techniques. International journal for numerical methods in engineering, vol. 40, no. 15, pp. 2891-2909.

Mayer, K. U., Benner, S. G., Frind, E. O., Thornton, S. F. and Lerner, D. N. 2001. Reactive transport modeling of processes controlling the distribution and natural attenuation of phenolic compounds in a deep sandstone aquifer. *Journal of Contaminant Hydrology*, 53(3-4):341–368.

Mayer, K. U.; Frind, E. O. & Blowes, D. W. 2002. Multicomponent reactive transport modeling in variably saturated porous media using a generalized formulation for kinetically controlled reactions Water Resources Research, 38, 1174.

Meysman, F.J. R., Middelburg, J. J., Herman, P. M. J. and Heip, C. H. R. 2003. Reactive transport in surface sediments. i. model complexity and software quality. *Computers & Geosciences*, 29(3):291–300.

McCaffrey, M. A., Lazar, B. and Holland, H. D., 1987. The evaporation path of seawater and the coprecipitation of br- and k+ with halite. *Journal of Sedimentary Research*, 57(5):928–937.

Mills, R., Lu, C., Lichtner, P.C. and Hammond, G. 2007. Simulating Subsurface Flow and Transport on Ultrascale Computers using PFLOTRAN, *Journal of Physics Conference Series* , 78, 012051 doi:10.1088/1742-6596/78/1/012051.

Molinero, J. and Samper, J. 2006. Large-scale modeling of reactive solute transport in fracture zones of granitic bedrocks. *Journal of Contaminant Hydrology*, 82(3-4):293–318.

Molins, Sergi, Carrera, Jesús, Ayora, Carlos, & Saaltink, Maarten W. 2004. A formulation for decoupling components in reactive transport problems. *Water Resour. Res.*, 40(10), W10301.

Molins, S. and Mayer, K. U. 2007. Coupling between geochemical reactions and multicomponent gas and solute transport in unsaturated media: A reactive transport modeling study. Water Resources Research, 43(5):W05435.

Norton, C. D., Decyk, V. and Slottow, J. , 1998. Applying fortran 90 and object-oriented techniques to scientific applications. *Object-Oriented Technology*, vol. 1543, pp. 462-463.

Olivella, S., Gens, A., Carrera, J., and Alonso, E.E. 1996. Numerical formulation for a simulator (code_bright) for the coupled analysis of saline media. *Engineering Computations*, 13:87–112.

Parkhurst, D.L., Kipp, K.L., Engesgaard, Peter, and Charlton, S.R. 2004. PHAST—A program for simulating ground-water flow, solute transport, and multicomponent geochemical reactions: U.S. Geological Survey Techniques and Methods 6–A8, 154 p.

Pidaparti, R.M.V., Hudli, A.V. 1993. Dynamic analysis of structures using object-oriented techniques. Computers andStructures; 49(1):149–156.

Pitzer, S. Thermodynamics of electrolytes. I. 1973. Theoretical basis and general equations. Journal of Physical Chemistry 77 (2), 268–277.

Pruess, K., Oldenburg, C. and Moridis, G. *1999.* TOUGH2 User's Guide, Version 2.0*, Lawrence Berkeley National Laboratory Report LBNL-43134, Berkeley, CA.*

Pruess, K. and Battistelli, A. TMVOC 2002. User's guide*, Lawrence Berkeley National Laboratory* Report Report LBNL-49375, Berkeley, CA.

Reeves, H., Kirkner, D.J. , 1988. Multicomponent mass transport with homogeneous and heterogeneous chemical reactions: effect of the chemistry on the choice of numerical algorithm: 2. Numerical results. Water Recourses Research 24 (10), 1730–1739.

Risacher, F., & Clement, A. 2001. A computer program for the simulation of evaporation of natural waters to high concentration. *Computers & Geosciences*, 27(2), 191–201.

Risacher, F., Alonso, H., & Salazar, C. 2003. The origin of brines and salts in Chilean salars: a hydrochemical review. *Earth-Science Reviews*, 63(3-4), 249–293.

Rubin, J. 1983. Transport of reacting solutes in porous media: Relation between mathematical nature of problem formulation and chemical nature of reactions, Water Resour. Res., 19(5), 1231–1252.

Saaltink, M. W., Ayora, C., & Carrera, J. 1998. A mathematical formulation for reactive transport that eliminates mineral concentrations. *Water Resources Research*, 34(7), 1649–1656.

Saaltink, M. W., Carrera, J. and Ayora, C. 2001. On the behavior of approaches to simulate reactive transport. *Journal of Contaminant Hydrology*, 48(3-4):213–235.

Saaltink, M. W., Batlle, F., Ayora, C., Carrera, J., and Olivella, S. 2004. Retraso, a code for modeling reactive transport in saturated and unsaturated porous media. Geologicaacta, 2, Nº3:235–251.

Sánchez-Moral, S., Ordóñez, S., García del Cura, M. A., Hoyos, M., & Cañaveras, J. C. 1998. Penecontemporaneous diagenesis in continental saline sediments: bloeditization in Quero playa lake (La Mancha, Central Spain). *Chemical Geology*, 149(3-4), 189–207.

Sánchez-Moral, S., Ordóñez, S., Benavente, D., & García del Cura, M. A. 2002. The water balance equations in saline playa lakes: comparison between experimental and recent data from Quero Playa Lake (central Spain). *Sedimentary Geology*, 148(1-2), 221–234.

Sanford, W. E., & Wood, W. W. 1991. Brine evolution and mineral deposition in hydrologically open evaporite basins. *Am J Sci*, 291(7), 687–710.

Shao, H., Dmytrieva, S. V., Kolditz, O., Kulik, D. A., Pfingsten, W. and Kosakowski, G. 2009. Modeling reactive transport in non-ideal aqueous-solid solution system. *Applied Geochemistry*, 24(7):1287–1300.

Silva, E.J., Mesquita, P, Saldanha, R.R., Palmeira, P.F.M. 1994. An object-oriented finite element program for electromagnetic field computation. IEEE Transactions on Magnetics; 30:3618–3621.

Silva, O., and J. Grifoll, 2007. A soil-water retention function that includes the hyper-dry region through the BET adsorption isotherm, Water Resources Research, 43, W11420, doi:10.1029/2006WR005325.

Simmons, C. T., & Narayan, K. A. 1998. Modelling density-dependent flow and solute transport at the Lake Tutchewop saline disposal complex, Victoria. *Journal of Hydrology*, 206(3-4), 219–236.

Sleep, B. E., and Sykes, J. F. 1993. Compositional simulation of groundwater contamination by organic compounds 1. Model development and verification, Water Resources Research, 29 (6), 1697-1708.

Slooten, L. J. 2008. *An Object Oriented approach to groundwater optimization and simulation problems*. Ph.D. thesis, Technical University of Catalonia (UPC).

Slooten, L.J., Batlle, F., and Carrera, J. 2010. An XML based Problem Solving Environment for Hydrological Problems. XVIII Conference on Computational Methods in Water Resources (CMWR) http://congress.cimne.com/cmwr2010

Steefel, C. I. and MacQuarrie, K.T.B. 1996. Approaches to modeling of reactive transport in porous media. *Reviews in Mineralogy and Geochemistry (Reactive Transport in Porous Media) January 1996; v. 34;1; p. 85-129*, 34:85–129.

Steefel, C. I., DePaolo, D. J. and Lichtner, P. C. 2005. Reactive transport modeling: An essential tool and a new research approach for the earth sciences. *Earth and Planetary Science Letters*, 240(3-4):539–558.

Unger, A. J. A., Sudicky, E. A. and Forsyth, P. A. 1995. Mechanisms controlling vacuum extraction coupled with air sparging for remediation of heterogeneous formations contaminated by dense non-aqueous phase liquids, Water Resources Research, 31 (8), 1913-1925.

van der Lee, j., De Windt, L., Lagneau, V. and Goblet, P. 2003. Module-oriented modeling of reactive transport with hytec. *Computers & Geosciences*, 29(3):265–275.

Wang, W. and Kolditz, O. 2007. Object-oriented finite element analysis of thermo-hydro-mechanical (THM) problems in porous mediaInt. J. Numer. Meth. Engng; 69:162-201.

Weiß, M., & Menzel, L. 2008. A global comparison of four potential evapotranspiration equations and their relevance to stream flow modelling in semi-arid environments. *Advances in Geosciences*, 18, 15–23.

Wissmeier, L. and Barry, D.A. 2008. Reactive transport in unsaturated soil: Comprehensive modelling of the dynamic spatial and temporal mass balance of water and chemical components. *Advances in Water Resources*, 31(5):858–875.

Wood, W. W., & Sanford, W. E. 1990. Ground-water control of evaporite deposition. *Economic Geology*, 85(6), 1226–1235.

Yan, J. P., Hinderer, M., & Einsele, G. 2002. Geochemical evolution of closed-basin lakes: general model and application to Lakes Qinghai and Turkana. *Sedimentary Geology*, 148(1-2), 105–122.

Yeh, G. T., and V. S. Tripathi, 1989. A critical evaluation of recent developments in hydrogeochemical transport models of reactive multichemical components, Water Resour. Res., 25(1), 93–108.

Yechieli, Y., & Wood, W. W. 2002. Hydrogeologic processes in saline systems: playas, sabkhas, and saline lakes. *Earth-Science Reviews*, 58(3-4), 343–365.

Xu, T., Pruess, K. 1998. Coupled modeling of non-isothermal multiphase flow, solute transport and reactive chemistry in porous and fractured media: 1. Model development and validation. Lawrence Berkeley National Laboratory Report LBNL-42050, Berkeley, California, 38 pp.

Zimmermann, T., Bomme, P., Eyheramendy, D., Vernier, L. and Commend, S. 1998. Aspects of an object-oriented finite element environment. Computers & Structures, vol. 68, no. 1-3, pp. 1-16.